Environmental Processes
https://doi.org/10.1007/s40710-021-00536-w

ORIGINAL ARTICLE

Simultaneous Removal of Soluble Metal Species and Nitrate from Acidic and Saline Industrial Wastewater in a Pilot-Scale Biofilm Reactor

Panagiota Mendrinou[1] · Artin Hatzikioseyian[1] · Pavlina Kousi[1] · Paschalis Oustadakis[1] · Petros Tsakiridis[1] · Emmanouella Remoundaki[1]

Received: 19 May 2021 / Accepted: 18 August 2021/Published online: 07 September 2021

Abstract

The hydrometallurgical treatment of waste printed circuit boards for the recovery of precious metals generates acidic wastewater containing nitrate, chloride and residual base metals. The scope of this work is the study of a biological treatment process for the concurrent metal sequestering, nitrate reduction and wastewater neutralization. A pilot-scale packed-bed biofilm reactor was set up, inoculated with the strain *H. denitrificans* and experimentally monitored. The range of operating parameters examined included: (a) nitrate concentration 750–5750 mg/L NO_3^-; (b) pH 3–8; (c) Cu, Ni, Zn and Fe at 50 mg/L and 100 mg/L; and (d) chloride concentration 5%–10% as NaCl. The presence of metals did not affect denitrification at the concentrations examined. *H. denitrificans* completely reduced nitrate and the intermediately produced nitrite at elevated chloride levels. Denitrification shifted pH towards circumneutral to alkaline values, where iron, zinc, copper and nickel were sequestered quantitatively from solution via bioprecipitation. The proposed simple, robust and low-cost biological treatment unit is advantageous compared to the conventional wastewater treatment, where metal precipitation is based on chemical neutralization and the problem of nitrate removal remains unresolved.

Keywords Bioprecipitation · *Halomonas denitrificans* · Metal removal · Nitrate reduction · Packed-bed biofilm reactor · Salinity

Article highlights • Denitrification is achieved at elevated metal, nitrate and chloride concentrations.
• Metal ions are sequestered via bioprecipitation.
• The effluent is neutralized.

✉ Artin Hatzikioseyian
artin@metal.ntua.gr

Extended author information available on the last page of the article

1 Introduction

Waste Electrical and Electronic Equipment (WEEE) ranks among the fastest growing waste streams in the world. The global generation of e-waste grew to 53.6 Mt in 2019 with the perspective to reach 74.7 Mt by 2030 (Forti et al. 2020). Among e-waste, printed circuit boards (PCBs) consist of 30% of base and precious metals (copper and iron 10%–20%, gold, silver, platinum) as well as rare earths. Their metal content is much higher than the natural ores, making metal recovery from PCBs a worldwide priority for circular economy (Işıldar 2018). Hydrometallurgical processing can be established in local WEEE recycling industries permitting the decentralized "green" production of pure metals (Tuncuk et al. 2012; Tunsu and Retegan 2016). These processes involve essentially two steps: (a) leaching of metals, which is generally achieved by means of strong acids such as nitric, hydrochloric and their mixtures (aqua regia); and (b) separation/selective extraction of the metals of interest from the leachate. Thus, the effluents from the separation and recovery stages contain residual anions such as NO_3^-, Cl^- as well as residual metal ions which have not been recovered. Neutralization of these streams resolves the problem of acidity, removes part of the soluble metal ions as hydroxides and part of sulfate as calcium sulfate when $Ca(OH)_2$ is used as neutralizing agent. However, the concentration of nitrate and chloride does not alter significantly as these anions remain mobile.

Soluble nitrogen compounds, i.e., nitrate or nitrite, can cause serious environmental and human health problems when discharged untreated into water bodies. The established discharge limit for nitrate in drinking water is 50 mg/L NO_3^- (or 11 mg/L NO_3^--N), and for nitrite 5 mg/L NO_2^- (Ward et al. 2018). Removal of chloride, nitrate and sulfate with conventional treatment options, such as reverse osmosis and ion exchange, is costly. Biological denitrification is a promising, cost effective alternative process which has proven efficiency and selectivity (Matějů et al. 1992). It is based on the ability of the microorganisms to use nitrate and nitrite as electron acceptors instead of molecular oxygen, and involves the reduction of nitrate to nitrite and ultimately to nitrous oxide and nitrogen gas via four enzymatic steps (Reactions 1–4):

$$NO_3^- + 2e^- + 2H^+ \rightarrow NO_2^- + H_2O \quad (1)$$

$$NO_2^- + e^- + 2H^+ \rightarrow NO + H_2O \quad (2)$$

$$2NO + 2e^- + 2H^+ \rightarrow N_2O + H_2O \quad (3)$$

$$N_2O + 2e^- + 2H^+ \rightarrow N_2 + H_2O \quad (4)$$

In the first step (Reaction 1), the reduction of nitrate to nitrite, is catalyzed by a molybdenum-containing nitrate reductase. Nitrite is further reduced to nitric oxide (Reaction 2) that can be catalyzed by either cytochrome *cd1* or copper-containing enzymes.

In the third step (Reaction 3), nitric oxide is reduced to nitrous oxide, a greenhouse gas. This is accomplished by a nitric oxide reductase that contains heme c, heme b and non-heme iron cofactors. Finally, a copper-containing enzyme (nitrous oxide reductase) drives the fourth and last step (Reaction 4) where nitrous oxide is reduced to dinitrogen (Tavares et al. 2006; Pang and Wang 2021). The overall denitrification reaction can be expressed as a single redox (Reaction 5):

$$2NO_3^- + 10e^- + 12H^+ \rightarrow N_2 + 6H_2O \quad (5)$$

Heterotrophic denitrification has been demonstrated feasible and efficient for the treatment of industrial wastewater which is characterized by elevated nitrate concentrations and no or low metal content. For example, Fernández-Nava et al. (2008) reported that the biological reduction of nitrate in the presence of calcium, from rinse wastewater generated during the manufacturing process of stainless steel, was feasible by achieving 98% nitrate removal in 7 h although they observed that increased calcium concentrations had negative effect on the denitrification rate. Similarly, successful biological reduction of nitrate has been reported for wastewater from the metal-finishing industry (Gabaldón et al. 2007) and nitrocellulose industry (Ugurlu and Ozturkcu 2018), as well as for simulated mine and mill effluents (Koren et al. 2000) and mine water (Mattila et al. 2007). Since industrial wastewater contains little or no organic carbon and most of the known denitrifiers derive their energy from the oxidation of organic substrates, including single carbon compounds (Lin et al. 2009; Pang and Wang 2021), a suitable carbon source/electron donor must be provided to achieve biological denitrification, such as methanol (Gabaldón et al. 2007; Koren et al. 2000; Fernández-Nava et al. 2008; Mattila et al. 2007), ethanol (Papirio et al. 2014; Zou et al. 2014) or acetate (Constantin and Fick 1997).

In the case of industrial metal-bearing wastewater, where metal sequestering is also essential for the safe discharge of the effluent, the biological activity should be sustained in order to simultaneously achieve denitrification and metal bioprecipitation. The later may occur as a result of the alkalinity produced via the biological activity; insoluble metal hydroxides and carbonates precipitate as pH shifts towards more alkaline values and carbonates are produced due to the oxidation of organic carbon. When sulfates are also fed in the reactor, and the prevailing conditions favor sulfate reduction, metal sulfides may also form. These processes, collectively termed as bioprecipitation, are well documented in the literature (Remoudaki et al. 2003; Tsezos et al. 2007; Kousi et al. 2011). Moreover, in conjunction with bioprecipitation, the metal precipitates formed in the bulk solution may be naturally trapped or chemically absorbed by the Extracellular Polymeric Substances (EPS) which are produced by bacteria as a resistance to toxic compounds (Teitzel and Parsek 2003). EPS encase biofilms and decelerate metal diffusion within them, affecting the overall sequestering of soluble metal species. Furthermore, metal sorption on cells and cellular components is controlled by a variety of physical-chemical mechanisms and interactions, such as ion exchange, complexation, adsorption and diffusion through cell walls and membranes (Flemming 1995; Gadd 2002; van Hullebusch et al. 2003).

However, metals have been reported to inhibit denitrifiers in soil, sediments and activated sludge (Baeseman et al. 2006; Magalhães et al. 2007; Sakadevan et al. 1999; Ochoa-Herrera et al. 2011). It has also been experimentally demonstrated, via batch assays, that the

denitrifying activity is affected in the case of synthetic mineral solutions containing Fe (Ramírez et al. 2018; Papirio et al. 2014), Ni (Ramírez et al. 2018; Zou et al. 2014), Co (Zou et al. 2014) and Cr (Ramírez et al. 2018), due to the accumulation of undesirable intermediates such as NO_2^- and N_2O (Ramírez et al. 2018). Special attention has been given to the effect of copper (Woolfenden et al. 2013; Felgate et al. 2012; Papirio et al. 2014; Zhao et al. 2020; Cheng et al. 2019), due to the copper-containing enzyme regulating the reduction of nitrous oxide into nitrogen.

To bypass the potential adverse effects of heavy metals on the nitrogen removal capacity of microbial biomass, recent studies have focused on selected metal-resistant bacteria (Zhang et al. 2019; Sun et al. 2016). Zhang et al. (2019) reported that the inhibitory effect of heavy metals on ammonium removal decreased in the order $Ni^{2+} > Cr^{6+} > Zn^{2+} > Cu^{2+}$, whereas Sun et al. (2016) found that efficient removal of ammonium occurred at 20 mg/L Zn^{2+} or 10 mg/L Ni^{2+} or 8 mg/L Cu^{2+} or 5 mg/L Cr^{6+}. Few studies have investigated the potential of biofilm reactors to efficiently remove nitrate from metal-bearing wastewater (Hirata et al. 2001; Zou et al. 2015). Hirata et al. (2001) monitored a fluidized-bed bioreactor treating actual, diluted wastewater generated during the recovery process of precious metals from printed circuit boards and demonstrated that it is feasible to remove soluble nitrogen in the presence of high salinity and metal concentrations. However, their study did not involve any data on pH or the concentration of soluble metal species. Zou et al. (2015) showed that fluidized-bed denitrifying cultures tolerated soluble Ni concentrations up to 500 mg/L; however, nickel remained soluble at concentrations 60–500 mg/L Ni in the feed solution. Thus, the microbially-mediated simultaneous removal of nitrate and metals remains challenging.

Another challenging characteristic of the wastewater to be treated is the high chloride content (i.e., salinity) due to the leaching agents (i.e., hydrochloric acid or aqua regia) commonly used for the hydrometallurgical recovery of metals from WEEE (Tuncuk et al. 2012). High chloride content is expected to have negative effects on microbial activity. Hirata et al. (2001) attempted to overcome these negative effects via long-term acclimation of the microbial culture, as previous studies on the effect of salt concentration showed that the nitrification ability was greatly decreased when salt concentration exceeded 2.3% (Vredenbregt et al. 1997) whereas over 2% of sodium chloride greatly reduced denitrification rate (Yang et al. 1995).

The purpose of the present work is to experimentally investigate and demonstrate the feasibility of biological denitrification of industrial wastewater via studying the effects of key factors such as acidity, salinity and metal content which generally stress bacteria and limit the microbial activity leading to nitrate reduction. The proposed single-stage process should meet three essential goals: (a) effluent neutralization; (b) nitrate removal; and (c) soluble metal species sequestering. To the best of our knowledge, such results have not been yet reported in the literature.

To this end, a pilot-scale packed-bed biofilm reactor was set up with a novel porous packing material which embeds trace elements for supporting the micronutrient requirements of an active biofilm. The bioreactor was inoculated with *Halomonas denitrificans*, a halophilic denitrifier capable of completely reducing nitrate to elemental nitrogen in the presence of high chloride, nitrate and metal content. The denitrifying capacity of the reactor was tested at extreme conditions of elevated nitrate (≈ 6 g/L NO_3^-) and chloride (10% w/v NaCl) levels in the presence of 100 mg/L Zn, Cu, Fe and Ni.

2 Materials and Methods

2.1 Bioreactor Set-up

A pilot-scale packed-bed reactor was selected as the bioreactor configuration for the treatment of wastewater containing nitrate and metal ions. The reactor is shown schematically in Fig. 1(a) and physically in Supplementary Material (SM) Fig. SM1. Such a bioreactor set-up was previously tested and found highly efficient for the treatment of acidic, sulphate- and metal-bearing wastewater (Kousi et al. 2007; Kousi et al. 2011). The reactor was made from transparent PVC (height: 50 cm; I.D.: 9.5 cm).

Two types of packing material for biofilm support were used: (a) spherical porous sintered-glass beads of average diameter 1.5–3.0 cm (Biohome Supergravel; Fig. 1b) at the bottom of the column creating a 5 cm high layer; and (b) cylindrical porous sintered-glass pieces of average length 2.5–3.5 cm and average diameter 1 cm (Biohome Ultimate Marine; Fig. 1c) filling the rest 40 cm of the column. At the top of the column, a headspace of 5 cm facilitated the release of the produced gases, providing for safety.

The packing material was produced and provided by Aqua Bio UK Ltd. (https://filterpro.co.uk/). It was selected due to its durability, the low pressure drop, the high porosity (approximately 50% according to the technical data sheet of the supplier), the good wetting properties and the trace element content which facilitates the development of active biofilm by providing the required trace elements for microbial growth (mainly Fe and Mn). The microscopic structure of the packing material is shown in Fig. 1d and e for Biohome Supergravel and Biohome Ultimate, respectively. The relevant EDS spectra at selected sites show characteristic peaks of silicon (Si) and oxygen (O) confirming that both Biohome Supergravel (Fig. 1f) and Biohome Ultimate (Fig. 1g) consist mainly of sintered glass. Both materials are also proprietarily enriched with trace elements, such as aluminum (Al), iron (Fe), manganese (Mn), chromium (Cr), sodium (Na), bromine (Br), calcium (Ca), titanium (Ti) and magnesium (Mg).

In all experiments, the reactor was run upflow in sequencing batch mode, meaning that the effluent returned into a well-mixed continuous stirred tank reactor (CSTR) from where it was fed again by means of a peristaltic pump (Shenchen LabM6). The working volume of the CSTR was 1 L and the liquid volume retained in the bioreactor was 1.7 L, corresponding to 53% void space. Thus, in each batch, a total volume of 2.7 L was treated.

2.2 Microbial Culture – Growth Medium

The bioreactor was inoculated with a pure culture of the strain *Halomonas denitrificans* (DSM-18045), which was obtained from the Deutsche Sammlung von Mikroorganismen und Zellkulturen (DSMZ, Germany), in pre-grown liquid culture in Bacto Marine Broth medium (DSMZ medium 514 + 8% NaCl) containing (in g/L): Bacto peptone (5.0), yeast extract (1.0), Fe^{3+} citrate (0.10), $MgCl_2.6H_2O$ (12.61), Na_2SO_4 (3.24), $CaCl_2.2H_2O$ (2.66), KCl (0.55), $NaHCO_3$ (0.16), KBr (0.08), H_3BO_3 (0.022), NH_4NO_3 (0.0016) and Na_2HPO_4 (0.008).

H. denitrificans was first isolated from saline water in Anmyeondo, Korea (Kim et al. 2007). The strain was selected for this study based on two specific characteristics: (a) its halotolerant nature which allows its growth in environments of high salinity, i.e., high chloride content (Miao et al. 2015); and (b) its phylogenetic traits which denote its ability to reduce completely nitrate to nitrogen gas (González-Domenech et al. 2010; Felgate et al. 2012; Wang

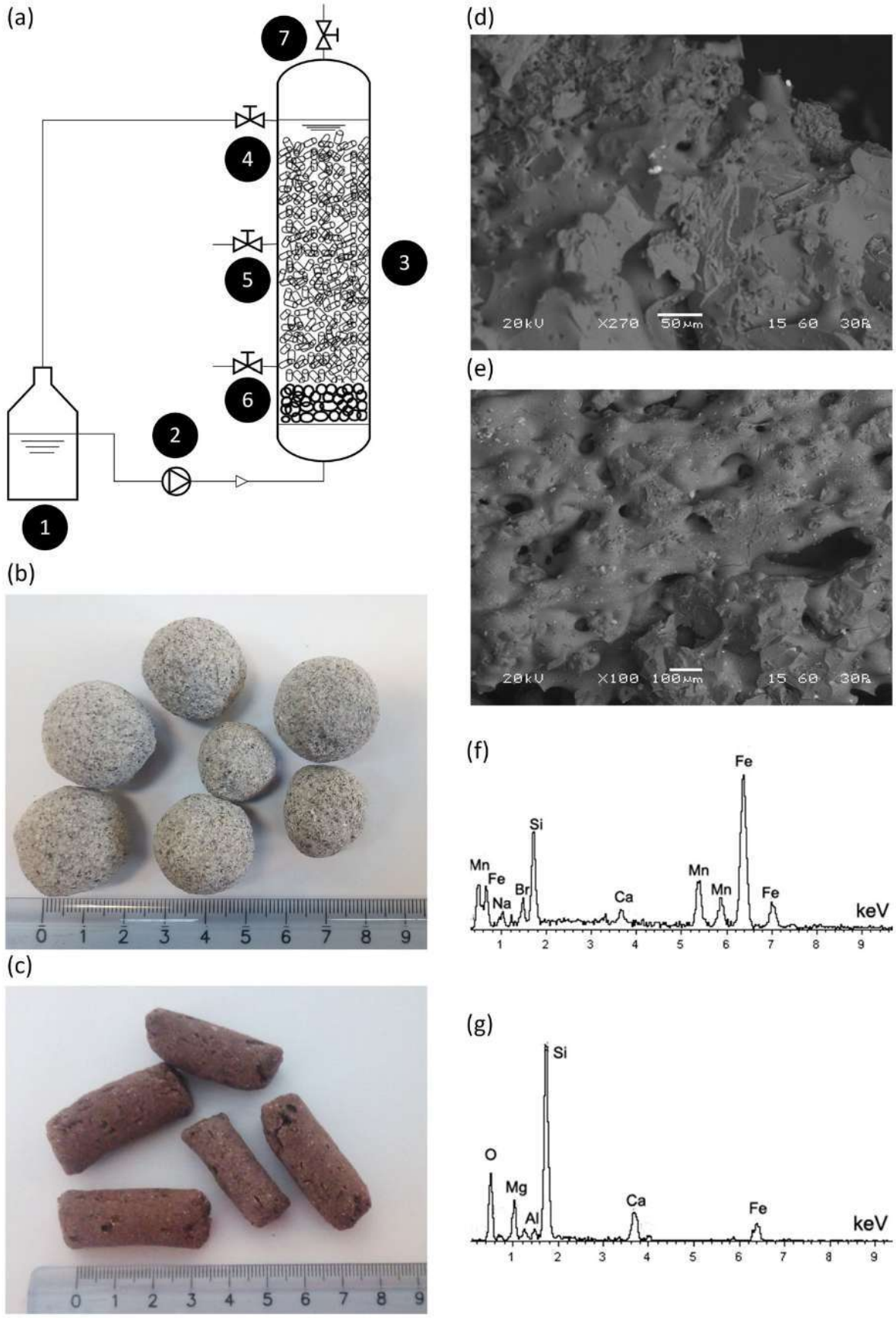

Fig. 1 (**a**) Layout of the denitrification unit: (1) feed from the completely stirred tank reactor (CSTR), (2) peristaltic pump, (3) packed-bed bioreactor, (4) reactor outflow, (5/6) sampling ports, (7) gas vent; photos of (**b**) Biohome Supergravel and (**c**) Biohome Ultimate packing materials; SEM micrographs for (**d**) Biohome Supergravel and (**e**) Biohome Ultimate; EDS spectra at selected sites on the surface of (**f**) Biohome Supergravel and (**g**) Biohome Ultimate

and Shao 2021). To the best of our knowledge, there are no bibliographic reports that the strain can tolerate elevated concentrations of metal ions or has been used in industrial wastewater treatment; these are investigated in this work for the first time.

2.3 Bioreactor Start-Up

Before inoculation, the column, the packing material and the silicon tubing were sterilized by recirculating 70% ethanol for 3 h followed by thorough rinsing with 3 L sterile deionized water. Bacto Marine Broth supplemented with 10% w/v NaCl and 1000 mg/L NO_3^- was used as growth medium for culture growth and transfer. An inoculum of 3 L was used for the first and subsequent inoculations of the reactor. The inoculation process was repeated four times: each phase lasted 5 days during which the reactor was run in sequencing batch mode for establishing an active biofilm on the surface and the pores of the packing material. The reactor was self-running with fresh medium (without microorganisms) after 21 days from the initial inoculation, indicating that an active biofilm was already established in the reactor. Subsequent experiments were performed in non-sterile clean conditions, while the reactor was periodically (on average, monthly) re-inoculated to ensure the dominance of *H. denitrificans* in the biofilm.

2.4 Experimental Set-up

In order to investigate the denitrification capacity, metal tolerance and metal sequestering capacity at high chloride concentration, different operating conditions were tested in the bioreactor. Four groups of experiments were designed and are reported in this work. All experiments were carried out at ambient temperature and in duplicate.

(a) In order to examine the tolerance and the denitrifying capacity of the biofilm, three different levels of initial nitrate concentration were tested: 750 mg/L, 2750 mg/L and 5750 mg/L NO_3^-. The ability of the microbial culture to tolerate and respire only on nitrite was also examined via feeding the reactor with solutions containing 2000 mg/L NO_2^-.

(b) The effect of pH on the denitrification process was investigated at initial pH 3, 4, 5, 6 and 8 at initial concentration 1250 mg/L NO_3^-. Due to the acidity of the wastewater to be treated, it is essential to study denitrification at low pH (i.e., 3–5). However, as denitrification progresses, pH shifts towards alkaline values. Thus, it is also important to study denitrification at circumneutral pH (i.e., 6–8). The initial pH of the medium was adjusted by the addition of 0.1 N HCl or 0.1 N NaOH as appropriate.

(c) The effect of salinity on the denitrification process was studied at pH 3 (the lowest of the tested pH) by adjusting the concentration of NaCl to 10% w/v (at 1250 mg/L NO_3^-), 7.5% w/v (at 2750 mg/L NO_3^-) and 5% w/v (at 3250 mg/L NO_3^-).

(d) To examine the effect of metal ions on the denitrification process as well as the fate of the metals during denitrification, a set of experiments was carried out at pH 3, nitrate concentration 2750–3250 mg/L NO_3^- and 5% w/v NaCl at two different initial metal concentrations: 50 mg/L and 100 mg/L. Four divalent metal ions were added separately (acclimation period 4 days before sampling): Fe^{2+} was added as $FeSO_4 \cdot 7H_2O$, Cu^{2+} was added as $CuCl_2 \cdot 2H_2O$, Ni^{2+} was added as $NiCl_2 \cdot 6H_2O$ and Zn^{2+} was added as $ZnCl_2$.

2.5 Sampling and Monitoring of the Reactor

Samples were collected from the reactor outflow (stream returning to the CSTR compartment) hourly for the first 6 h and once every 24 h for each run as appropriate. pH was determined on unfiltered samples. For all subsequent analytical determinations, the samples were vacuum filtered through 0.20 μm sterile membrane filters (Whatman ME 24/21 ST). The concentration of nitrate and nitrite was determined by colorimetry (Merck method 1.09713.0001 for nitrate adjusted to Hach DR/2500 at 340 nm and Merck method 1.14776.0002 for nitrite adjusted to Hach DR/2500 at 550 nm, respectively). The measuring range for nitrate and nitrite was 0–20 mg/L NO_3^--N and 0.02–1 mg/L NO_2^--N, respectively. Total organic carbon (TOC) was determined by colorimetry (Hach method 10129, DR/2500, measuring range: 0–20 mg/L TOC). The concentrations of soluble copper, nickel, iron and zinc were determined by flame atomic absorption spectroscopy (AAS) after acidification of the samples by adding HNO_3. All results were plotted as mean values with error bars representing one standard deviation.

The sludge generated within the reactor was examined by Scanning Electron Microscopy (SEM) using a Jeol 6380 LV microscope (accelerating voltage: 15 kV at low vacuum 30 Pa) and a backscattered electron detector. Microanalysis was performed by an Oxford INCA Energy Dispersive Spectrometer (EDS) connected to the SEM. SEM was performed on polished sections, which had been produced by vacuum impregnation of the selected sample in a low viscosity epoxy resin. After removing a small surface by cutting in micro-saw, the sample was grinded and polished with 1 μm diamond paste, on a lapping disk.

3 Results and Discussion

3.1 Kinetics of Nitrate and Nitrite Reduction

The kinetics of nitrate reduction are presented in Fig. 2a. Complete nitrate removal is attained within 4 h and 6 h for 750 mg/L and 2750 mg/L NO_3^-, respectively, whereas for 5750 mg/L NO_3^-, nitrate is completely removed within 25 h. The parallel monitoring of nitrite concentration verified that nitrate was reduced via the formation of intermediate nitrite. Nitrite profiles (Fig. 2b) represent typical kinetic curves of an intermediately produced and sequentially consumed in a sequence of reactions in series; thus, the peaks of the curves (Fig. 2b) correspond to the time when the nitrite reduction rate was higher than the nitrite production rate. The same profiles also show that the maximum nitrite concentration depends on the initial nitrate concentration: profile peaks at 200 mg/L, 580 mg/L and 1000 mg/L NO_2^- are observed for 750 mg/L, 2750 mg/L and 5750 mg/L NO_3^-, at 2 h, 4 h and 5 h, respectively. Complete nitrite reduction was observed within 4 h for 750 mg/L NO_3^- and less than 25 h for 2750 mg/L and 5750 mg/L NO_3^-. The results demonstrate the high denitrifying capacity of the biofilm reactor inoculated with *H. denitrificans*. All soluble nitrogen species (i.e., NO_3^- and NO_2^-) were completely removed from solution within 25 h, in compliance with the WHO established discharge limit, even for initial nitrate concentrations as high as 6 g/L, verifying similar findings for biofilm reactors reported in the literature (Mattila et al. 2007; Hirata et al. 2001).

Monitoring pH vs. time (Fig. 2c) verified that pH shifted towards more alkaline values as the reduction of nitrate to nitrogen progressed via the consumption of protons (Reaction 5). The rise of pH depends on the extent of nitrate reduction: higher initial nitrate concentrations correspond to higher final pH values. Moreover, pH profiles show a consistent pattern: initial

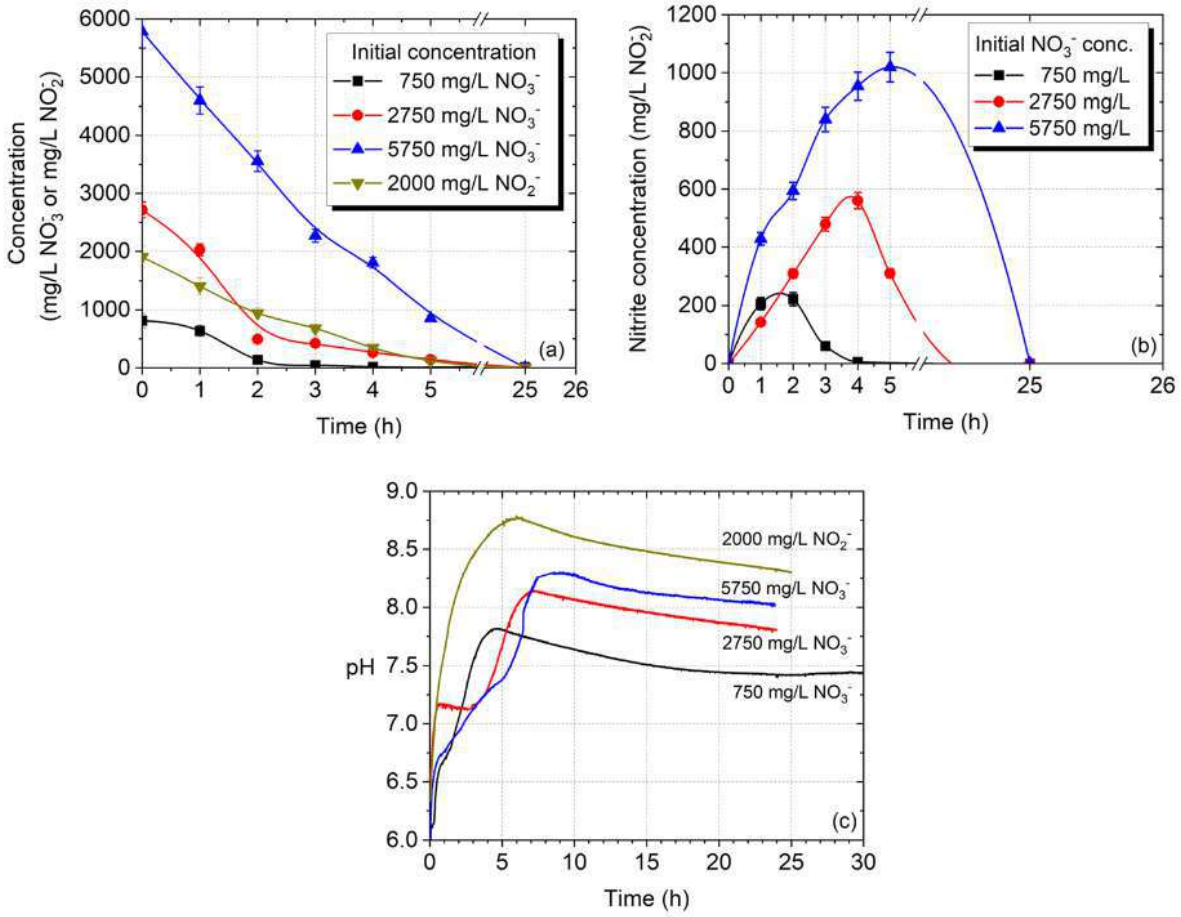

Fig. 2 Effect of initial nitrate/nitrite concentration on the denitrification process: (**a**) nitrate/nitrite concentration profiles; (**b**) produced nitrite concentration profiles; and (**c**) pH profiles

pH (6.2–7.2) rose steeply to reach a peak value from where it kept decreasing slowly towards an equilibrium value. The peak values 7.6, 8.3 and 8.6 for an initial concentration of 750 mg/L, 2750 mg/L and 5750 mg/L NO_3^-, respectively, coincide with zero residual nitrate concentration.

The ability of *H. denitrificans* to grow only by reducing nitrite in the absence of nitrate was investigated by conducting an experiment feeding the reactor with 2000 mg/L NO_2^- as the sole electron acceptor. The results shown in Fig. 2a prove that there is no apparent delay of nitrite reduction which is completely reduced to elemental nitrogen within 6 h. Therefore, it is confirmed that *H. denitrificans* can grow in the absence of nitrate by using only nitrite as terminal electron acceptor (nitrite respiration). This is consistent with the observed consumption of the nitrite produced as intermediate during nitrate reduction. It should be noted that, when only nitrite was present, the pH of the effluent reached a peak of 8.8 while maintaining the highest observed equilibrium pH value of 8.3 (Fig. 2c). Complete reduction of nitrate to the harmless elemental nitrogen is a significant prerequisite for the successful treatment of any nitrate-containing wastewater. Residual concentrations of nitrite are undesirable after wastewater treatment. It should be noted that only selected microbial species can carry out complete denitrification; several species stop the reduction process at an intermediate product such as nitrite, nitric oxide (NO) or nitrous oxide (N_2O) or start the reduction process from these intermediates (Kim et al. 2007; Holmes et al. 2019; You et al. 2020).

The results from TOC monitoring (data not shown) indicate that about 87% of TOC originates from bacto peptone while the rest 13% from the yeast extract contained in the

growth medium. TOC degradation reached about 50% in all runs representing the conversion of the organic fraction of peptones and yeast into CO_2. Thus, it was ensured that the carbon source was never in growth-limiting conditions and did not limit the denitrification process.

3.2 The Effect of Initial pH on Denitrification

Although the scope of this study is the treatment of acidic wastewater, the effect of the initial pH on the denitrification process was investigated over a wider range of values. To this end, the effect of the initial pH was studied at pH 3, 4, 5, 6 and 8 (Fig. 3a-f) versus the non-adjusted pH of the feed solution (pH = 6.8). All experiments were carried out with nitrate as electron acceptor at 1250 mg/L NO_3^-. These experiments also confirmed that denitrification progressed through the formation of nitrite and the subsequent reduction of nitrite to nitrogen (Fig. 3a-d). However, the initial pH of the medium significantly affected the concentration of nitrite (Fig. 3c-d). Both nitrate and nitrite were reduced within 4 h for acidic initial pH values. For pH 3, 4 and 5, the maximum nitrite concentration was lower than 75 mg/L, while for the circum-neutral and alkaline initial pH values, i.e., 6, 6.8 and 8, nitrite concentration was significantly higher (120 mg/L - 200 mg/L) and complete reduction was observed at 24 h. Therefore, it can be concluded that, under acidic pH, lower nitrite maxima are observed; this can be attributed either to the increased rate of nitrite reduction and/or to the decreased rate of nitrate reduction. This result is on the benefit of the proposed process aiming at the treatment of highly acidic streams with short residence times concerning nitrate reduction and low peak nitrite concentrations.

The control experiment at pH 6.8 showed a typical profile with a peak at pH 8 and a tail reaching equilibrium at pH 7.8. When the initial pH of the feed solution was adjusted to 3, 4 and 5, pH increased considerably to an equilibrium value of around 7.5 (Fig. 3e). When the initial pH was adjusted to 6 and 8, the corresponding equilibrium pH was 7.3 and 7.8, respectively (Fig. 3f). These findings are consistent with other results reported in literature for *Halomonas* species; pure or mixed cultures of *Halomonas* species retained high denitrification rates over a wide range of pH (Zhu and Liu 2017).

The steep increase of pH, especially in the case of acidic values (i.e., 3, 4 and 5), demonstrates the efficiency of the treatment unit to tolerate and neutralize acidic wastewater originating from WEEE acid leaching processes. It has been experimentally shown that biofilm reactors tolerate feed pH as low as 2.5 (Papirio et al. 2014) or 4.0 (Ugurlu and Ozturkcu 2018) with no adverse effects on denitrification. In the present work also, the established biofilm tolerated acidic feeds (pH = 3) and achieved both aims, namely wastewater neutralization and soluble nitrogen removal, within 4 h (Figs. 3a-d). Furthermore, the inherent increase of pH to 7.5–8.0, during denitrification, affects the solubility and mobility of the present metal ions as it will be discussed in the following.

3.3 The Effect of Salinity on Denitrification

The effect of salinity on the denitrification process was studied at three different chloride levels (NaCl: 5% w/v, 7.5% w/v and 10% w/v). These experiments simulated the presence of chloride in the wastewater due to the use of hydrochloric acid/aqua regia as leaching agents as well as the high ionic strength of the solution to be treated due to the presence of various dissolved species (i.e., nitrate, chloride and metal ions).

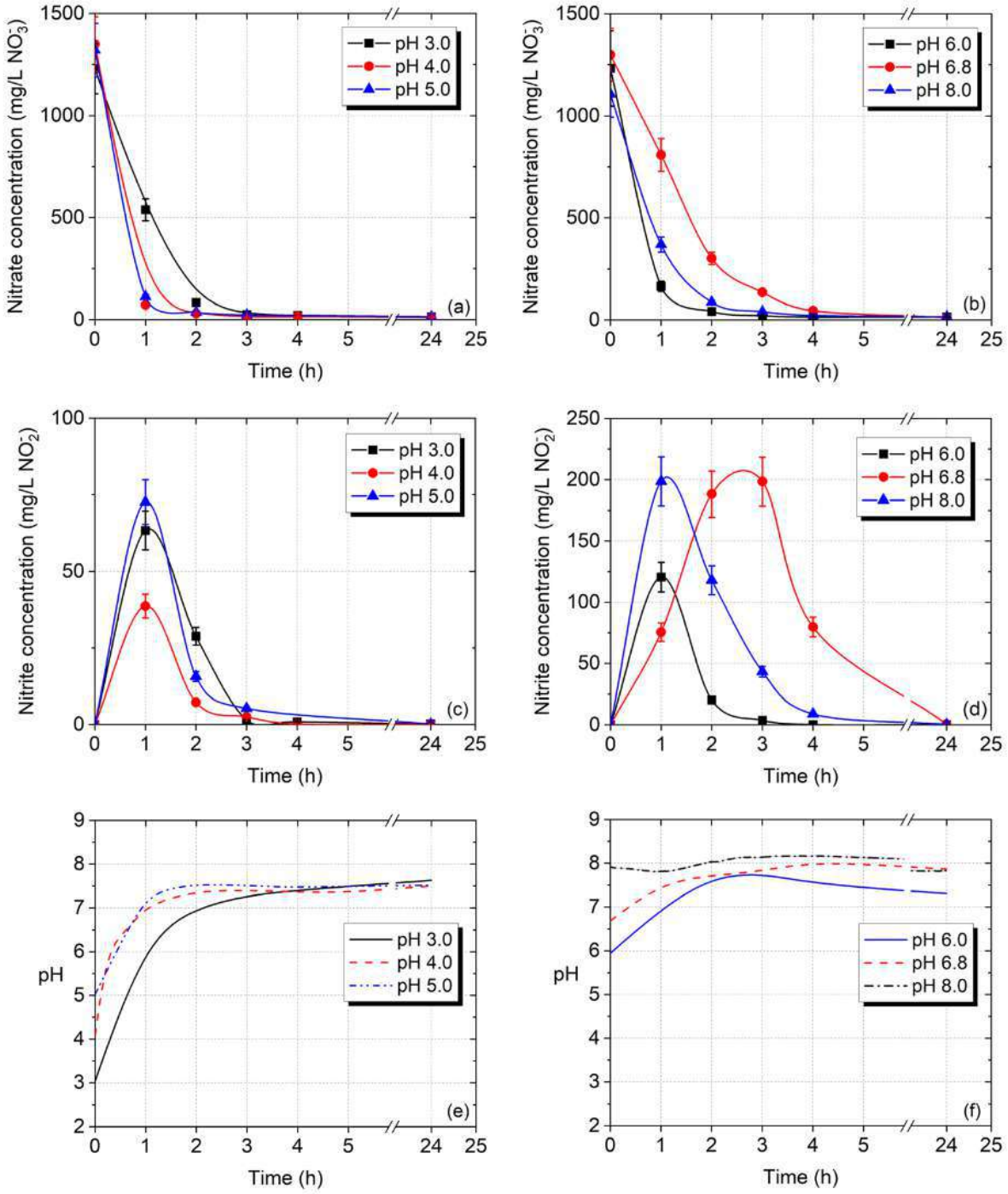

Fig. 3 Effect of initial pH on the denitrification process: (**a**)-(**b**) nitrate concentration profiles; (**c**)-(**d**) nitrite concentration profiles; and (**e**)-(**f**) pH profiles

The results reported in this study prove that the increased salinity did not affect the denitrification process which was completed within 4 h for different initial nitrate concentrations (Fig. 4a). However, Fig. 4b shows that salinity affected the temporal accumulation of nitrite in the medium, implying a direct effect on the physiology of *H. denitrificans*, as the decrease of NaCl stress may enhance the biodiversity of the denitrifying bacteria (Miao et al. 2015). Accumulation of nitrite was also observed in an anoxic packed-bed reactor that treated metallurgical wastewater as salinity increased (Yoshie et al. 2002). This phenomenon can be attributed to the decreasing diversity of the nitrite reductase genes as salinity increases (Yoshie

et al. 2004). Figure 4c indicates that, starting from pH 3, pH increased steeply within 2 h close to neutral values (7.0–7.7) regardless of the salinity level.

These findings are consistent with other results reported in the literature for *Halomonas* species; *H. campisalis* was shown to completely reduce nitrate at 12.5% NaCl and pH 9 (Peyton et al. 2001) whereas a recent study testing 14 *Halomonas* strains in a medium containing 6% NaCl demonstrated that the ability to remove nitrogen from saline media is a common property of *Halomonas* bacteria (Wang et al. 2019).

3.4 The Effects of Zn, cu, Fe and Ni on Denitrification

The effect of zinc, copper, iron and nickel on the denitrification process was studied, for each metal individually, at two initial concentrations: 50 mg/L and 100 mg/L. The synergistic effect of these metals was also studied with feed solutions containing 20 mg/L and 50 mg/L Zn, Cu, Fe and Ni (Fig. SM2 and SM3).

Figure 5a-f present the profiles for nitrate/nitrite concentration and pH vs. time compared to the control experiment which was conducted without any metal addition in the feed solution. Complete nitrate reduction was systematically observed within 5 h for all four metals tested at both concentrations (Fig. 5a-b) indicating that there is no significant inhibition on the denitrification process due to the presence of the metal ions. This is also indicated by the pH profiles (Fig. 5e-f) which show that, for all metals and at both concentrations, starting from pH 3, pH shifts to 7.2–7.5 within 2 h and equilibrates at a value close to 8.0.

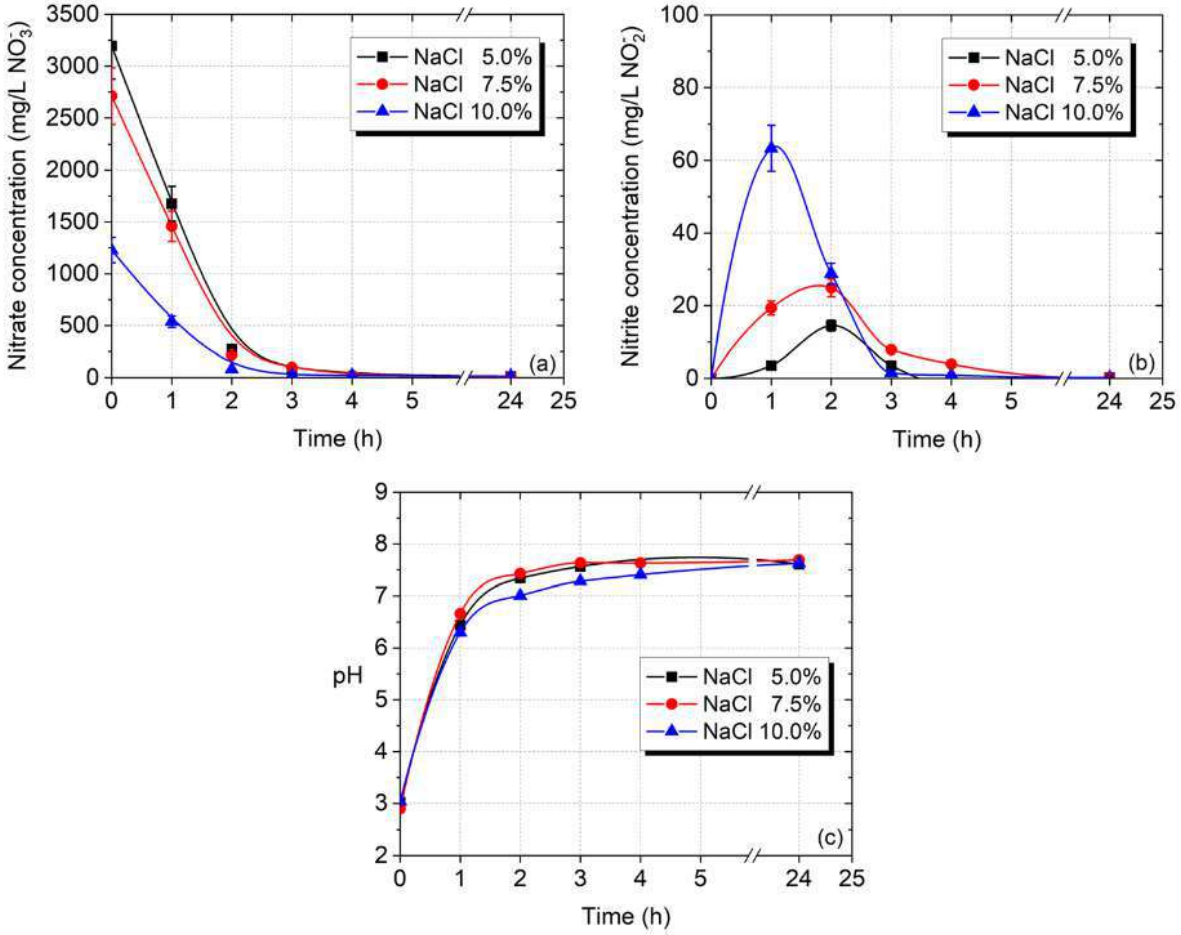

Fig. 4 Effect of salinity on the denitrification process: (**a**) nitrate concentration profiles; (**b**) nitrite concentration profiles; and (**c**) pH profiles

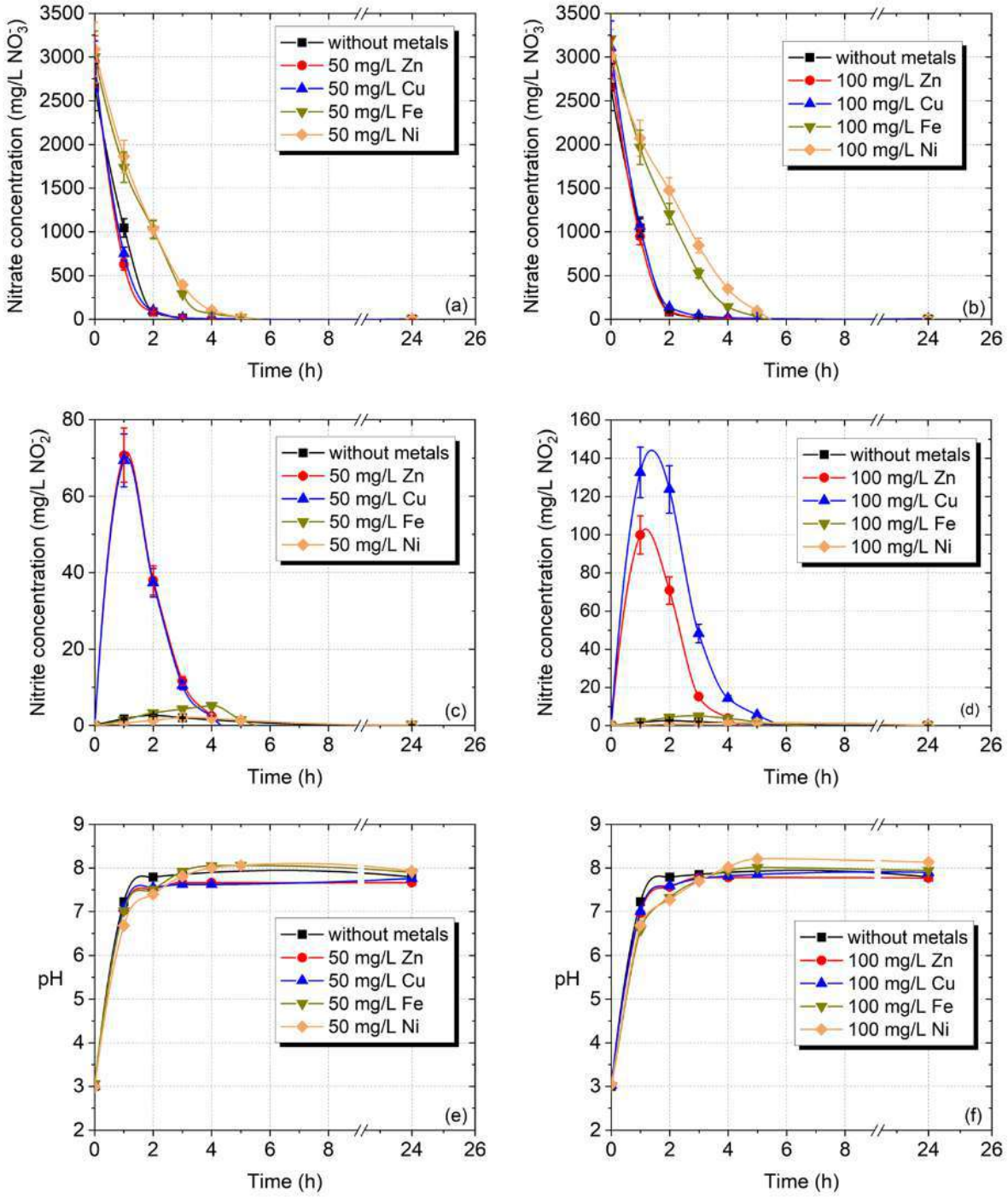

Fig. 5 Effect of Zn, Cu, Fe and Ni on (**a**)-(**b**) nitrate reduction; (**c**)-(**d**) nitrite production; and (**e**)-(**f**) pH

However, regarding their effect on the denitrifying physiology of *H. denitrificans*, the tested metals can be clustered into two groups: (a) zinc and copper; and (b) iron and nickel. Figure 5a-b indicate that, in presence of Zn and Cu, denitrification was completed within 3 h, as in the case without metals addition, while, in presence of Fe and Ni, denitrification was retarded and was completed within 5 h. The effects of these metals are more noticeable on the nitrite concentration profiles (Fig. 5c-d): nitrite concentration was much higher when Zn or Cu was added to the feed solution compared to Fe or Ni; in the latter case, nitrite reduction proceeded as in the case without metals addition. Specifically, for Zn or Cu, peak concentrations of 75 mg/L and 100–150 mg/L NO_2^- were observed (Fig. 5c-d) for 50 mg/L and 100 mg/L metal concentration, respectively. This indicates that Ni and Fe significantly affect the

microbial activity by decelerating nitrate reduction and accelerating nitrite reduction. The opposite behavior is observed in case of Zn and Cu where nitrate reduction rates are high but nitrite reduction rates are low.

Copper and iron are expected to positively affect individual steps of the overall process as they are needed in traces for supporting the catalyzing activity of the enzymes leading to the reduction of nitrite (Reaction 2, Cu-containing reductase), nitric oxide (Reaction 3, Fe-containing reductase) and nitrous oxide (Reaction 4, Cu-containing reductase). Thus, it has been shown that copper stimulates both growth and activity of denitrifying bacteria, resulting in the accumulation of nitrogen oxides in copper-deficient cultures (Granger and Ward 2003; Woolfenden et al. 2013). However, at elevated copper concentrations, accumulation of nitrite was observed (Cheng et al. 2019) and the activity of nitrate and nitric oxide reductase was suppressed (Zhao et al. 2020). This effect was reversed and the denitrifying activity recurred rapidly as the bioavailable Cu decreased due to immobilization (Jacinthe and Tedesco 2009). Papirio et al. (2014) also found that copper inhibited the removal of nitrate whereas iron stimulated the activity of denitrifiers increasing the denitrification rate in a fluidized-bed reactor.

Moreover, ZnO nanoparticles, and thus, the released zinc ions inhibited the catalytic activity of key denitrifying enzymes, resulting in negative effects on the reduction of nitrate and N_2O (Zheng et al. 2014). Nickel was also found to inhibit the last two steps of denitrification (Zou et al. 2014) or cause accumulation of intermediates (Ramírez et al. 2018). Nevertheless, nickel did not inhibit denitrification at pH 7 when its initial concentration did not exceed 50 mg/L but denitrification was repressed at soluble Ni levels between 50 mg/L and 100 mg/L; at 100 mg/L, nitrate removal only reached 30% after 6 h (Zou et al. 2013).

3.5 The Fate of Zn, cu, Fe and Ni during Denitrification

The concentration profiles of soluble Zn, Cu, Fe and Ni during denitrification at 50 mg/L and 100 mg/L initial concentrations are presented in Figs. 6a-d, respectively. Soluble metals fed in the reactor either separately (Figs. 6a-d) or concurrently (Figs. SM2 and SM3) were sequestered from solution within 6 h except nickel which exhibited an S-shaped kinetic profile (Figs. 6d and SM3d). The eventual sequestering of all metals explains the resistance of denitrifiers to initial heavy metal concentrations as high as 100 mg/L.

As it has already been shown (Figs. 2c, 3e-f, 4c, 5e-f), the solution pH always shifted to 7.5–8.0 within 2 h due to the complete reduction of the negatively charged nitrate/nitrite ions to neutral elemental nitrogen. Under these conditions, the excess of hydroxyl ions can react with the soluble metal species and form the corresponding metal hydroxide precipitates (Figs. SM4a and SM4b). The formation of metal carbonates, utilizing the bicarbonate ions (HCO_3^-) which are generated as a result of the oxidation of the carbon source, is also possible. In addition, when biological sulfate reduction is favored, the formation of metal sulfides can occur (Figs. SM2c and SM4c) and dominates the bioprecipitation mechanism due to the lower solubility of sulfides compared to metal hydroxides and carbonates (Lewis 2010). All these precipitation mechanisms have been reported for Ni in denitrifying fluidized-bed bioreactors in earlier studies (Zou et al. 2015; Zou et al. 2014).

To explain the sequestering pattern of Ni, a set of abiotic experiments were carried out (section SM.3) to elucidate the role of organic moieties in forming stable complexes with nickel ions. The results (Fig. SM5) revealed that, when the organic content of nickel solutions is high, nickel remains soluble and does not form insoluble nickel hydroxides when pH ranges

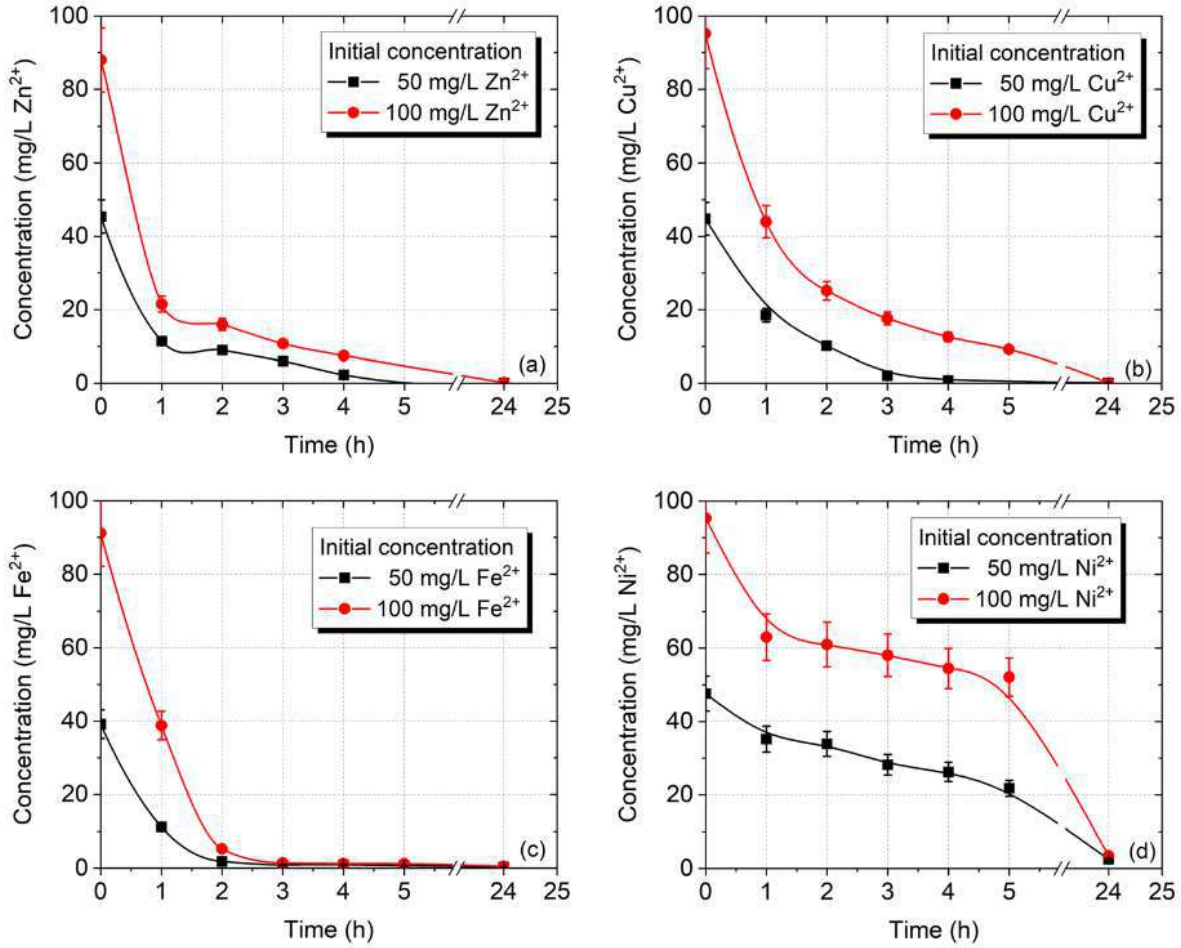

Fig. 6 Concentration profiles of Zn, Cu, Fe and Ni during denitrification

from 3 to 8 due to the formation of metal-organic complexes. Similar behavior regarding the solubility of metal ions in presence of organic matter has also been observed for chromium (Remoundaki et al. 2003; Remoundaki et al. 2007). Therefore, the S-shaped kinetic profile of nickel and the slow sequestering during the first 5 h is attributed to the soluble complexes formed with the organic content of the medium. Thus, Ni^{2+} bioavailability and toxicity decreased (Ramírez et al. 2018), improving the tolerance of *H. denitrificans* to higher initial Ni content. Moreover, as the degradation of the organic substrate proceeds, these complexes are dissociated permitting the formation of insoluble nickel species.

4 Conclusions

This work presents an effective biological process for the simultaneous removal of metals and nitrate from acidic, highly saline wastewater. The process is robust and capable of treating metal-bearing wastewater at pH values as low as 3, nitrate at concentrations as high as 5750 mg/L NO_3^- and tolerate salinity as high as 10% as NaCl. The experimental results demonstrated that the reactor may operate over a wide range of values of the above parameters, maintaining a high efficiency. It is anticipated that even more extreme conditions in terms of lower pH, higher NO_3^- and higher metal content could be tackled successfully which is the aim of the ongoing research activity. This work demonstrates that the proposed pilot-scale biological system achieved, in one stage, to neutralize the treated solution, completely remove

nitrate without residual forms of reduced nitrogen and precipitate the metal content of the solution (i.e., Zn, Cu, Fe and Ni each at 100 mg/L) via bioprecipitation. As a result, the proposed process could be applied as a main treatment or polishing scheme for any relevant wastewater which needs to be treated for safe discharge.

Supplementary Information The online version contains supplementary material available at https://doi.org/10.1007/s40710-021-00536-w.

Availability of Data and Material (Data Transparency) All data will be available by the authors upon request.

Code Availability Not applicable.

Authors' Contributions Artin Hatzikioseyian, Pavlina Kousi and Emmanouella Remoundaki contributed to the study conception and design. Material preparation, data collection and analysis were performed by Panagiota Mendrinou, Paschalis Oustadakis and Petros Tsakiridis. All authors contributed equally to the interpretation of the results and provided critical feedback. The first draft of the manuscript was written by Panagiota Mendrinou and revised by all authors who read and approved the final manuscript.

Funding This research has been co-financed by the European Regional Development Fund of the European Union and Greek national funds through the Operational Program Competitiveness, Entrepreneurship and Innovation, under the call RESEARCH – CREATE – INNOVATE (project code: T1EDK-00219).

Declarations

Ethics Approval Not applicable.

Consent to Participate Not applicable.

Consent for Publication (Include Appropriate Statements) Not applicable.

Conflicts of Interest/Competing Interests The authors declare no conflict of interest.

References

Baeseman JL, Smith RL, Silverstein J (2006) Denitrification potential in stream sediments impacted by acid mine drainage: effects of pH, various electron donors and iron. Microb Ecol 51(2):232–241. https://doi.org/10.1007/s00248-005-5155-z

Cheng YF, Zhang Q, Li GF, Xue Y, Zheng XP, Cai S, Zhang ZZ, Jin RC (2019) Long-term effects of copper nanoparticles on granule-based denitrification systems: performance, microbial communities, functional genes and sludge properties. Bioresour Technol 289:121707. https://doi.org/10.1016/j.biortech.2019.121707

Constantin H, Fick M (1997) Influence of C-sources on the denitrification rate of a high-nitrate concentrated industrial wastewater. Water Res 31(3):583–589. https://doi.org/10.1016/S0043-1354(96)00268-0

Felgate H, Giannopoulos G, Sullivan MJ, Gates AJ, Clarke TA, Baggs E, Rowley G, Richardson DJ (2012) The impact of copper, nitrate and carbon status on the emission of nitrous oxide by two species of bacteria with biochemically distinct denitrification pathways. Environ Microbiol 14(7):1788–1800. https://doi.org/10.1111/j.1462-2920.2012.02789.x

Fernández-Nava Y, Marañón E, Soons J, Castrillón L (2008) Denitrification of wastewater containing high nitrate and calcium concentrations. Bioresour Technol 99(17):7976–7981. https://doi.org/10.1016/j.biortech.2008.03.048

Flemming H-C (1995) Sorption sites in biofilms. Water Sci Technol 32(8):27–33. https://doi.org/10.2166/wst.1995.0256

Forti V, Baldé CP, Kuehr R, Bel G (2020) The global e-waste monitor 2020: quantities, flows and the circular economy potential. United Nations University (UNU)/United Nations Institute for training and research (UNITAR) – co-hosted SCYCLE Programme, international telecommunication union (ITU) & international solid waste association (ISWA), Bonn/Geneva/Rotterdam

Gabaldón C, Izquierdo M, Martínez-Soria V, Marzal P, Penya-roja J-M, Javier Alvarez-Hornos F (2007) Biological nitrate removal from wastewater of a metal-finishing industry. J Hazard Mater 148(1):485–490. https://doi.org/10.1016/j.jhazmat.2007.02.071

Gadd GM (2002) Microbial interactions with metals/radionuclides: the basis of bioremediation. In: Keith-Roach MJ, Livens FR (eds) Interactions of microorganisms with radionuclides. Radioactivity in the environment, vol 2. Elsevier, Amsterdam, pp 179–203

González-Domenech CM, Martínez-Checa F, Béjar V, Quesada E (2010) Denitrification as an important taxonomic marker within the genus *Halomonas*. Syst Appl Microbiol 33(2):85–93. https://doi.org/10.1016/j.syapm.2009.12.001

Granger J, Ward BB (2003) Accumulation of nitrogen oxides in copper-limited cultures of denitrifying bacteria. Limnol Oceanogr 48(1):313–318. https://doi.org/10.4319/lo.2003.48.1.0313

Hirata A, Nakamura Y, Tsuneda S (2001) Biological nitrogen removal from industrial wastewater discharged from metal recovery processes. Water Sci Technol 44(2–3):171–179. https://doi.org/10.2166/wst.2001.0767

Holmes DE, Dang Y, Smith JA (2019) Nitrogen cycling during wastewater treatment. Adv Appl Microbiol 106:113–192. https://doi.org/10.1016/bs.aambs.2018.10.003

Işıldar A (2018) 10 - biotechnologies for metal recovery from electronic waste and printed circuit boards. In: Vegliò F, Birloaga I (eds) Waste Electrical and Electronic Equipment Recycling. Woodhead Publishing, pp. 241–269. https://doi.org/10.1016/B978-0-08-102057-9.00010-X

Jacinthe PA, Tedesco LP (2009) Impact of elevated copper on the rate and gaseous products of denitrification in freshwater sediments. J Environ Qual 38(3):1183–1192. https://doi.org/10.2134/jeq2007.0666

Kim KK, Jin L, Yang HC, Lee S-T (2007) *Halomonas gomseomensis* sp. nov., *Halomonas janggokensis* sp. nov., *Halomonas salaria* sp. nov. and *Halomonas denitrificans* sp. nov., moderately halophilic bacteria isolated from saline water. Int J Syst Evol Microbiol 57(4):675–681. https://doi.org/10.1099/ijs.0.64767-0

Koren DW, Gould WD, Bédard P (2000) Biological removal of ammonia and nitrate from simulated mine and mill effluents. Hydrometallurgy 56(2):127–144. https://doi.org/10.1016/S0304-386X(99)00088-2

Kousi P, Remoundaki E, Hatzikioseyian A, Battaglia-Brunet F, Joulian C, Kousteni V, Tsezos M (2011) Metal precipitation in an ethanol-fed, fixed-bed sulphate-reducing bioreactor. J Hazard Mater 189(3):677–684. https://doi.org/10.1016/j.jhazmat.2011.01.083

Kousi P, Remoundaki E, Hatzikioseyian A, Tsezos M (2007) A study of the operating parameters of a sulphate-reducing fixed-bed reactor for the treatment of metal-bearing wastewater. Adv Mater Res 20-21:230–234. https://doi.org/10.4028/www.scientific.net/AMR.20-21.230

Lewis AE (2010) Review of metal sulphide precipitation. Hydrometallurgy 104(2):222–234. https://doi.org/10.1016/j.hydromet.2010.06.010

Lin Y-M, Tay J-H, Liu Y, Hung Y-T (2009) Biological nitrification and denitrification processes. In: Wang LK, Pereira NC, Hung Y-T (eds) Handbook of environmental engineering, Vol. 8: Biological treatment processes. Humana Press, Totowa, pp 539–588. https://doi.org/10.1007/978-1-60327-156-1_13

Magalhães C, Costa J, Teixeira C, Bordalo AA (2007) Impact of trace metals on denitrification in estuarine sediments of the Douro River estuary, Portugal. Mar Chem 107(3):332–341. https://doi.org/10.1016/j.marchem.2007.02.005

Matějů V, Čižinská S, Krejčí J, Janoch T (1992) Biological water denitrification-a review. Enzym Microb Technol 14(3):170–183. https://doi.org/10.1016/0141-0229(92)90062-S

Mattila K, Zaitsev G, Langwaldt J (2007) Biological removal of nutrients from mine waters (final report). Finnish Forest Research Institute - Rovaniemi Unit, Rovaniemi

Miao Y, Liao R, Zhang X-X, Liu B, Li Y, Wu B, Li A (2015) Metagenomic insights into salinity effect on diversity and abundance of denitrifying bacteria and genes in an expanded granular sludge bed reactor treating high-nitrate wastewater. Chem Eng J 277:116–123. https://doi.org/10.1016/j.cej.2015.04.125

Ochoa-Herrera V, León G, Banihani Q, Field JA, Sierra-Alvarez R (2011) Toxicity of copper(II) ions to microorganisms in biological wastewater treatment systems. Sci Total Environ 412-413:380–385. https://doi.org/10.1016/j.scitotenv.2011.09.072

Pang Y, Wang J (2021) Various electron donors for biological nitrate removal: a review. Sci Total Environ 794:148699. https://doi.org/10.1016/j.scitotenv.2021.148699

Papirio S, Ylinen A, Zou G, Peltola M, Esposito G, Puhakka JA (2014) Fluidized-bed denitrification for mine waters. Part I: low pH and temperature operation. Biodegradation 25(3):425–435. https://doi.org/10.1007/s10532-013-9671-0

Peyton BM, Mormile MR, Petersen JN (2001) Nitrate reduction with *Halomonas campisalis*: kinetics of denitrification at pH 9 and 12.5% NaCl. Water Res 35(17):4237–4242. https://doi.org/10.1016/S0043-1354(01)00149-X

Ramírez JE, Rangel-Mendez JR, Limberger Lopes C, Gomes SD, Buitrón G, Cervantes FJ (2018) Denitrification of metallurgic wastewater: mechanisms of inhibition by Fe, Cr and Ni. J Chem Technol Biotechnol 93(2): 440–449. https://doi.org/10.1002/jctb.5374

Remoudaki E, Hatzikioseyian A, Kousi P, Tsezos M (2003) The mechanism of metals precipitation by biologically generated alkalinity in biofilm reactors. Water Res 37(16):3843–3854. https://doi.org/10.1016/S0043-1354(03)00306-3

Remoundaki E, Hatzikioseyian A, Kaltsa F, Tsezos M (2003) The role of metal-organic complexes in the treatment of chromium containing effluents in biological reactors. In: Tsezos M, Remoudaki E, Hatzikioseyian A (eds) Biohydrometallurgy: A Sustainable Technology in Evolution, Proceedings of the International Biohydrometallurgy Symposium IBS 2003. National Technical University of Athens (NTUA), Athens, pp 711–718

Remoundaki E, Hatzikioseyian A, Tsezos M (2007) A systematic study of chromium solubility in the presence of organic matter: consequences for the treatment of chromium-containing wastewater. J Chem Technol Biotechnol 82(9):802–808. https://doi.org/10.1002/jctb.1742

Sakadevan K, Zheng H, Bavor HJ (1999) Impact of heavy metals on denitrification in surface wetland sediments receiving wastewater. Water Sci Technol 40(3):349–355. https://doi.org/10.1016/S0273-1223(99)00471-0

Sun Z, Lv Y, Liu Y, Ren R (2016) Removal of nitrogen by heterotrophic nitrification-aerobic denitrification of a novel metal resistant bacterium *Cupriavidus* sp. S1. Bioresour Technol 220:142–150. https://doi.org/10.1016/j.biortech.2016.07.110

Tavares P, Pereira AS, Moura JJG, Moura I (2006) Metalloenzymes of the denitrification pathway. J Inorg Biochem 100(12):2087–2100. https://doi.org/10.1016/j.jinorgbio.2006.09.003

Teitzel GM, Parsek MR (2003) Heavy metal resistance of biofilm and planktonic *Pseudomonas aeruginosa*. Appl Environ Microbiol 69(4):2313–2320. https://doi.org/10.1128/AEM.69.4.2313-2320.2003

Tsezos M, Remoundaki E, Hatzikioseyian A (2007) Bioprocessing - principles and applications for metal immobilization from waste-water streams. In: Cox M, Negre P, Yurramendi L (eds) A guide book on the treatment of effluents from the mining/metallurgy, paper. Plating and Textile Industries. INASMET-Tecnalia, Spain, pp 233–246

Tuncuk A, Stazi V, Akcil A, Yazici EY, Deveci H (2012) Aqueous metal recovery techniques from e-scrap: hydrometallurgy in recycling. Miner Eng 25(1):28–37. https://doi.org/10.1016/j.mineng.2011.09.019

Tunsu C, Retegan T (2016) Chapter 6 - hydrometallurgical processes for the recovery of metals from WEEE. In: Cote G, Ekberg C, Nilsson M, Retegan T (eds) Chagnes A. Elsevier, WEEE Recycling, pp 139–175. https://doi.org/10.1016/B978-0-12-803363-0.00006-7

Ugurlu A, Ozturkcu SD (2018) Treatment of nitrocellulose industry watewaters by upflow denitrification filter: effect of packing media and recirculation. Environmental Processes 5(1):81–94. https://doi.org/10.1007/s40710-017-0282-3

van Hullebusch E, Zandvoort M, Lens P (2003) Metal immobilisation by biofilms: mechanisms and analytical tools. Rev Environ Sci Biotechnol 2(1):9–33. https://doi.org/10.1023/B:RESB.0000022995.48330.55

Vredenbregt LHJ, Nielsen K, Potma AA, Kristensen GH, Sund C (1997) Fluid bed biological nitrification and denitrification in high salinity wastewater. Water Sci Technol 36(1):93–100. https://doi.org/10.1016/S0273-1223(97)00341-7

Wang L, Shao Z (2021) Aerobic denitrification and heterotrophic sulfur oxidation in the genus *Halomonas* revealed by six novel species characterizations and genome-based analysis. Front Microbiol 12:652766. https://doi.org/10.3389/fmicb.2021.652766

Wang T, Zhang L, Bo L, Zhu Y, Tang X, Liu W (2019) Simultaneous heterotrophic nitrification and aerobic denitrification at high concentrations of NaCl by *Halomonas* bacteria. IOP Conference Series: Earth and Environmental Science 237:052033. https://doi.org/10.1088/1755-1315/237/5/052033

Ward MH, Jones RR, Brender JD, de Kok TM, Weyer PJ, Nolan BT, Villanueva CM, van Breda SG (2018) Drinking water nitrate and human health: an updated review. Int J Env Res Public Health 15(7):1557. https://doi.org/10.3390/ijerph15071557

Woolfenden HC, Gates AJ, Bocking C, Blyth MG, Richardson DJ, Moulton V (2013) Modeling the effect of copper availability on bacterial denitrification. MicrobiologyOpen 2(5):756–765. https://doi.org/10.1002/mbo3.111

Yang PY, Nitisoravut S, Wu JS (1995) Nitrate removal using a mixed-culture entrapped microbial cell immobilization process under high salt conditions. Water Res 29(6):1525–1532. https://doi.org/10.1016/0043-1354(94)00296-J

Yoshie S, Noda N, Miyano T, Tsuneda S, Hirata A, Inamori Y (2002) Characterization of microbial community in nitrogen removal process of metallurgic wastewater by PCR-DGGE. Water Sci Technol 46(11–12):93–98. https://doi.org/10.2166/wst.2002.0722

Yoshie S, Noda N, Tsuneda S, Hirata A, Inamori Y (2004) Salinity decreases nitrite reductase gene diversity in denitrifying bacteria of wastewater treatment systems. Appl Environ Microbiol 70(5):3152–3157. https://doi.org/10.1128/AEM.70.5.3152-3157.2004

You Q-G, Wang J-H, Qi G-X, Zhou Y-M, Guo Z-W, Shen Y, Gao X (2020) Anammox and partial denitrification coupling: a review. RSC Adv 10(21):12554–12572. https://doi.org/10.1039/D0RA00001A

Zhang N, Chen H, Lyu Y, Wang Y (2019) Nitrogen removal by a metal-resistant bacterium, *pseudomonas putida* ZN1, capable of heterotrophic nitrification-aerobic denitrification. J Chem Technol Biotechnol 94(4):1165–1175. https://doi.org/10.1002/jctb.5863

Zhao S, Su X, Wang Y, Yang X, Bi M, He Q, Chen Y (2020) Copper oxide nanoparticles inhibited denitrifying enzymes and electron transport system activities to influence soil denitrification and N_2O emission. Chemosphere 245:125394. https://doi.org/10.1016/j.chemosphere.2019.125394

Zheng X, Su Y, Chen Y, Wan R, Liu K, Li M, Yin D (2014) Zinc oxide nanoparticles cause inhibition of microbial denitrification by affecting transcriptional regulation and enzyme activity. Environ Sci Technol 48(23):13800–13807. https://doi.org/10.1021/es504251v

Zhu IX, Liu JR (2017) Effects of salinity on biological nitrate removal from industrial wastewater. In: Zhu IX (ed) Nitrification and Denitrification IntechOpen https://doi.org/10.5772/intechopen.69438

Zou G, Papirio S, van Hullebusch ED, Puhakka JA (2015) Fluidized-bed denitrification of mining water tolerates high nickel concentrations. Bioresour Technol 179:284–290. https://doi.org/10.1016/j.biortech.2014.12.044

Zou G, Papirio S, Ylinen A, Di Capua F, Lakaniemi AM, Puhakka JA (2014) Fluidized-bed denitrification for mine waters. Part II: effects of Ni and co. Biodegradation 25(3):417–423. https://doi.org/10.1007/s10532-013-9670-1

Zou G, Ylinen A, Di Capua F, Papirio S, Lakaniemi AM, Puhakka J (2013) Impact of heavy metals on denitrification of simulated mining wastewaters. Adv Mater Res 825:500–503. https://doi.org/10.4028/www.scientific.net/amr.825.500

Affiliations

Panagiota Mendrinou [1] · Artin Hatzikioseyian [1] · Pavlina Kousi [1] · Paschalis Oustadakis [1] · Petros Tsakiridis [1] · Emmanouella Remoundaki [1]

Panagiota Mendrinou
giouli@metal.ntua.gr

Pavlina Kousi
pkousi@metal.ntua.gr

Paschalis Oustadakis
oustadak@metal.ntua.gr

Petros Tsakiridis
ptsakiri@central.ntua.gr

Emmanouella Remoundaki
remound@metal.ntua.gr

[1] School of Mining and Metallurgical Engineering, National Technical University of Athens (NTUA), Heroon Polytechniou 9, 15780 Zografou, Greece

Journal of Environmental Management 344 (2023) 118334

Contents lists available at ScienceDirect

Journal of Environmental Management

journal homepage: www.elsevier.com/locate/jenvman

Research article

Hydrometallurgical recovery of silver and gold from waste printed circuit boards and treatment of the wastewater in a biofilm reactor: An integrated pilot application

Dimitrios Vlasopoulos [a], Panagiota Mendrinou [a], Paschalis Oustadakis [a], Pavlina Kousi [a], Athanasios Stergiou [b], Spyridon-Dionysios Karamoutsos [b], Artin Hatzikioseyian [a], Petros E. Tsakiridis [a], Emmanouella Remoundaki [a,*], Styliani Agatzini-Leonardou [a]

[a] School of Mining and Metallurgical Engineering, National Technical University of Athens (NTUA), Heroon Polytechniou 9, 15780, Zografou, Greece
[b] Ecoreset S.A., Thessi Agios Georgios, 193 00, Aspropyrgos, Greece

ARTICLE INFO

Keywords:
Printed circuit boards
Silver
Gold
Hydrometallurgy
Denitrification

ABSTRACT

A hydrometallurgical process for the recovery of gold and silver from waste printed circuit boards (PCBs) was experimentally verified and tested at pilot scale. The process comprises four sequential leaching stages; the first two based on HCl, correspond to base metals (e.g. Sn, Cu) removal, while the third is based on HNO_3 for Ag leaching and the final on aqua regia for Au leaching. After base metals leaching, the solid residue, enriched in silver and gold about 5 times, contained silver almost quantitively as insoluble AgCl and significant losses (Ag loss <8%) were avoided. The necessary reduction of Ag in the solid phase was achieved with a solution of 0.5 M N_2H_4 and 3 M NaOH, at 80 °C and S/L ratio 10%. Leaching of silver by 4 M HNO_3 was followed by its recovery from nitrate solution by 0.08 M N_2H_4 at ambient temperature with an efficiency of 83%. Gold was leached by aqua regia and quantitively recovered by 0.13 M N_2H_4 at ambient temperature. Wastewater resulting from the process, rich in nitrate (5 g/L) and chloride (50 g/L), was treated by an effective and novel biological denitrification system tolerating metals at ppm level, to comply with zero nitrate and residual metals discharge guidelines. The overall process requires low reagents and energy input and has zero discharge for liquid effluents. The scheme is appropriate to be applied at local small to medium industrial units, complying with decentralized circular economy principles for metal recovery from electronic waste.

1. Introduction

Waste Electrical and Electronic Equipment (WEEE) ranks among the fastest growing waste streams in the world. The global generation of e-waste grew to 53.6 Mt in 2019 with the perspective to reach 74.7 Mt by 2030 (Forti et al., 2020). Among e-waste, printed circuit boards (PCBs) comprise 30–40% base and precious metals as well as rare earths. Their metal content is typically ten to hundred times higher than primary ores (Rao et al., 2020), making metal recovery from PCBs a worldwide priority for circular economy. More specifically, silver content in PCBs ranges from 0.080% to 0.130% (w/w) and gold content from 0.014% to 0.035% (w/w) while base metal content varies from 2.00% to 3.30% and 9.70%–47.50% (w/w) for tin and copper, respectively (Mishra et al., 2021).

Selective metal recovery from PCBs is a problem with complex solutions as they contain up to 60 different elements (Lu and Xu, 2016). PCBs treatment involves size reduction (dismantling, shredding, grinding) and magnetic separation (Rocchetti et al., 2018); followed by metals recovery via pyrometallurgical, hydrometallurgical, electrometallurgical or biohydrometallurgical processes (Birloaga and Vegliò, 2018a, 2018b; Hubau and Bryan, 2023; Kaya, 2016). Hydrometallurgical processing (Birloaga and Vegliò, 2016, 2022) can be established in local WEEE recycling industries permitting the decentralized "green" production of pure metals (Tuncuk et al., 2012; Tunsu and Retegan, 2016) compared to pyrometallurgy which is by far more energy intensive requiring expensive and complicated facilities (Copani et al., 2019). Hydrometallurgy involves essentially two steps: (a) leaching of metals; and (b) separation/selective extraction of the metals of interest from the pregnant leaching solution (PLS). As far as the hydrometallurgical recovery of silver and gold from PCBs is concerned, main challenges

* Corresponding author.
E-mail addresses: astergiou@ecoreset.gr (A. Stergiou), sdkaramoutsos@ecoreset.gr (S.-D. Karamoutsos), remound@metal.ntua.gr (E. Remoundaki).

https://doi.org/10.1016/j.jenvman.2023.118334
Received 31 January 2023; Received in revised form 1 June 2023; Accepted 4 June 2023

addressed are: (i) the efficient removal of base metals in upstream stages (Wu et al., 2022) leaving silver and gold quantitatively in the solid residue; (ii) the enrichment of both in this solid residue from which they may be extracted; (iii) their selective separation and recovery. In this context, the scope of this work was to selectively recover silver and gold from PCBs following a hydrometallurgical scheme also involving the recovery of base metals such as tin and copper. The scheme was designed with minimum number of reagents (i.e., hydrochloric acid, nitric acid, hydrazine hydrate) rendering successful the downstream wastewater treatment in a novel denitrifying biological system (Mendrinou et al., 2021).

Gold extraction from primary ores has been dominated by cyanide (Medina and Anderson, 2020) which has been successfully applied to Au extraction from PCBs (Akcil et al., 2015; Rao et al., 2020). However, due to the toxicity of cyanide, research has focused on other lixiviants, such as halogens, thiosulphate and thiourea, for precious metal leaching (Au, Ag and Pt) from PCBs (Mir and Dhawan, 2022). Among them, aqua regia (a 3:1 hydrochloric/nitric acid mixture) is greatly efficient forming $AuCl_4^-$ and is preferred due to high dissolution rate, easy operation, flexibility and low capital requirements (Huy Do et al., 2023). Metallic gold may then be formed by chemical reduction. Among the reagents used for Au recovery from aqueous tetrachloroaurate (III) $(AuCl_4^-)$ solutions, i.e., sodium metabisulfite/urea (Barnwal and Dhawan, 2020) or iron sulfate (Dehchenari et al., 2017), hydrazine (N_2H_4) is a simple and powerful reducing agent (Cotton and Wilkinson, 1998). Hydrazine hazardous effects are mitigated using hydrazine hydrate instead of hydrazine and by its use at concentrations lower than 5% (w/w) (about 1.5 M) (IARC, 2018; Niemeier and Kjell, 2013). Moreover, when used as reducing agent, hydrazine is oxidized to N_2 and NH_3 or just N_2 depending on the electrons transferred in the redox system (Audrieth and Mohr, 1948). Ammonia is easily removed from solution by air stripping whereas unutilized hydrazine can also be removed by aeration as it is oxidized into nitrogen gas (Chen and Lim, 2002). Hence, lacking dangerous byproducts, hydrazine may be considered as an environmentally friendly reducing agent.

To avoid an additional silver/gold separation process due to partial dissolution of silver in aqua regia (Park and Fray, 2009), metallic Ag can be selectively leached by nitric acid before gold leaching (Birloaga and Veglio, 2018b; Sadrnezhaad et al., 2006). Soluble silver can then be recovered as pure metallic Ag upon reduction by hydrazine (Cheng et al., 2000) or as AgCl by adding Cl^- (Theocharis et al., 2022). In the present work, AgCl was formed during leaching by HCl and HCl–H_2O_2 for tin and copper recovery, respectively. Thus, Ag was maintained in the solid residue avoiding significant losses due to Ag dissolution during base metal leaching. Consequently, silver had to be reduced from the solid AgCl and converted into metallic Ag prior to leaching by HNO_3. This reduction can also be achieved by hydrazine (Gautam et al., 2022; Marinato et al., 2023).

This work presents experimental data for the definition of the values of main parameters such as solid/liquid ratio, lixiviant and other reagents concentration and temperature. Once the sets of parameters were selected, they were used in a pilot application. The results of the pilot application demonstrated the efficiency of a process based on (a) base metal (i.e., Cu, Sn) removal/recovery by HCl; (b) reduction of AgCl by N_2H_2; (c) leaching of Ag by HNO_3 and recovery by reduction or precipitation; (d) leaching of Au by aqua regia; (e) recovery of Au by N_2H_2. The proposed process involves only two leaching agents, i.e., HCl and HNO_3, and two pretreatment stages for base metal recovery while N_2H_2 is used as a reducing agent for both Au and Ag.

The effluents are rich in NO_3^-, Cl^- and contain residual metal ions. Neutralization of these streams removes part of the soluble metal species by precipitation without altering the content of nitrate and chloride. However, the removal of nitrate and residual metals from wastewater is a priority and in the present work, was addressed via a microbially-mediated process. Heterotrophic denitrification has been demonstrated feasible and efficient for the treatment of wastewater which is characterized by elevated nitrate and chloride concentrations and presence of soluble metal species such as Fe, Ni, Cu, and Zn (Mendrinou et al., 2021). Thus, the results obtained from the downstream treatment of the wastewater by a packed-bed biofilm reactor are also presented in this work.

2. Materials and methods

2.1. Sample characterization and pretreatment

The waste PCB samples originated from the material retained by filter bags during PCB shredding in a local WEEE recycling facility (Ecoreset, Greece). The metallic fraction of the material was obtained after treatment in a shaking table and characterized in terms of granulometry. The chemical composition of all solid samples (selected fraction of raw dust and intermediate/final solid residues) was determined after eutectic fusion at 1000 °C and dissolution in HCl. The metal content of all leachates and effluents was determined by flame Atomic Absorption Spectrometry (AAS). Scanning Electron Microscopy (SEM) elucidated the characteristics of the solids. All experiments were conducted in triplicate and results are expressed as mean values.

The samples were pretreated (i) with HCl and (ii) with HCl–H_2O_2 to leach tin and copper respectively and remove most of the other co-existing metals such as Fe, Ni, Zn. Consequently, the mass of the samples was significantly reduced, and the produced solid residue was treated for Ag and Au extraction. As it will be presented in Section 3, this residue was significantly enriched in Ag and Au.

2.2. Determination of parameters for silver extraction and recovery

Laboratory-scale experimental investigation of parameters was conducted before the pilot application. Silver in PCBs appears mostly as metallic Ag which, in reaction with hydrochloric acid and an oxidant such as hydrogen peroxide, turns into chloride salt (Reaction (1)). Silver chloride is a white crystalline solid, with low solubility in water and acids, which remains in the solid residue after the two pretreatment stages and cannot be further dissolved or separated from gold. Silver in AgCl may be reduced upon direct contact of the solid material with an alkaline hydrazine solution (James, 1940). Hydrazine is a strong reducing agent forming metallic Ag (Reaction (2)) which, then, may be extracted via leaching with HNO_3.

$$2Ag + 2HCl + H_2O_2 \rightarrow 2AgCl + 2H_2O \quad (1)$$

$$4AgCl + N_2H_4 + 4NaOH \rightarrow 4Ag + N_2 + 4NaCl + 4H_2O \quad (2)$$

The parameters, which were chosen to be studied to determine their possible effect on silver reduction occurring directly on the solid AgCl, were: hydrazine concentration (0.05–2 M), NaOH concentration (0.5–3 M), contact time (30–160 min for 0.5 M/2 M N_2H_4) and temperature (25–80 °C). Following the reduction of silver, 4 M HNO_3 was used as leaching agent (S/L ratio: 0.1 g/mL; agitation speed: 300 rpm; contact time: 2 h; 1 M H_2O_2 was added to enhance oxidizing conditions). The reduction efficiency is represented by the leaching efficiency, assuming that metallic Ag was leached quantitatively by HNO_3 (Theocharis et al., 2022).

Soluble silver in the pregnant nitrate solution was then recovered as metallic Ag upon reduction using hydrazine hydrate (0.08 M; 0.5 h; 25 °C; 300 rpm - Reactions (3) and (4) (Cheng et al., 2000)). These conditions represent a hydrazine hydrate concentration 20% over stoichiometry. Alternatively, silver was precipitated as AgCl by 0.05 M NaCl (Reaction (5)).

$$4Ag^+ + N_2H_4 \rightarrow 4Ag + N_2 + 4H^+ \quad (3)$$

$$2Ag^+ + 2N_2H_4 \rightarrow 2Ag + N_2 + 2NH_3 + 2H^+ \quad (4)$$

$$AgNO_3 + NaCl \rightarrow AgCl + NaNO_3 \quad (5)$$

Hydrazine may be efficient as a reducing agent both in alkaline and acidic solutions according to the standard redox potentials (Audrieth and Mohr, 1948) of hydrazine (Reaction (6)) and the hydrazinium ion (Reaction (7)).

$$N_2H_4 + 4OH^- \rightarrow N_2 + 4H_2O + 4e^- \quad E_0 = +1.15V \quad (6)$$

$$N_2H_5^+ \rightarrow N_2 + 5H^+ + 4e^- \quad E_0 = +0.17V \quad (7)$$

All reagents used were of analytical grade. Hydrochloric acid, nitric acid, and hydrazine hydrate were supplied by Merck and the solutions used in the experimental part were prepared in the desired concentrations via dilution with deionized water.

2.3. Determination of parameters for gold extraction and recovery

After silver extraction, the solid residue was leached with aqua regia ($HCl–HNO_3$: 3:1) (Reactions (8) and (9)). The leaching temperature was kept constant at 90 °C (Elomaa et al., 2017; Patel et al., 2017; Sheng and Etsell, 2007) and the contact time was 3 h. Experiments were carried out for S/L ratio ranging from 1% to 10%.

$$2Au + 11HCl + 3HNO_3 \rightarrow 2HAuCl_4 + 3NOCl + 6H_2O \quad (8)$$

$$Au + 4HCl + HNO_3 \rightarrow HAuCl_4 + 2H_2O + NO \quad (9)$$

Gold was then recovered as metallic Au upon reduction using hydrazine hydrate (0.13 M; 0.5 h; 25 °C; 300 rpm - Reactions (10)–(14) (Streszewski et al., 2014; Tatarchuk et al., 2011),). These conditions represent a hydrazine concentration 20% over stoichiometry.

$$Au^{III} \rightarrow Au^{I} \rightarrow Au^0 \quad (10)$$

$$AuCl_4^- + N_2H_4 \leftrightarrow Au(N_2H_4)Cl_3 + Cl^- \quad (11)$$

$$3Au(N_2H_4)Cl_3 \rightarrow 3AuCl_2^- + 3Cl^- + 4H^+ + 2NH_4^+ + 2N_2 \quad (12)$$

$$AuCl_2^- + N_2H_4 \leftrightarrow Au(N_2H_4)Cl + Cl^- \quad (13)$$

$$2Au(N_2H_4)Cl \rightarrow 2Au + 2Cl^- + 2NH_4^+ + N_2 \quad (14)$$

2.4. Pilot-scale application, wastewater characterization and remediation

The parameters corresponding to efficiency maxima were selected for pilot application. The selected sample fraction (sample mass: 1000 g) was treated in 20-L tank reactors (Emak, Turkey). According to the flowsheet depicted in Fig. 1, four reactors operated in batch mode for leaching tin, copper, silver and gold. Each of these cylindrical reactors were shaped with conical bottom and bottom output (diam.: 30 cm; cylinder height: 40 cm; cone height: 10 cm); they were made from polypropylene (for base metal and silver leaching) and titanium (for gold leaching) to operate from 25 °C to 130 °C. They were fitted with an overhead stirrer (200–600 rpm) and lid with inlets for pH electrode, temperature probe and acid/base addition. Heating, pH and agitation were regulated via an integrated controller. The gases produced in the reactors were led from a dedicated lid outlet into fume scrubbers containing appropriate neutralization/reduction filters in order to treat HCl/HNO_3 emissions.

The four distinct effluents (WW1-WW4), which were generated during the relevant leaching stages, were characterized in terms of pH, chloride, nitrate, and residual soluble metal content. A packed-bed denitrifying biofilm reactor was previously set up, inoculated with *Halomonas denitrificans* and operated upflow in fed-batch mode. The treating capacity of the bioreactor was 2.7 L per batch. The bioreactor was fed with Bacto Marine Broth medium (DSMZ medium 514 + 8% NaCl). The denitrifying system was acclimated to a wide variety of initial feed conditions with synthetic solutions: (a) 750–10,000 mg/L nitrate, (b) pH 3–8, (c) salinity 5–10% and (d) metal concentrations (Fe, Cu, Ni, Zn) up to 100 mg/L (Mendrinou et al., 2021).

Samples were collected from the reactor outlet and essential parameters were monitored: pH, nitrate, nitrite, chloride, soluble metals (specifically, copper, nickel, iron, zinc, and lead). pH was determined on

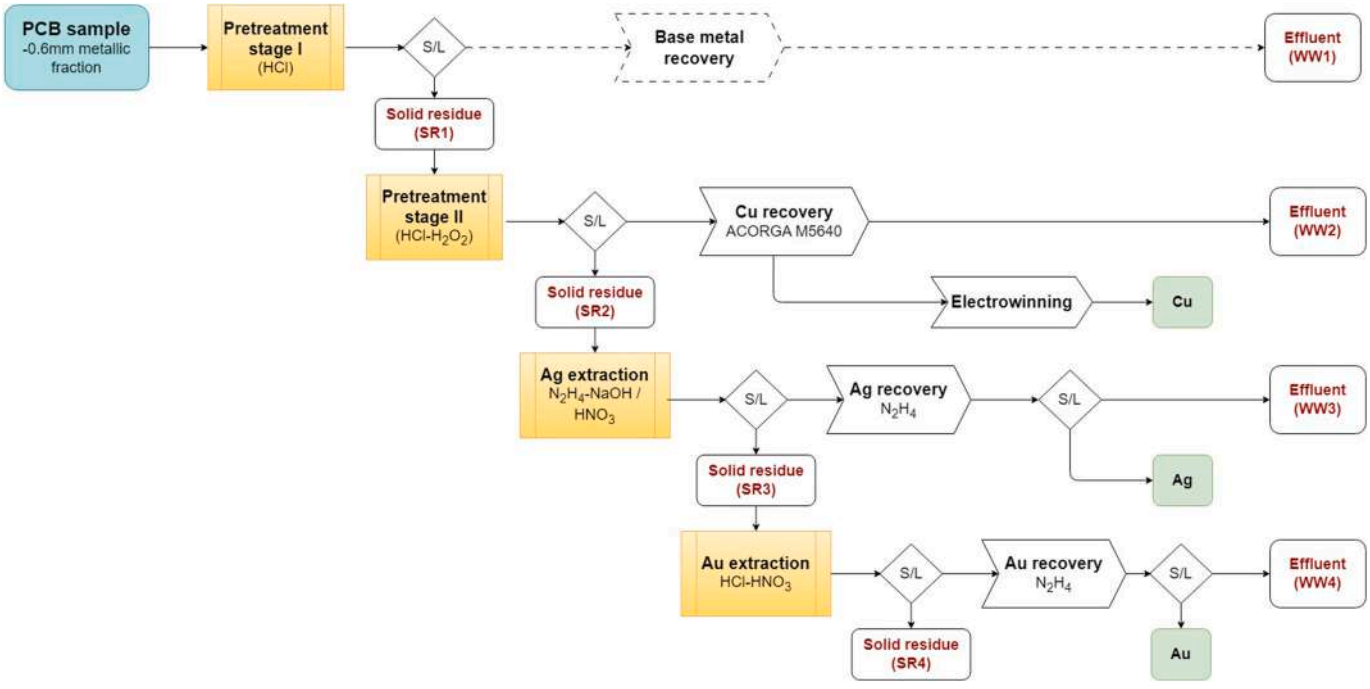

Fig. 1. Hydrometallurgical flowsheet for Ag and Au recovery from waste PCBs.

unfiltered samples while all other parameters were determined on vacuum filtered samples through 0.20 μm sterile membrane filters (Whatman ME 24/21 ST). Nitrate and nitrite were colorimetrically determined by Merck method 1.09713.0001 and 1.14776.0002, respectively. Chloride content was determined by titration with 0.1 M $AgNO_3$ (Mohr's method using 0.25 M K_2CrO_4 as indicator). Soluble copper, nickel, iron, zinc, and lead were determined by flame Atomic Absorption Spectrometry (AAS) after acidification of the samples by adding HNO_3. All experiments were conducted in triplicate and results are expressed as mean values.

3. Results and discussion

3.1. Sample composition and pretreatment

The metallic fraction of the waste PCB sample was characterized in terms of granulometry. According to the results (Table S1 and Figure S1), 78% of the mass corresponded to the −0,6 mm fraction. This fraction was used in all laboratory scale and pilot experiments. Table 1 shows the chemical composition of the selected sample fraction and the resulted solid residues after the first (HCl) and the second (HCl–H_2O_2) pretreatment stage. These data show that more than 90% of the initial base metals (Fe, Zn, and Sn) content was removed after the first pretreatment stage. During the second pretreatment stage, more than 95% of Cu and 90% of Ni were leached. Soluble copper was recovered via solvent extraction with ACORGA M5640 (Vlasopoulos et al., 2021). The second solid residue (Table 1) was further enriched in silver and gold: Ag by 4.2 times and Au by 4.75 times. A loss of silver mass of about 8% occurred during the second leaching step. Gold remained intact in the solid residue. This solid residue, enriched in precious metals, was further treated for silver and gold recovery.

3.2. Determination of parameters for silver extraction and recovery

Fig. 2 shows SEM-EDS results for the enriched solid residue in Ag and Au. Silver in the solid appeared in the presence of chloride, while no metallic silver was detected. The morphology of particles consists of crystalline aggregates of tenths micrometers, agglomerating each other and formed by micro crystals of relatively spherical form, with sizes varying from 1 μm to 10 μm. The great similarity of the values for Ag and Cl indicated that the silver in the silver-bearing residue existed in the form of silver chloride. This is due to the formation of AgCl after leaching by HCl in the two pretreatment stages which were carried out to remove base metals (e.g., Fe, Zn, Ni, Sn, Cu) from the PCB sample. Thus, with low losses (<8%, see section 3.1), silver remained enriched in the solid residue; this would not be possible if other leaching agents were used. For example, in leaching by H_2SO_4 and H_2O_2 (Vlasopoulos et al., 2021), a significant amount of silver co-dissolves along with copper (our unpublished data and (Birloaga et al., 2014; Tuncuk, 2019)). The advantage of selecting HCl ensures that Ag remains, almost quantitatively, in the solid phase until being finally extracted.

Since AgCl cannot be leached by common leaching agents, it must be reduced to metallic form and then leached by HNO_3. Hydrazine hydrate, in alkaline environment, was used as reducing agent for silver reduction. The effects of hydrazine concentration, solution alkalinity in terms of sodium hydroxide concentration, contact time and temperature on Ag reduction were studied.

Fig. 3(a) shows that increasing hydrazine concentration from 0.05 M to 2 M slightly affected the efficiency of Ag reduction reaching a maximum extraction level at 55% while, for both 0.5 M and 2 M N_2H_4, Ag extraction reached maximum levels in 120 min (Fig. 3(c)). However, the reaction rate was faster for 2 M N_2H_4. This finding is supported by literature where it has been reported that higher N_2H_4 concentration accelerates the reaction, provided that NaOH concentration is sufficient (Purna et al., 2010). It is also stated that, for the reduction reaction to proceed, silver particles and chloride ions should be able to leave the surface of the solid material, exposing new AgCl to the reducing agent. Otherwise, electron transfer is interrupted regardless of available hydrazine in solution; this may explain the outcome of our experiments.

Fig. 3(b) shows that an increase of NaOH concentration from 0.5 M to 3 M increased silver reduction from 43% to 50%; thus, the solution alkalinity did not significantly affect the reduction efficiency. Fig. 3(d) shows that the increase of temperature affected the reduction efficiency positively. At room temperature (25 °C), less than 55% of the Ag content was extracted while, at 80 °C, Ag extraction reached 83%. These results led to the choice of the following parameter values for the pilot application: 0.5 M N_2H_4, 3 M NaOH, S/L ratio: 10% and T = 80 °C.

After leaching by 4 M HNO_3, silver was recovered from the pregnant solution either as AgCl via precipitation (Theocharis et al., 2022) or as metallic Ag via reduction with N_2H_4. In both cases, Ag was recovered quantitatively.

3.3. Determination of parameters for gold extraction and recovery

The solid residue after the Ag extraction stage was leached with aqua regia. Fig. 4 shows that, for quantitative extraction of Au, S/L ratio should be less than 0.05 g/mL. Gold is in the form $AuCl_4^-$ and is quantitatively recovered as elemental Au after reduction by N_2H_4. Fig. 5 presents SEM-EDS of the precipitate solid obtained after reduction by H_2N_4. It consisted of pure gold particles which were in the form of aggregates of fine crystallites. The aggregates had an irregular shape and a homogeneous size of about 20 μm (longest dimension). Minor impurities, associated with refractory metals such as W, Nb or Ti, identified through EDS analysis (Figure S2), have been deposited among gold agglomerates, forming smaller aggregates, presenting an irregular morphology with a size of about 20 μm. Particle morphology, shape and size examination under SEM revealed both spherical particles with a size of about 1 μm and rods shape particles with a size in the range of 5 μm. These are, either due to residual phases, containing Ag and Sn, which were not leached during the upstream processes, or constituents containing W, Sb, Nb and Ti, which remained undissolved during the process. As hot aqua regia is not selective, aggressively digested both Au and the other unleached metallic values, which were finally co-deposited with Au.

Dehchenari et al. who proposed grinding, leaching in nitric acid for silver recovery, leaching in aqua regia and precipitation by iron sulfate for gold recovery, achieved 82.3% Au recovery (Dehchenari et al., 2017).

Table 1
Chemical composition of the initial PCB sample and the solid residues originating from the first and second pretreatment stages.

Metal	Metal content (% w/w)		
	−0.6 mm metallic fraction of the PCB sample	Solid residue after 1st pretreatment stage	Solid residue after 2nd pretreatment stage
Au	0.04	0.05	0.19
Ag	0.07	0.08	0.29
Cu	54.01	65.38	8.70
Fe	3.86	1.23	0.17
Zn	1.00	0.33	0.05
Sn	10.20	1.84	1.36
Pb	3.81	1.96	0.20
Ni	0.93	0.94	0.05
Total	73.92	71.81	11.01

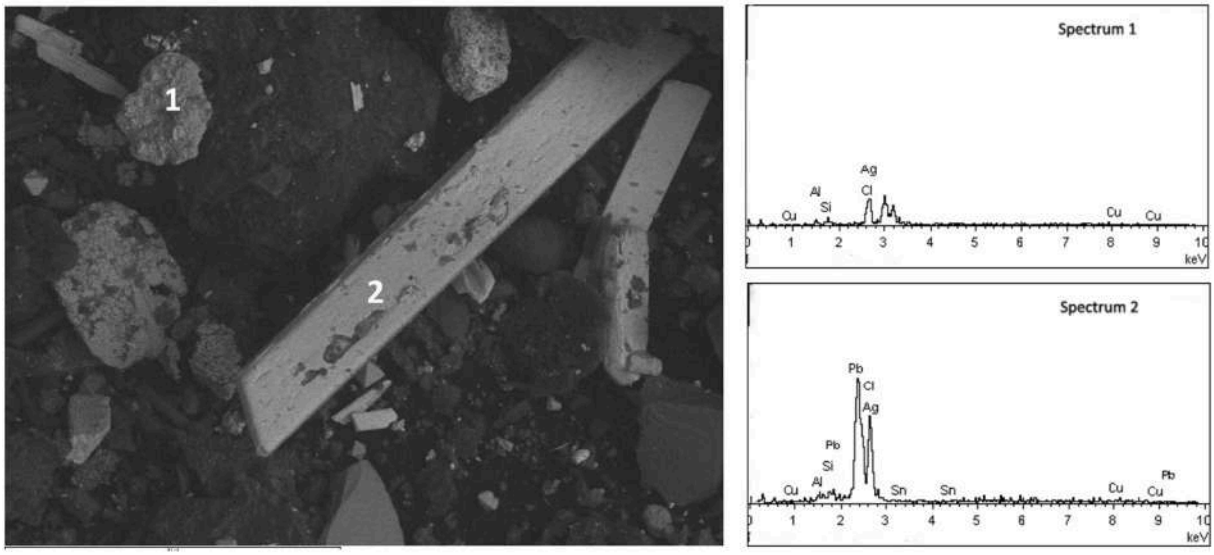

Fig. 2. SEM-EDS analysis of the solid residue upon the second pretreatment stage (scale: 200 μm).

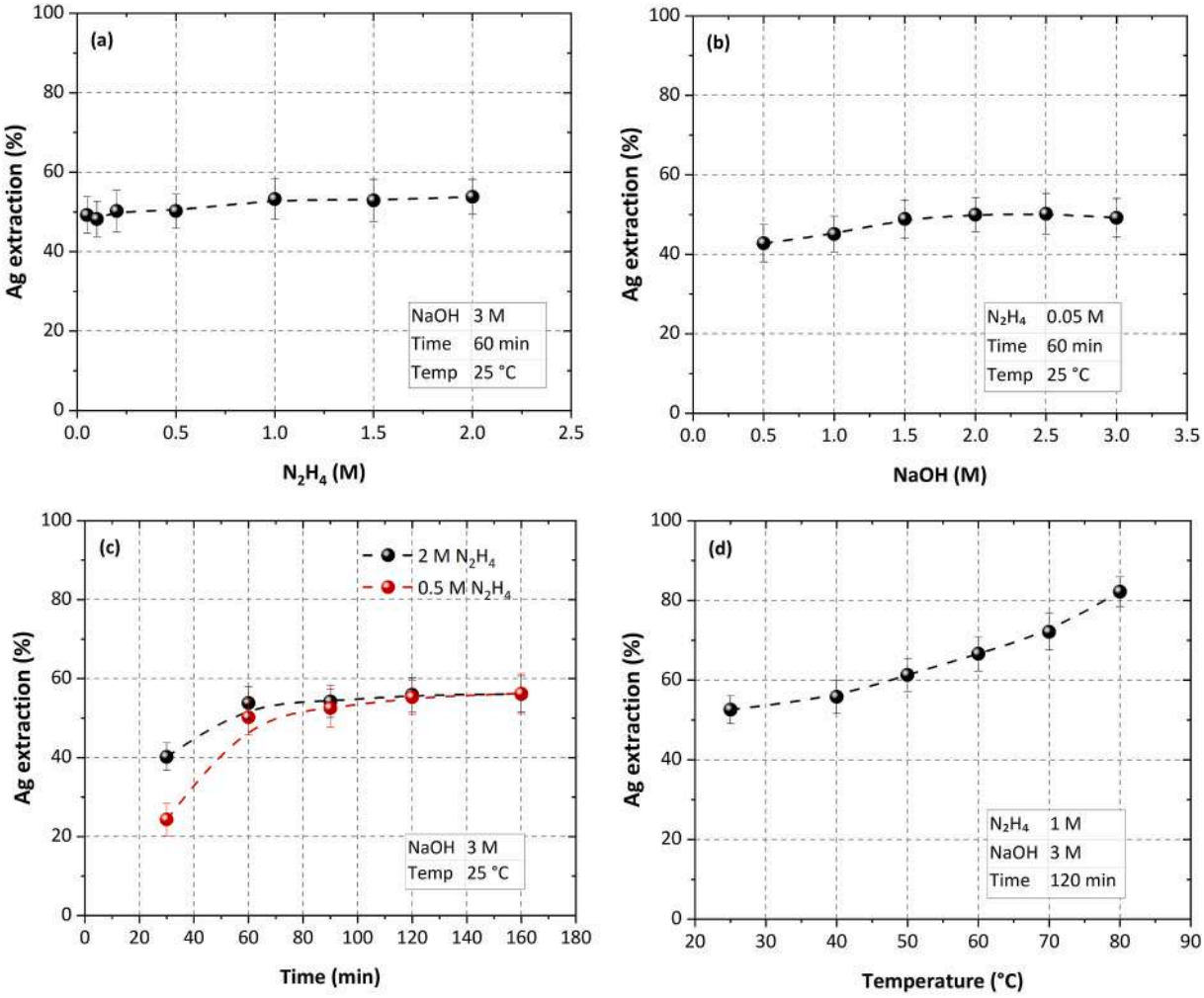

Fig. 3. Effect of (a) hydrazine concentration; (b) NaOH concentration; (c) contact time; and (d) temperature on Ag reduction and subsequent extraction with 5 M HNO_3.

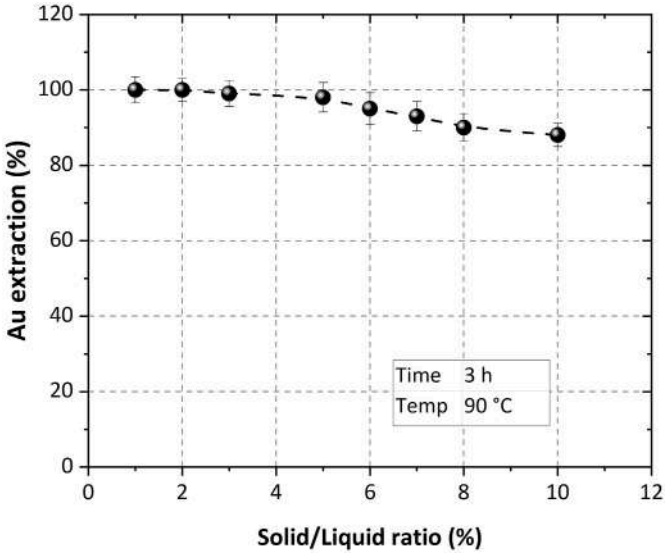

Fig. 4. Effect of solid/liquid ratio on Au extraction with aqua regia.

3.4. Pilot-scale application, wastewater composition and treatment

Table 2 shows the results for the composition of the pregnant solutions and the solid residues from the four leaching stages of the pilot application. For 1000 g of initial material, the obtained pregnant solutions contained the elements of interest at concentrations ranging from 1 g/L to 40 g/L for base metals and 90 mg/L to 200 mg/L for Au and Ag, respectively. The successive reduction of the mass of the material along the leaching stages is also shown in Table 2. In the first leaching stage, Sn, Fe and Zn were removed from the material at percentages of about 70–87%. The second stage is characterized by the quantitative leaching of copper. Nickel was also leached in this stage. In the third stage, Ag was leached with an efficiency of 83% leaving gold in the solid residue. Finally, gold was leached by aqua regia quantitatively. Table 3 summarizes the parameters and the obtained results for silver and gold extraction and recovery. Silver was recovered from the pregnant solution by 99.9% via N_2H_4 reduction. The recovery of gold via N_2H_4 reduction reached 99.9%. The purity of the produced silver and gold precipitates was determined at 97.3% and 90.6%, respectively.

The effluents originating from the stages of the hydrometallurgical process for Ag and Au recovery based on the flowsheet shown in Fig. 1 and the parameter values shown in Table 3, are acidic and contain soluble species at levels shown in Table 4. The ranges of the concentrations of the varied species correspond to the pilot application but also to additional datasets produced from raw materials of different initial composition. WW1 and WW2 are poor in nitrate while WW3 and WW4 nitrate content is much above the reactor acclimation threshold (i.e., 10 g/L). Moreover, pH and soluble metal content are well beyond the reactor acclimation thresholds (i.e., pH = 3 and [Me] = 100 mg/L, respectively). To attain lower nitrate content in the reactor feed, equal volumes of WW1-WW4 were mixed. Additionally, the resulting solution was neutralized by 5 M NaOH. Thus, soluble metals were precipitated as insoluble species and, upon 24-h sedimentation and microfiltration (0.20 μm) of the clarified supernatant, a neutral solution with low metal content (1–10 mg/L) was generated (mixW, Table 5). Then, mixW was diluted with nutrient broth by 1:6 (1 part of mixW and 5 parts of broth). Thus, the high chloride content of the mixed effluent solution was reduced while the biofilm was provided with all the essential organic and inorganic substances for denitrification. Upon chloride and nitrate determination, chloride concentration was further corrected by adding NaCl to correspond to 5% salinity. Finally, peptone and yeast were added as 1.5 g/g NO_3^- and 0.3 g/g NO_3^-, respectively (PR-mixW, Table 5), to feed the bioreactor.

Biological denitrification was achieved in the bioreactor (Table 5 and Fig. 6). The presence of metals, such as Fe, Ni, Cu, Zn and Pb at concentrations up to 10 mg/L, did not affect the denitrification process (Table 5). The kinetic profiles of nitrate and nitrite reduction as well as pH and concentration profiles of Zn, Cu, Fe and Ni during denitrification are presented in Fig. 6 (and Table S2). Denitrification proceeded through the formation of nitrite as intermediate which was sequentially reduced completely into nitrogen (Fig. 6(a and b)). After 28 h, nitrate removal reached 99.8% and nitrite concentration remained below 0.1 mg/L (Fig. 6(a and b)). Residual metal concentrations were at 1 mg/L level. A slight increase in Ni concentration was observed (Fig. 6(d)) and may be due to Ni distribution between insoluble forms and organic complexes formed due to the presence of peptone in the nutrient (Mendrinou et al., 2021).

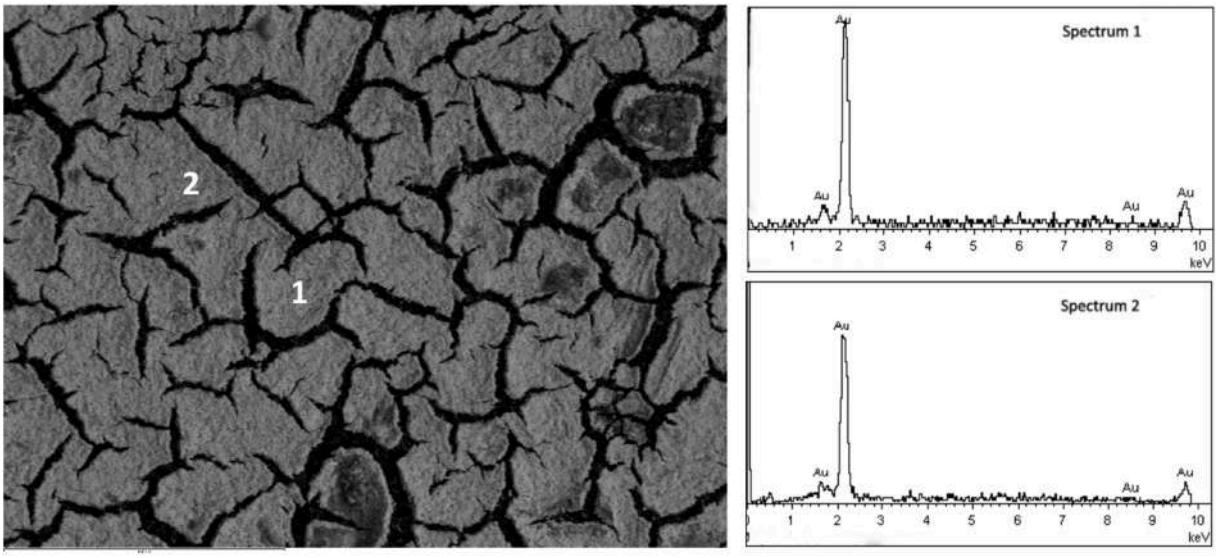

Fig. 5. SEM-EDS analysis of the precipitate upon gold recovery (scale: 100 μm).

Table 2
Composition of the pregnant solutions (PLS) and the solid residues (RES) from the four leaching stages of the pilot application.

		Au	Ag	Cu	Fe	Zn	Sn	Pb	Ni
Initial material (m = 1000 g)									
	Metal content (% w/w)	0.04	0.07	54.01	3.86	1.00	10.20	3.81	0.93
1st pretreatment stage	PLS (V = 4.78 L)								
	Concentration (g/L)	$<10^{-4}$	$<5x10^{-5}$	0.06	5.96	1.66	18.45	4.44	0.50
	Leaching efficiency[a] (%)	–	–	0.05	73.77	79.70	86.48	55.68	25.60
	RES (m = 843.3 g)								
	Metal content (% w/w)	0.05	0.08	64.38	1.57	0.36	2.83	1.64	0.94
2nd pretreatment stage	PLS (V = 13.5 L)								
	Concentration (g/L)	$<10^{-4}$	$4x10^{-3}$	38.62	0.95	0.22	1.37	0.91	0.55
	Leaching efficiency (%)	–	8.25	96.53	33.26	29.72	18.18	32.10	79.96
	RES (m = 221.7 g)								
	Metal content (% w/w)	0.21	0.29	9.47	0.17	0.05	2.36	0.20	0.05
Ag leaching	PLS (V = 2.5 L)								
	Concentration (g/L)	$<10^{-4}$	0.23	8.17	0.05	0.02	1.17	0.16	0.02
	Leaching efficiency (%)	–	83.38	3.78	0.36	0.59	2.87	1.03	0.52
	RES (196.0 g)								
	Metal content (% w/w)	0.22	0.04	0.13	0.12	0.02	0.03	0.02	0.03
Au leaching	PLS (V = 4.63 L)								
	Concentration (mg/L)	9.28	1.15	4.67	4.37	0.26	0.93	0.55	0.62
	Leaching efficiency (%)	99.90	7.58	0.04	0.52	0.12	0.04	0.07	0.31
	RES (m = 188.6 g)								
	Metal content (% w/w)	0.01	0.01	0.06	0.02	0.02	0.01	0.00	0.02

[a] Leaching efficiency after each stage was calculated based on the composition of the initial material.

Table 3
Conditions of silver and gold leaching and recovery in pilot application.

Stage	Agents	Time (h)	Temperature (°C)	Agitation (rpm)	Efficiency (%)	Efficiency (%)
Ag reduction	0.5 M N_2H_4 3 M NaOH S/L ratio: 10%	1.5	80	300	83	
Ag extraction	4 M HNO_3 1 M H_2O_2 S/L ratio: 10%	1.0	25	300	83	
Ag recovery	N_2H_4: 0.08 M Alternatively, 0.05 M NaCl	0.5	25	300	99.9	
Au extraction	HCl:HNO_3 3:1 (AR) S/L ratio: 5%	5.0	90	300		99.9
Au recovery	N_2H_4: 0.13 M	0.5	25	300		99.9

Table 4
Composition of the effluents generated by the hydrometallurgical processing of the waste PCB sample.

Effluent	pH	Anion content (g/L)		Metal content (mg/L)				
		NO_3^-	Cl^-	Fe^{2+}	Cu^{2+}	Ni^{2+}	Zn^{2+}	Pb^{2+}
WW1	1.74–2.10	0	56–102	1310–7500	140–142	180–700	3030–3500	730–1300
WW2	~0	0	30–78	845–1500	440–1950	750–920	490–970	600–1250
WW3	~0	190–223	0.5–1.2	15–20	5–10	15–20	5–10	1–5
WW4	~0	48.3–173	49–102	230–290	430–510	30–50	35–130	12–1380

Table 5
Chemical composition of the pretreated and treated wastewater solutions.

Solution	pH	Anion content (g/L)		Metal content (mg/L)				
		NO_3^-	Cl^-	Fe^{2+}	Cu^{2+}	Ni^{2+}	Zn^{2+}	Pb^{2+}
mixW	~0.20	15.6–75.5	54–90	2900–5800	810–1830	320–860	1330–1540	900–1120
PR-mixW	6.70	4.9	50	1.60	6.19	1.22	8.06	<1
Treated	7.96	0.008	50	1.09	0.30	9.40	3.14	<1

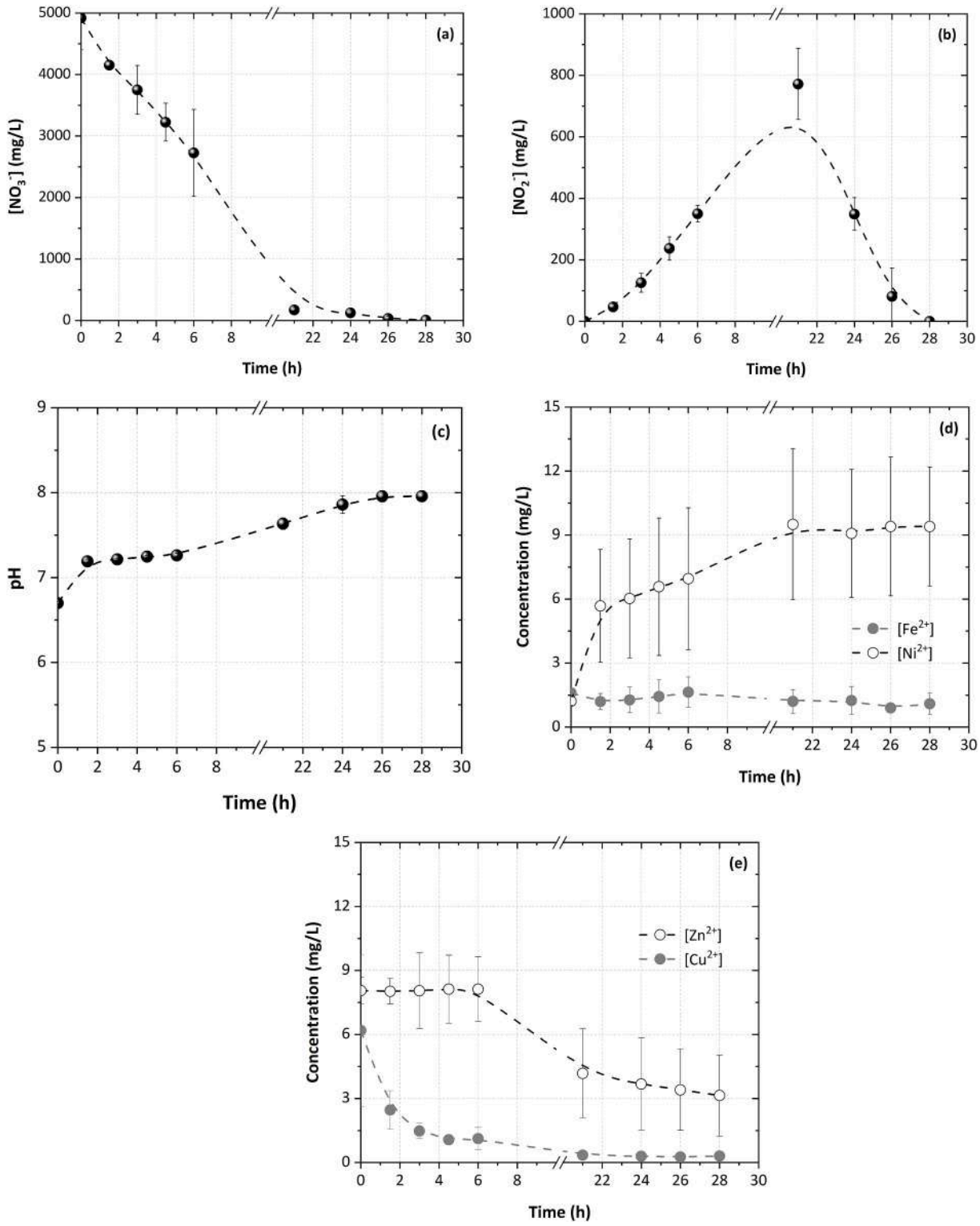

Fig. 6. (a) Nitrate; (b) nitrite; (c) pH; (d) Fe and Ni; (e) Zn and Cu kinetic profiles during denitrification of pretreated wastewater.

4. Conclusions

This paper presents an experimental work including hydrometallurgical recovery of silver and gold from waste PCBs and treatment of the effluents by a biofilm packed-bed reactor, which led to a successful pilot application. The main achievements are:

- A hydrometallurgical process for the extraction of base and precious metals by only two leaching agents: HCl and HNO_3.
- Separation and selective recovery of silver and gold by 83% and 100%, respectively.
- Optimal parameters experimentally verified for the efficient reduction and recovery of gold by hydrazine hydrate: 0.13 M N_2H_4 at ambient temperature.

- Optimal parameters experimentally verified for the efficient reduction of silver in solid phase (0.5 M N_2H_4, 3 M NaOH, 80 °C and S/L ratio 10%) and its recovery from nitrate solution by hydrazine hydrate (0.08 M N_2H_4 at ambient temperature).
- An effective and novel solution for treating wastewater streams after appropriate pretreatment: microbial denitrification in presence of metals at ppm level and high chloride content, in a packed-bed biofilm reactor.
- The overall process requires low reagents and energy input and has zero discharge for liquid effluents.

Credit author statement

Dimitrios Vlasopoulos: Investigation, Visualization, Writing - Original Draft. **Panagiota Mendrinou:** Investigation, Visualization, Writing - Original Draft. **Paschalis Oustadakis:** Methodology, Writing - Original Draft. **Pavlina Kousi:** Methodology, Writing - Original Draft. **Athanasios Stergiou:** Resources; Project administration, Funding acquisition. **Spyridon-Dionysios Karamoutsos:** Resources; Project administration, Funding acquisition. **Artin Hatzikioseyian:** Methodology, Writing - Original Draft. **Petros E. Tsakiridis:** Methodology, Writing - Original Draft. **Styliani Agatzini-Leonardou:** Conceptualization, Methodology, Supervision. **Emmanouella Remoundaki:** Conceptualization, Methodology, Writing - Review & Editing, Supervision.

Declaration of competing interest

The authors declare that they have no known competing financial interests or personal relationships that could have appeared to influence the work reported in this paper.

Data availability

Data will be made available on request.

Acknowledgments-Funding

This research has been co-financed by the European Regional Development Fund of the European Union and Greek national funds through the Operational Program Competitiveness, Entrepreneurship and Innovation, under the call RESEARCH – CREATE – INNOVATE (project code: T1EDK-00219). Mr. D. Vlasopoulos and Ms. P. Mendrinou also acknowledge the financial support they received from the State Scholarships Foundation of Greece (IKY) for the implementation of their doctoral theses which was co-financed by Greece and the European Union (European Social Fund-ESF) through the Operational Programme "Human Resources Development, Education and Lifelong Learning" in the context of the Act "Enhancing Human Resources Research Potential by undertaking a Doctoral Research" Sub-action 2: IKY Scholarship Programme for PhD candidates in the Greek Universities".

Appendix A. Supplementary data

Supplementary data to this article can be found online at https://doi.org/10.1016/j.jenvman.2023.118334.

References

Akcil, A., Erust, C., Gahan, C.S., Ozgun, M., Sahin, M., Tuncuk, A., 2015. Precious metal recovery from waste printed circuit boards using cyanide and non-cyanide lixiviants – a review. Waste Manag. 45, 258–271. https://doi.org/10.1016/j.wasman.2015.01.017.

Audrieth, L.F., Mohr, P.H., 1948. The chemistry of hydrazine. Chemical & Engineering News Archive 26 (51), 3746–3749. https://doi.org/10.1021/cen-v026n051.p3746.

Barnwal, A., Dhawan, N., 2020. Recycling of discarded mobile printed circuit boards for extraction of gold and copper. Sustainable Materials and Technologies 25, e00164. https://doi.org/10.1016/j.susmat.2020.e00164.

Birloaga, I., Coman, V., Kopacek, B., Vegliò, F., 2014. An advanced study on the hydrometallurgical processing of waste computer printed circuit boards to extract their valuable content of metals. Waste Manag. 34 (12), 2581–2586. https://doi.org/10.1016/j.wasman.2014.08.028.

Birloaga, I., Vegliò, F., 2016. Study of multi-step hydrometallurgical methods to extract the valuable content of gold, silver and copper from waste printed circuit boards. J. Environ. Chem. Eng. 4 (1), 20–29. https://doi.org/10.1016/j.jece.2015.11.021.

Birloaga, I., Vegliò, F., 2018a. 4 - hydrometallurgical processing of waste printed circuit boards. In: Vegliò, F., Birloaga, I. (Eds.), Waste Electrical and Electronic Equipment Recycling. Woodhead Publishing, pp. 95–113. https://doi.org/10.1016/B978-0-08-102057-9.00004-4.

Birloaga, I., Vegliò, F., 2018b. Overview on hydrometallurgical procedures for silver recovery from various wastes. J. Environ. Chem. Eng. 6 (2), 2932–2938. https://doi.org/10.1016/j.jece.2018.04.040.

Birloaga, I., Vegliò, F., 2022. An innovative hybrid hydrometallurgical approach for precious metals recovery from secondary resources. J. Environ. Manag. 307, 114567 https://doi.org/10.1016/j.jenvman.2022.114567.

Chen, J.P., Lim, L.L., 2002. Key factors in chemical reduction by hydrazine for recovery of precious metals. Chemosphere 49 (4), 363–370. https://doi.org/10.1016/S0045-6535(02)00305-3.

Cheng, D., Feng, C., Xu, D., Xia, S., Xu, Y., 2000. The directional reaction of hydrazine with silver complexes. Part 2. Influence of acidity and temperature. Transit. Met. Chem. 25 (3), 320–323. https://doi.org/10.1023/A:1007057720133.

Copani, G., Colledani, M., Brusaferri, A., Pievatolo, A., Amendola, E., Avella, M., Fabrizio, M., 2019. Integrated technological solutions for zero waste recycling of Printed Circuit Boards (PCBs). In: Tolio, T., Copani, G., Terkaj, W. (Eds.), Factories of the Future: the Italian Flagship Initiative. Springer International Publishing, Cham, pp. 149–169. https://doi.org/10.1007/978-3-319-94358-9_7.

Cotton, F.A., Wilkinson, G., 1998. Advanced Inorganic Chemistry, fifth ed. Wiley Interscience, New York.

Dehchenari, M.A., Hosseinpoor, S., Aali, R., Salighehdar, N., Mehdipour, M., 2017. Simple method for extracting gold from electrical and electronic wastes using hydrometallurgical process. Environmental Health Engineering and Management Journal 4 (1), 55–58. https://doi.org/10.15171/ehem.2017.08.

Elomaa, H., Seisko, S., Junnila, T., Sirviö, T., Wilson, B.P., Aromaa, J., Lundström, M., 2017. The effect of the redox potential of aqua regia and temperature on the Au, Cu, and Fe dissolution from WPCBs. Recycling 2 (3). https://doi.org/10.3390/recycling2030014.

Forti, V., Baldé, C.P., Kuehr, R., Bel, G., 2020. The Global E-Waste Monitor 2020: Quantities, Flows and the Circular Economy Potential. United Nations University (UNU)/United Nations Institute for Training and Research (UNITAR) – co-hosted SCYCLE Programme, International Telecommunication Union (ITU) & International Solid Waste Association (ISWA), Bonn/Geneva/Rotterdam.

Gautam, P., Behera, C.K., Sinha, I., Gicheva, G., Singh, K.K., 2022. High added-value materials recovery using electronic scrap-transforming waste to valuable products. J. Clean. Prod. 330, 129836 https://doi.org/10.1016/j.jclepro.2021.129836.

Hubau, A., Bryan, C.G., 2023. Metal recovery from e-wastes. In: Johnson, D.B., Bryan, C. G., Schlömann, M., Roberto, F.F. (Eds.), Biomining Technologies: Extracting and Recovering Metals from Ores and Wastes. Springer International Publishing, Cham, pp. 239–259. https://doi.org/10.1007/978-3-031-05382-5_14.

Huy Do, M., Tien Nguyen, G., Dong Thach, U., Lee, Y., Huu Bui, T., 2023. Advances in hydrometallurgical approaches for gold recovery from E-waste: a comprehensive review and perspectives. Miner. Eng. 191, 107977 https://doi.org/10.1016/j.mineng.2022.107977.

IARC, 2018. Monographs on the Evaluation of Carcinogenic Risks to Humans - Some Industrial Chemicals, vol. 115. International Agency for Research on Cancer (IARC), France.

James, T.H., 1940. Surface conditions of silver halides and the rate of reaction. III. Reduction of silver chloride by hydrazine. J. Am. Chem. Soc. 62 (7), 1654–1658. https://doi.org/10.1021/ja01864a006.

Kaya, M., 2016. Recovery of metals and nonmetals from electronic waste by physical and chemical recycling processes. Waste Manag. 57, 64–90. https://doi.org/10.1016/j.wasman.2016.08.004.

Lu, Y., Xu, Z., 2016. Precious metals recovery from waste printed circuit boards: a review for current status and perspective. Resour. Conserv. Recycl. 113, 28–39. https://doi.org/10.1016/j.resconrec.2016.05.007.

Marinato, Y., Pavoski, G., Rosario, C.G.A., de Andrade, L.M., Espinosa, D.C.R., 2023. Ag recovery from waste printed circuit boards of cell phone for synthesis of Ag nanoparticles and their antibacterial activity. J. Mater. Cycles Waste Manag. 25 (2), 970–984. https://doi.org/10.1007/s10163-022-01579-3.

Medina, D., Anderson, C.G., 2020. A review of the cyanidation treatment of copper-gold ores and concentrates. Metals 10 (7). https://doi.org/10.3390/met10070897.

Mendrinou, P., Hatzikioseyian, A., Kousi, P., Oustadakis, P., Tsakiridis, P., Remoundaki, E., 2021. Simultaneous removal of soluble metal species and nitrate from acidic and saline industrial wastewater in a pilot-scale biofilm reactor. Environmental Processes 8 (4), 1481–1499. https://doi.org/10.1007/s40710-021-00536-w.

Mir, S., Dhawan, N., 2022. A comprehensive review on the recycling of discarded printed circuit boards for resource recovery. Resour. Conserv. Recycl. 178, 106027 https://doi.org/10.1016/j.resconrec.2021.106027.

Mishra, G., Jha, R., Rao, M.D., Meshram, A., Singh, K.K., 2021. Recovery of silver from waste printed circuit boards (WPCBs) through hydrometallurgical route: a review. Environmental Challenges 4, 100073. https://doi.org/10.1016/j.envc.2021.100073.

Niemeier, J.K., Kjell, D.P., 2013. Hydrazine and aqueous hydrazine solutions: evaluating safety in chemical processes. Org. Process Res. Dev. 17 (12), 1580–1590. https://doi.org/10.1021/op400120g.

Park, Y.J., Fray, D.J., 2009. Recovery of high purity precious metals from printed circuit boards. J. Hazard Mater. 164 (2), 1152–1158. https://doi.org/10.1016/j.jhazmat.2008.09.043.

Patel, S., Patel, R., Gautam, A., Gautam, S., 2017. Influence of oxidizing agent on recovery of metals including gold and silver from printed circuit boards. International Research Journal of Engineering and Technology 4 (1), 830–834.

Purna, G., Rao, C., Yang, J., 2010. Chemical reduction method for preparation of silver nanoparticles on a silver chloride substrate for application in surface-enhanced infrared optical sensors. Appl. Spectrosc. 64 (10), 1094–1099. https://doi.org/10.1366/000370210792973640.

Rao, M.D., Singh, K.K., Morrison, C.A., Love, J.B., 2020. Challenges and opportunities in the recovery of gold from electronic waste. RSC Adv. 10 (8), 4300–4309. https://doi.org/10.1039/C9RA07607G.

Rocchetti, L., Amato, A., Beolchini, F., 2018. Printed circuit board recycling: a patent review. J. Clean. Prod. 178, 814–832. https://doi.org/10.1016/j.jclepro.2018.01.076.

Sadrnezhaad, S.K., Ahmadi, E., Mozammel, M., 2006. Kinetics of silver dissolution in nitric acid from Ag-Au0:04-Cu0:10 and Ag-Cu0:23 scraps. J. Mater. Sci. Technol. 22 (5), 696–700.

Sheng, P.P., Etsell, T.H., 2007. Recovery of gold from computer circuit board scrap using aqua regia. Waste Manag. Res. 25 (4), 380–383. https://doi.org/10.1177/0734242x07076946.

Streszewski, B., Jaworski, W., Szaciłowski, K., Pacławski, K., 2014. Kinetics and mechanism of redox reaction between tetrachloroaurate(III) ions and hydrazine. Int. J. Chem. Kinet. 46 (6), 328–337. https://doi.org/10.1002/kin.20850.

Tatarchuk, V.V., Sergievskaya, A.P., Druzhinina, I.A., Zaikovsky, V.I., 2011. Kinetics and mechanism of the growth of gold nanoparticles by reduction of tetrachloroauric acid by hydrazine in Triton N-42 reverse micelles. J. Nanoparticle Res. 13 (10), 4997. https://doi.org/10.1007/s11051-011-0481-1.

Theocharis, M., Pavlopoulos, C., Kousi, P., Hatzikioseyian, A., Zarkadas, I., Tsakiridis, P. E., Remoundaki, E., Zoumboulakis, L., Lyberatos, G., 2022. An integrated thermal and hydrometallurgical process for the recovery of silicon and silver from end-of-life crystalline Si photovoltaic panels. Waste and Biomass Valorization 13, 4027–4041. https://doi.org/10.1007/s12649-022-01754-5.

Tuncuk, A., 2019. Lab scale optimization and two-step sequential bench scale reactor leaching tests for the chemical dissolution of Cu, Au & Ag from waste electrical and electronic equipment (WEEE). Waste Manag. 95, 636–643. https://doi.org/10.1016/j.wasman.2019.07.008.

Tuncuk, A., Stazi, V., Akcil, A., Yazici, E.Y., Deveci, H., 2012. Aqueous metal recovery techniques from e-scrap: hydrometallurgy in recycling. Miner. Eng. 25 (1), 28–37. https://doi.org/10.1016/j.mineng.2011.09.019.

Tunsu, C., Retegan, T., 2016. Chapter 6 - hydrometallurgical processes for the recovery of metals from WEEE. In: Chagnes, A., Cote, G., Ekberg, C., Nilsson, M., Retegan, T. (Eds.), WEEE Recycling. Elsevier, pp. 139–175. https://doi.org/10.1016/B978-0-12-803363-0.00006-7.

Vlasopoulos, D., Oustadakis, P., Agatzini-Leonardou, S., Tsakiridis, P., Remoundaki, E., 2021. A hydrometallurgical process for Cu recovery from printed circuit boards. Materials Proceedings 5 (1), 56. https://doi.org/10.3390/materproc2021005056.

Wu, C., Awasthi, A.K., Qin, W., Liu, W., Yang, C., 2022. Recycling value materials from waste PCBs focus on electronic components: technologies, obstruction and prospects. J. Environ. Chem. Eng. 10 (5), 108516 https://doi.org/10.1016/j.jece.2022.108516.

Journal of Environmental Management 342 (2023) 118285

Contents lists available at ScienceDirect

Journal of Environmental Management

journal homepage: www.elsevier.com/locate/jenvman

Research article

Modeling biological denitrification in the presence of metal ions and elevated chloride content: Insights into abiotic and biotic mechanisms regulating metal bioprecipitation

Artin Hatzikioseyian *, Panagiota Mendrinou, Pavlina Kousi, Emmanouella Remoundaki

School of Mining and Metallurgical Engineering, National Technical University of Athens (NTUA), Heroon Polytechniou 9, 15772, Zografou, Greece

ARTICLE INFO

Keywords:
AQUASIM
Biological denitrification
Metal bioprecipitation
Model

ABSTRACT

Biological denitrification is a critical process in which microorganisms convert nitrate to nitrogen gas. Metal ions, such as those found in industrial wastewater, can be toxic to microorganisms and impede denitrification. It is critical to identify the mechanisms that allow microorganisms to tolerate metal ions and understand how these mechanisms can be utilized to improve denitrification efficiency by modeling the process. This study presents a mathematical model of biological denitrification in the presence of metal ions. The model includes key biotic and abiotic mechanisms and is based on pilot scale results. The model predicts the bioprecipitation of metal ions due to pH shift and alkalinity production during the metabolic activity of microorganisms. The model parameters are estimated to fit the experimental results and the mechanisms regulating metal detoxification via biological metal precipitation are presented. The model provides a valuable tool for understanding the behavior of denitrification systems in the presence of metal ions and can be used to optimize these systems for more efficient and effective treatment of industrial wastewater.

1. Introduction

Industrial denitrification is the process of removing nitrate and nitrite from industrial wastewater before it is released into the environment. The procedure is usually carried out to comply with environmental regulations and to avoid negative effects on aquatic ecosystems. Industrial denitrification is similar to denitrification in natural systems such as soil and aquatic environments, and it typically involves the use of microorganisms such as bacteria and fungi to convert nitrogen compounds into nitrogen gas (Revsbech and Sørensen, 2013). Denitrification is essential for regulating nitrate and nitrite levels in ecosystems and is an important component of the global nitrogen cycle (Golterman, 2013). In wastewater treatment plants, denitrification is commonly used to remove excess nitrogen, which can cause eutrophication and other negative effects on aquatic ecosystems (Gerardi, 2003). It is also used to remove nitrogen from drinking water as the World Health Organization (WHO) recommends a guideline value of 50 mg/L for nitrate and 3 mg/L for nitrite (WHO 2017). The United States Environmental Protection Agency (EPA) has set a maximum contaminant level (MCL) of 10 mg/L for nitrate and of 1 mg/L for nitrite (EPA, 2009).

There are several methods for industrial denitrification, including chemical, physical and biological methods (Bhatnagar and Sillanpää, 2011; Burghate and Ingole, 2014). The most common chemicals used for denitrification is sodium bisulfite ($NaHSO_3$), sodium metabisulfite ($Na_2S_2O_5$) and sodium dithionite ($Na_2S_2O_4$) (Tanaka et al., 1979) and less widely used zero-valent iron (Zhang et al., 2010) or magnesium (Kumar and Chakraborty, 2006). The choice of chemicals depends on the specific application and the initial concentration of nitrate and nitrite in the water. Chemical denitrification is a fast process, it does not require a complex treatment system and it can be used in combination with other methods such as biological or physical denitrification. However, the use of chemicals can create issues such as the generation of secondary pollutants and the increase of the treatment costs. Additionally, the use of chemicals can also affect the pH and dissolved oxygen levels of the treated water. Therefore, it's important to carefully evaluate the feasibility and sustainability of chemical denitrification methods before applying them in practice.

In physical denitrification nitrates and nitrites are removed from the water or the wastewater through physical means. This can be done through methods such as adsorption (Bhatnagar et al., 2010; Bhatnagar and Sillanpää, 2011; Öztürk and Bektaş, 2004), ion-exchange (Richard,

* Corresponding author.
E-mail address: artin@metal.ntua.gr (A. Hatzikioseyian).

https://doi.org/10.1016/j.jenvman.2023.118285
Received 31 January 2023; Received in revised form 20 May 2023; Accepted 26 May 2023
Available online 31 May 2023

1989), reverse osmosis (Schoeman and Steyn, 2003), electrodialysis (Wan et al., 2010; Wisniewski et al., 2001) or catalytic denitrification (Pintar et al., 2001).

However, the most widely used treatment method for nitrate removal is biological denitrification which uses microorganisms that can convert oxidized nitrogen to elemental nitrogen (Gerardi, 2003). This anaerobic process can be engineered in bioreactors, where microorganisms are grown in planktonic or immobilized form and use nitrate and/or nitrite as terminal electron acceptors. Biological denitrification has several advantages; it is cost-effective, a natural process that mimics the nitrogen cycle, highly efficient, flexible in its application, able to be combined with other treatment processes and produces harmless nitrogen gas as a by-product. However, there are also several challenges that need to be considered, including the sensitivity of microorganisms to pH and temperature, inhibition by other compounds such as heavy metals, the need for a carbon source in heterotrophic denitrification, lower reaction rates than other methods, the requirement for regular monitoring and maintenance, the potential to generate unwanted gases such as nitric oxide (NO) and nitrous oxide (N_2O), and the susceptibility to biological and chemical interference. Nevertheless, biological denitrification remains a safe and effective method for removing oxidized nitrogen from water and wastewater.

The recycling of the end of life (EoL) waste electronic equipment with hydrometallurgical processes aims to recover metals and other materials from e-wastes such as printed circuit boards (PCBs), smartphones, TV sets, and other electronic devices that contain valuable metals such as copper, tin, zinc, lead, silver, gold and palladium (Thakur and Kumar 2020). E-waste recycling is carried out in sequential steps including mechanical processes such as shredding, grinding, and separation, as well as chemical processes such as leaching (hydrometallurgy) or smelting (pyrometallurgy). The methods chosen depend on the type and condition of the e-waste, as well as the desired end products. However, the recycling of e-waste with hydrometallurgy over pyrometallurgy has several benefits, including (Holuszko et al., 2022; Kaya, 2019; Khan and Asiri, 2019):

(a) Energy savings: Pyrometallurgical methods are more energy demanding.
(b) Pollution reduction: Recycling e-waste with hydrometallurgical processes reduces the emissions of toxic volatile emissions.
(c) Economic benefits: Capital investments and operating costs of hydrometallurgical processes are lower compared to pyrometallurgical processes.

However, it should be realized that the recycling of e-wastes by hydrometallurgical methods can be complex and requires specialized knowledge and equipment. It is also important to ensure that the recycling process is done in an environmentally responsible manner to minimize potential negative impacts on human health and the environment. For example, during hydrometallurgical processing of printed circuit boards (PCBs) mineral acids such as nitric and hydrochloric acid or mixtures of them - also known as aqua regia in molar ratio 1:3 - are often used in order to dissolve base metals such as copper, zinc, lead and tin and precious metals such as gold and silver. Different methods are used to recover the target metals from these metal-laden acidic streams, including selective extraction with organic solvents and electrowinning as for the case of copper (Kordosky, 1992, 2002) or reductive precipitation as for the cases of gold and silver (Murali et al., 2022). Upon the recovery of targeted metals, the spent acidic streams are enriched with the consumed acids and are recycled to the dissolution process. A bleed stream is removed periodically to avoid accumulation of non-recovered/consumed build up chemicals. The resulting wastewater contains heavy metals, acidity, chlorides, nitrates, high levels of dissolved salts, and/or dissolved organic matter. If not properly treated, these pollutants can be toxic to aquatic life and have a negative impact on the local ecosystem and human health.

Wastewater from hydrometallurgy can be treated using a combination of physical, chemical, and biological processes such as precipitation, neutralization, and biological treatment. The type and concentration of pollutants in the wastewater will determine the treatment method used. Before neutralization the wastewater streams are characterized by low pH, residual non recovered metal ions at the level of hundred to thousand ppm and elevated concentrations of nitrate and chloride. Conventional wastewater treatment scheme includes neutralization of the wastewater to pH around 7 with the use of alkaline reagents such as sodium hydroxide or lime. Neutralization of the wastewater also precipitates the dissolved metal ions which can be settled and separated by sedimentation or filtration from the wastewater. However, nitrate and chloride content are not affected significantly during neutralization and metal precipitation. For these anions other techniques such as reverse osmosis or ion exchange should be used to reduce the level of these below the permissible discharge levels.

Although the metal ions could be considered harmful to microorganisms, previous work has shown that solutions with high nitrate levels can be effectively treated through biological denitrification (Hirata et al., 2001; Zou et al., 2015), despite the presence of elevated chloride levels and high levels of dissolved metals (Mendrinou et al., 2021).

In this work we present a mathematical model that elucidates how the microorganisms can tolerate high metal levels through pH shifts and alkalinity production. The model is based on already published experimental results regarding denitrification of synthetic solutions which simulate wastewater originating from the hydrometallurgical treatment of waste PCBs for the recovery of base and precious metals using hydrochloric and nitric acid (Mendrinou et al., 2021) and explains the mechanisms behind biological metal precipitation, which helps to detoxify the metal ions and remove them from the wastewater.

2. Materials and methods

The process concept, the experimental set-up and the results have been presented in detail in our previous work (Mendrinou et al., 2021). In summary, synthetic or real wastewater was treated in a pilot scale packed-bed reactor (working volume 2.7 L) filled with biofilm support sintered-glass packing material (Biohome Supergravel and Biohome Ultimate Marine) provided by Aqua Bio UK Ltd (https://filterpro.co.uk/). A schematic of the bioreactor and the connections with the wastewater holding vessel are illustrated in Fig. 1. The bioreactor was inoculated with a pure culture of the strain *Halomonas denitrificans* (DSM-18045), obtained from the Deutsche Sammlung von Mikroorganismen und Zellkulturen (DSMZ, Germany). *H. denitrificans* was first isolated from saline water in Anmyeondo, Korea (Kim et al., 2007) and was selected based on two specific characteristics: (a) its halotolerant nature which allows its growth in environments of high salinity (Miao et al., 2015); and (b) its phylogenetic traits which denote its ability to completely reduce nitrate to nitrogen gas (Felgate et al., 2012; González-Domenech et al., 2010; Wang and Shao, 2021). In addition, it has been proven that the strain can tolerate and grow in the presence of Zn^{2+}, Cu^{2+}, Fe^{2+} and Ni^{2+} at concentrations of at least up to 100 mg/L (Mendrinou et al., 2021). In order to study the denitrification kinetics under diverse operating conditions, an array of batch runs was carried out, with the reactor operating in upflow direction in batch closed loop mode. The synthetic wastewater was kept in a well-mixed holding vessel of 1 L and fed the reactor by means of a peristaltic pump.

To support the growth and denitrification activity of *Halomonas denitrificans,* the wastewater was supplemented with Bacto Marine Broth medium (DSMZ medium 514 + 8% NaCl) containing (in g/L): Bacto peptone (5.0), yeast extract (1.0), $MgCl_2.6H_2O$ (12.61), Na_2SO_4 (3.24), $CaCl_2{\cdot}2H_2O$ (2.66), KCl (0.55), $NaHCO_3$ (0.16), KBr (0.08), H_3BO_3 (0.022), NH_4NO_3 (0.0016) and Na_2HPO_4 (0.008). The denitrifying capacity of the reactor was evaluated for initial nitrate concentration between 750 mg/L and 6000 mg/L, for pH 3 to 8, for salinity levels from 5% up to 10% as NaCl and metal ions concentration up to 100 mg/L for

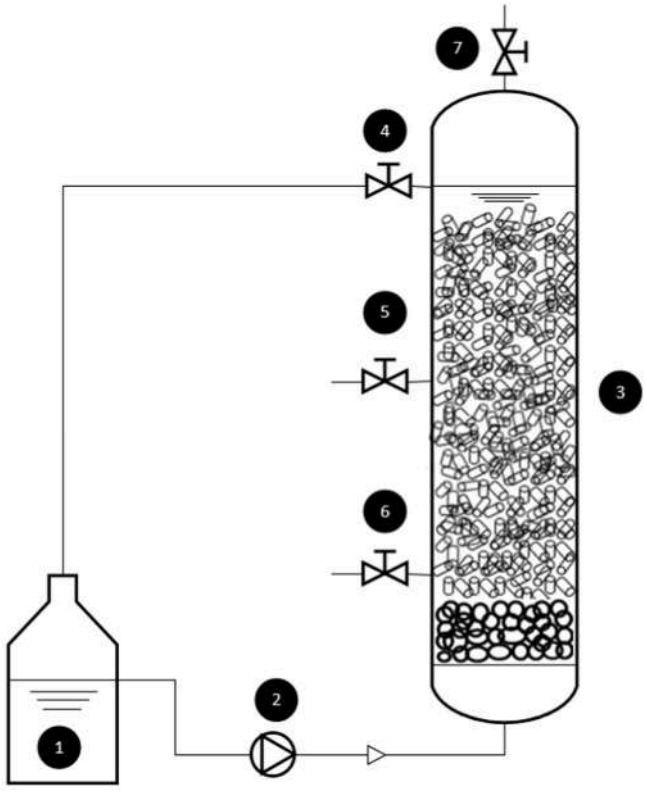

Fig. 1. Schematic layout of the experimental setup: (1) holding vessel, (2) peristaltic pump, (3) biological reactor (4, 5, 6) sampling points (7) gas vent.

the four divalent metals (Fe^{2+}, Cu^{2+}, Ni^{2+} and Zn^{2+}) which were added in the broth as $FeSO_4{\cdot}7H_2O$, $CuCl_2{\cdot}2H_2O$, $NiCl_2{\cdot}6H_2O$ and $ZnCl_2$, respectively. However, long term experiments revealed that the presence of sulfate competes denitrification and promotes sulfate reduction. Thus, Na_2SO_4 was excluded from the broth and $FeSO_4{\cdot}7H_2O$ was replaced by $FeCl_2{\cdot}4H_2O$. At 6000 mg/L organic content composed of 5000 mg/L bacto peptone and 1000 mg/L yeast extract, the initial TOC was 2300 ± 310 mg/L. At the end of each treatment cycle a remaining amount of 1305 ± 378 mg/L TOC was observed. Since there is an excess of organic carbon in the wastewater, nitrate is the limiting factor which is completely reduced before the consumption of the carbon source. To reduce the amount of excess organic content at the end of the treatment, the ratio of electron donor/electron acceptor needs to be further optimized. The pH of the treated wastewater was always above 7 and ranged between 7.3 and 8.3. In all cases, the effluent concentration of nitrate, nitrite, zinc, copper, iron and nickel were 6.78 ± 5.35 mg/L, 0.271 ± 0.222 mg/L, 0.229 ± 0.127 mg/L, 0.148 ± 0.0534 mg/L, 0.786 ± 0.798 mg/L and 20.6 ± 3.26 mg/L, respectively. The sampling, monitoring and the analytical procedures for the determination of nitrate, nitrite, metal ions and the total organic carbon (TOC) are presented in detail in the previous work (Mendrinou et al., 2021).

3. Model development

This work demonstrates the development of a biological denitrification model in the presence of metal ions. The model involves the most important biotic (biological) and abiotic (chemical) processes that take place in a biological reactor and predicts the fate of the metal ions under pH shift and alkalinity production.

3.1. Microbial denitrification

In this work only the case of heterotrophic denitrification is considered because *Halomonas denitrificans* is a heterotrophic denitrifier. Lithotrophic denitrification in an alternative option when the electron donor is an inorganic element such as iron (II), sulfur or hydrogen while the carbon source is carbon dioxide. This process is slower than heterotrophic denitrification, but it can be more effective at removing nitrate from water with low organic content. Lithoautotrophic denitrification is often used in groundwater and soil remediation, and it can be carried out in situ without adding organic carbon sources, making it potentially more cost-effective and environmentally friendly.

The simulation of the microbial activity in the model is based on the principles of bioenergetics. The methodology consists of the combination of three semi-reactions: (a) the electron donor reaction (R_d); (b) the electron acceptor reaction (R_a); and (c) the cell synthesis reaction (R_c) (Rittmann and McCarty, 2020). In heterotrophic denitrification, electrons released by the oxidation of the organic substrate (electron donor) are captured by the electron acceptor and the biomass synthesis reaction (Rittmann and McCarty, 2020).

In the present study, the electron donor and carbon source originate primarily from the peptone, and secondarily from the yeast extract used as a supplementary nutrient in the feed solution (Mendrinou et al., 2021). It has been experimentally proven that *Halomonas denitrificans* proceeds to complete denitrification via the formation of the intermediate nitrite (Mendrinou et al., 2021). Therefore, nitrate present in the original feed solution and nitrite which is produced during nitrate reduction, are specified as sequential electron acceptors (reactions (2) and (6)). Moreover, ammonium which is also provided in the feed solution is specified as nitrogen source for biomass synthesis (reactions (3) and (7)). Therefore, the stoichiometry of the overall biological activity can be written by combining the following semi-reactions:

For the reduction stage of nitrate (NO_3^-) to the intermediate nitrite (NO_2^-):

Electron donor reaction (R_d):

$$\left(\frac{1}{4x+y-2z-3w}\right) C_xH_yO_zN_{w\,(aq)} + \left(\frac{3x-z}{4x+y-2z-3w}\right) H_2O \rightarrow \left(\frac{w}{4x+y-2z-3w}\right) NH^+_{4(aq)} + \left(\frac{x}{4x+y-2z-3w}\right) HCO^-_{3(aq)} + \left(\frac{5x+y-2z-4w}{4x+y-2z-3w}\right) H^+_{(aq)} + e^- \quad (1)$$

Electron acceptor reaction (R_a):

$$\left(\frac{1-f_s}{2}\right) NO^-_{3(aq)} + (1-f_s) H^+_{(aq)} + (1-f_s) e^- \rightarrow \left(\frac{1-f_s}{2}\right) NO^-_{2(aq)} + \left(\frac{1-f_s}{2}\right) H_2O \quad (2)$$

Cell synthesis reaction (R_c):

$$\left(\frac{5f_s}{20}\right)\ HCO_{3(aq)}^{-}+\left(\frac{f_s}{20}\right)\ NH_{4(aq)}^{+}+\left(\frac{24f_s}{20}\right)\ H_{(aq)}^{+}+f_s\ e^{-}\rightarrow\left(\frac{f_s}{20}\right)\ C_5H_7O_2N+\left(\frac{13f_s}{20}\right)\ H_2O \tag{3}$$

Overall reaction (R):

where f_s is the fraction of electrons captured for biomass synthesis, $C_xH_yO_zN_w$ is a generalized formula used for the organic substrate which serves as carbon and electron donor and $C_5H_7O_2N$ is a "typical" formula used for the microbial cells in wastewater applications. The values of f_s depend on the nature of the organic substrate and the nature of the electron acceptor. For denitrification with organic electron donors such as methanol and BOD from municipal wastewater the maximum value of f_s is estimated as 0.36 and 0.52, respectively, while for inorganic electron donors such as hydrogen and sulfur 0.21 and 0.13, respectively (Rittmann and McCarty, 2020). In the model, for both denitrification stages - reactions (4) and (8) - the value of f_s is fixed to 0.5 meaning that 50% of the electrons from the oxidation reaction (R_d) is captured for cell synthesis (reaction R_c) while 50% is captured for energy production (reaction R_a).

$$\left(\frac{1}{4x+y-2z-3w}\right)\ C_xH_yO_zN_{w\ (aq)}+\left(\frac{1-f_s}{2}\right)\ NO_{3(aq)}^{-}+\left(\frac{3x-z}{4x+y-2z-3w}-\frac{1-f_s}{2}-\frac{13f_s}{20}\right)\ H_2O+\left((1-f_s)+\frac{24f_s}{20}-\frac{5x+y-2z-4w}{4x+y-2z-3w}\right)\ H_{(aq)}^{+}+\left(\frac{f_s}{20}-\frac{w}{4x+y-2z-3w}\right)\ NH_{4(aq)}^{+}\rightarrow\left(\frac{f_s}{20}\right)\ C_5H_7O_2N+\left(\frac{1-f_s}{2}\right)\ NO_{2(aq)}^{-}+\left(\frac{x}{4x+y-2z-3w}-\frac{5f_s}{20}\right)\ HCO_{3(aq)}^{-} \tag{4}$$

The corresponding reactions for the reduction stage of the intermediate nitrite (NO_2^-) to nitrogen (N_2) are:

Electron donor reaction (R_d):

$$\left(\frac{1}{4x+y-2z-3w}\right)\ C_xH_yO_zN_{w\ (aq)}+\left(\frac{3x-z}{4x+y-2z-3w}\right)\ H_2O\rightarrow\left(\frac{w}{4x+y-2z-3w}\right)\ NH_{4\ (aq)}^{+}+\left(\frac{x}{4x+y-2z-3w}\right)\ HCO_{3\ (aq)}^{-}+\left(\frac{5x+y-2z-4w}{4x+y-2z-3w}\right)\ H_{(aq)}^{+}+e^{-} \tag{5}$$

Electron acceptor reaction (R_a):

$$\left(\frac{1-f_s}{3}\right)\ NO_{2(aq)}^{-}+\left(\frac{4(1-f_s)}{3}\right)\ H_{(aq)}^{+}+(1-f_s)\ e^{-}\rightarrow\left(\frac{1-f_s}{6}\right)\ N_{2(g)}+\left(\frac{2(1-f_s)}{3}\right)\ H_2O \tag{6}$$

Cell synthesis reaction (R_c):

$$\left(\frac{5f_s}{20}\right)\ HCO_{3(aq)}^{-}+\left(\frac{f_s}{20}\right)\ NH_{4(aq)}^{+}+\left(\frac{24f_s}{20}\right)\ H_{(aq)}^{+}+f_s\ e^{-}\rightarrow\left(\frac{f_s}{20}\right)\ C_5H_7O_2N+\left(\frac{13f_s}{20}\right)\ H_2O \tag{7}$$

Overall reaction (R):

$$\left(\frac{1}{4x+y-2z-3w}\right)\ C_xH_yO_zN_{w\ (aq)}+\left(\frac{1-f_s}{3}\right)\ NO_{2(aq)}^{-}\rightarrow\left(\frac{f_s}{20}\right)\ C_5H_7O_2N+\left(\frac{x}{4x+y-2z-3w}-\frac{5f_s}{20}\right)\ HCO_{3(aq)}^{-}+\left(\frac{4(1-f_s)}{3}+\frac{24f_s}{20}-\frac{5x+y-2z-4w}{4x+y-2z-3w}\right)\ H_{(aq)}^{+}+\left(\frac{w}{4x+y-2z-3w}-\frac{f_s}{20}\right)\ NH_{4(aq)}^{+}+\left(\frac{1-f_s}{6}\right)\ N_{2(g)}+\left(-\frac{3x-z}{4x+y-2z-3w}+\frac{2(1-f_s)}{3}+\frac{13f_s}{20}\right)\ H_2O \tag{8}$$

Amino acids, proteins and other nitrogenous compounds can be typically represented by the empirical formula $C_{16}H_{24}O_5N_4$ (Rittmann and McCarty, 2020). Elemental analysis of the carbon and nitrogen content for the mixture of peptones and yeast extract supplemented in the wastewater indicated that the ratio of C/N in our study is close to 4.5/1. Thus, the empirical formula $C_{18}H_{24}O_5N_4$ ($x = 18$, $y = 24$, $z = 5$ and $w = 4$) was selected to represent the carbon/electron source in the model.

3.2. Microbial kinetics

The kinetic terms of the microbial growth consist of mixed Monod type equations including the two limiting substances i.e. the carbon

source, and the alternative electron acceptors NO_3^- (equation (9)) and NO_2^- (equation (10)), respectively:

(a) Reduction of nitrate to nitrite (9):

$$\frac{dX}{dt} = \mu_{max,NO_3} \cdot \frac{C_{org}}{K_{sorg} + C_{org}} \cdot \frac{C_{NO_3}}{K_{NO_3} + C_{NO_3}} \cdot X \quad (9)$$

(b) Reduction of nitrite to nitrogen (10):

$$\frac{dX}{dt} = \mu_{max,NO_2} \cdot \frac{C_{org}}{K_{sorg} + C_{org}} \cdot \frac{C_{NO_2}}{K_{NO_2} + C_{NO_2}} \cdot X \quad (10)$$

where $\mu_{max,NO3}$ and $\mu_{max,NO2}$ are the maximum specific growth rates for the reactions (4) and (8) respectively, C_{org}, C_{NO_3} and C_{NO_2} are the concentrations of the organic substrate, the nitrate and the nitrite, respectively, K_{sorg}, K_{NO_3} and K_{NO_2} are the half saturation constants of the organic substrate, the nitrate and the nitrite respectively, and X is the biomass concentration.

3.3. Abiotic reactions

The overall biological reactions as expressed by equations (4) and (8) quantitatively determine the concentrations of simple chemical species such as $NH_{4(aq)}^+$, $HCO_{3(aq)}^-$ and $H_{(aq)}^+$ consumed or produced during denitrification. These changes affect the microenvironment of the bacteria and the macroenvironment of the wastewater by altering the speciation of the dissolved metals due to the increase of the alkalinity and the pH of the wastewater. Acid-base equilibria between these species are included in the model by the hydrolysis reactions of $HCO_{3(aq)}^-$ and $NH_{4(aq)}^+$ and the dissociation of water. These reactions buffer the pH of the treated wastewater to circumneutral values. In the presence of metal ions such as Fe^{2+}, Cu^{2+}, Ni^{2+} and Zn^{2+} the model predicts the change of species mobility by including precipitation reactions of the metals in the form of insoluble $Me(OH)_{2(s)}$ and/or $MeCO_{3(s)}$. Depending on the corresponding solubility product constants and the abundance of OH^- and/or HCO_3^- - which affect the pH - the model can predict the fate of the soluble and particulate metal species formed in the bioreactor environment.

Therefore, the model is complemented by the following chemical reactions assuming that all are in equilibrium (values of equilibrium constants at 25 °C (Stumm and Morgan, 2012)):

Equilibrium of $H_2CO_3/HCO_3^-/CO_3^{2-}$:

$$H_2CO_3^*(aq) \rightleftarrows H_{(aq)}^+ + HCO_3^-(aq) \quad (11)$$

with equilibrium constant for the composite H_2CO_3* (the sum of $CO_{2(aq)}$ and $H_2CO_{3(aq)}$):

$$K_{a1(H_2CO_3)} = \frac{H_{(aq)}^+ \cdot HCO_{3(aq)}^-}{H_2CO_3^*(aq)} = 4.45 \cdot 10^{-7} \quad (12)$$

and bicarbonate dissociation to CO_3^{2-}:

$$HCO_3^-(aq) \rightleftarrows H_{(aq)}^+ + CO_{3(aq)}^{2-} \quad (13)$$

with equilibrium constant:

$$K_{a2(H_2CO_3)} = \frac{H_{(aq)}^+ \cdot CO_3^{2-}(aq)}{HCO_3^-(aq)} = 4.69 \cdot 10^{-11} \quad (14)$$

At any time, the total inorganic carbon in the wastewater is calculated by the mass balance equation (15):

$$\text{Total Inorganic Carbon} = TIC = H_2CO_3^*(aq) + HCO_3^-(aq) + CO_{3(aq)}^{2-} \quad (15)$$

while the fraction of the species as a function of $H_{(aq)}^+$ are given by equations (16)-(18):

$$a_0 = \frac{{H_{(aq)}^+}^2}{{H_{(aq)}^+}^2 + K_{a1(H_2CO_3)} \cdot H_{(aq)}^+ + K_{a1(H_2CO_3)} \cdot K_{a2(H_2CO_3)}} = \frac{H_2CO_3^*(aq)}{TIC} \quad (16)$$

$$a_1 = \frac{K_{a1(H_2CO_3)} \cdot H_{(aq)}^+}{{H_{(aq)}^+}^2 + K_{a1(H_2CO_3)} \cdot H_{(aq)}^+ + K_{a1(H_2CO_3)} \cdot K_{a2(H_2CO_3)}} = \frac{HCO_3^-(aq)}{TIC} \quad (17)$$

$$a_2 = \frac{K_{a1(H_2CO_3)} \cdot K_{a2(H_2CO_3)}}{{H_{(aq)}^+}^2 + K_{a1(H_2CO_3)} \cdot H_{(aq)}^+ + K_{a1(H_2CO_3)} \cdot K_{a2(H_2CO_3)}} = \frac{CO_3^{2-}(aq)}{TIC} \quad (18)$$

Equilibrium of NH_4^+/NH_3:

$$NH_4^+(aq) \rightleftarrows H_{(aq)}^+ + NH_{3(aq)} \quad (19)$$

with equilibrium constant:

$$K_{a1(NH_4^+)} = \frac{H_{(aq)}^+ \cdot NH_{3(aq)}}{NH_4^+(aq)} = 5.62 \cdot 10^{-10} \quad (20)$$

At any time, the concentration of total inorganic nitrogen is given by the mass balance equation (21):

$$\text{Total Inorganic Nitrogen} = TIN = NH_{3(aq)} + NH_4^+(aq) \quad (21)$$

while the fraction of the species as a function of $H_{(aq)}^+$ are given by equations (22) and (23):

$$a_0 = \frac{H_{(aq)}^+}{H_{(aq)}^+ + K_{a1(NH_4^+)}} = \frac{NH_4^+(aq)}{TIN} \quad (22)$$

$$a_1 = \frac{K_{a1(NH_4^+)}}{H_{(aq)}^+ + K_{a1(NH_4^+)}} = \frac{NH_{3(aq)}}{TIN} \quad (23)$$

Water dissociation:

$$H_2O \rightleftarrows H_{(aq)}^+ + OH_{(aq)}^- \quad (24)$$

with equilibrium constant:

$$K_w = H_{(aq)}^+ \cdot OH_{(aq)}^- = 10^{-14} \quad (25)$$

where K_w is the dissociation constant of water.

The model is completed by the charge balance equation (26):

$$H_{(aq)}^+ + NH_4^+(aq) + 2 \cdot Ca_{(aq)}^{2+} + 2 \cdot Cu_{(aq)}^{2+} + 2 \cdot Fe_{(aq)}^{2+} + 2 \cdot Ni_{(aq)}^{2+} + 2 \cdot Zn_{(aq)}^{2+} + Na_{(aq)}^+ = OH_{(aq)}^- + NO_{3(aq)}^- + NO_{2(aq)}^- + HCO_3^-(aq) + 2 \cdot CO_3^{2-}(aq) + Cl_{(aq)}^- \quad (26)$$

where $Na_{(aq)}^+$ and $Cl_{(aq)}^-$ are the concentrations of the positive and negative counter-ions, respectively assuming that all compounds supplemented in the wastewater are added in the form of sodium or chloride salts. Equation (26) is used to calculate the pH of the wastewater during denitrification.

The chemical species consumed or produced during microbial denitrification affect the concentration of the soluble metal ions in the wastewater. As the concentration of nitrates and nitrites decreases, the concentration of hydroxyl ions increases, shifting the pH of the waste-

Table 1
Solubility product constants for selected metal ions for metal hydroxides and carbonates (Speight, 2017).

Metal ion	$Me(OH)_2$	$MeCO_3$
Ca^{2+}	$5.50 \cdot 10^{-6}$	$2.80 \cdot 10^{-9}$
Cu^{2+}	$2.20 \cdot 10^{-20}$	$1.40 \cdot 10^{-10}$
Fe^{2+}	$4.87 \cdot 10^{-17}$	$3.13 \cdot 10^{-11}$
Ni^{2+}	$5.48 \cdot 10^{-16}$	$1.42 \cdot 10^{-7}$
Zn^{2+}	$3.00 \cdot 10^{-17}$	$1.46 \cdot 10^{-10}$

water to more alkaline values. In addition, the oxidation of the carbon from the organic substrate produces CO_2 which is kept dissolved in the wastewater forming HCO_3^- according to equation (11). Therefore, the mobility of the divalent metal ions is considered to be controlled mainly by the precipitation reactions (27) and (29):

$$Me^{2+}_{(aq)} + 2\ OH^-_{(aq)} \rightleftarrows Me(OH)_{2(s)} \quad (27)$$

with solubility constant:

$$K_{sp\ Me(OH)_2} = Me^{2+}_{(aq)} \cdot {OH^-_{(aq)}}^2 \quad (28)$$

$$Me^{2+}_{(aq)} + CO^{2-}_{3(aq)} \rightleftarrows MeCO_{3(s)} \quad (29)$$

with solubility constant:

$$K_{sp\ MeCO_3} = Me^{2+}_{(aq)} \cdot CO^{2-}_{3(aq)} \quad (30)$$

where $Me^{2+}_{(aq)}$ is the concentration of the divalent metal ion such as Ca^{2+}, Cu^{2+}, Fe^{2+}, Ni^{2+} and Zn^{2+} present in the wastewater, and $K_{sp\ Me(OH)_2}$ and $K_{sp\ MeCO_3}$ the corresponding solubility constants for metal hydroxides and carbonates, respectively. Values of $K_{sp\ Me(OH)_2}$ and $K_{sp\ MeCO_3}$ for the studied metals are presented in Table 1.

A metal ion could potentially precipitate in the solid phase in the form of $Me(OH)_2$ or $MeCO_3$ respectively when the corresponding saturation index (SI) under particular reactor operating conditions exceeds one. Therefore, in the model we consider that a metal ion precipitates when:

$$SI_{Me(OH)_2} = \frac{Me^{2+}_{(aq)} \cdot \left(OH^-_{(aq)}\right)^2}{K_{sp\ Me(OH)_2}} > 1 \quad (31)$$

$$SI_{MeCO_3} = \frac{Me^{2+}_{(aq)} \cdot CO^{2-}_{3(aq)}}{K_{sp\ MeCO_3}} > 1 \quad (32)$$

where $SI_{Me(OH)_2}$ and SI_{MeCO_3} are the saturation indices of $Me(OH)_2$ or $MeCO_3$, respectively. Inversely, we consider that an already formed solid phase, which has been already precipitated and retained in the reactor, could potentially dissolve when the corresponding saturation index under particular reactor operating conditions is less than one.

3.4. Model implementation

The set of equations presented in sections 3.1 to 3.3 constitute a system of differential-algebraic equations (DAE) which should be numerically solved simultaneously. The model has been implemented in AQUASIM (Reichert, 1994). AQUASIM (https://www.eawag.ch/en/department/siam/software/) is a freely available versatile software which can simulate biological and chemical processes in various compartments among which the mixed reactor, the biofilm reactor, the advective-diffusive reactor, the saturated soil, the river section, the lake, and the sediment compartments (Reichert, 1998). The compartments can be linked by diffusive or advective flows to simulate the particular process flowsheet. A typical workflow with AQUASIM is presented in Fig. S1. In the present configuration, as shown in Fig. 1, both the holding vessel (1) and the bioreactor (2) are simulated as a continuous flow stirred tank compartments. However, it is assumed, that denitrification occurs only in the bioreactor compartment and that no chemical or biological reactions occur in the holding vessel. The assumption is valid because the biofilm reactor holds significantly more biomass than the suspended planktonic biomass in the holding vessel. The compartments are connected with two advective links: (a) The feed flow link from the holding vessel to the inflow of the bioreactor, and (b) The return flow from the outflow of the bioreactor to the holding vessel. Therefore, the outflow of the bioreactor affects the inflow of the holding vessel while the output of the holding vessel affects the inflow of the bioreactor. This specific setup of periodic initial conditions in the two compartments creates significant difficulties when initiating the numerical integration algorithms in AQUASIM. To address these limitations, the simulated flowsheet includes a small dummy continuous input in the holding vessel and a corresponding small dummy continuous output from the bioreactor, allowing the closed loop to function as an internal recirculation pattern within an open flow system.

Another significant concern in simulating models using a system of differential algebraic equations (DAE) is the numerical stability of the algorithms, which can be affected by the combination of slow microbial growth processes and instantaneous chemical equilibrium reactions. Solving these stiff equations necessitates the use of specialized algorithms. However, a common workaround is to convert the instantaneous chemical reactions into fast dynamic processes that occur many times faster than the slower biological reactions that govern the overall reaction rates of the process. For example, for the fast dissociation reaction of water (equation (24)) the corresponding fast kinetic equation could be described by equation (33):

$$r_{H^+} = r_{OH^-} = k_{H_2O} \cdot (K_w - H^+ \cdot OH^-) \quad (33)$$

where r_{H^+} and r_{OH^-} are the volumetric rates of H^+ and OH^- production, respectively and k_{H_2O} is an apparent kinetic constant multiple times greater than the specific growth rates of the microorganism. At equilibrium, where the rates of H^+ and OH^- production are zero, equation (33) is equivalent to equation (25).

In a similar manner, the rate of metal precipitation as metal carbonate is written in the model by the equation (34):

$$r_{MeCO_3\ precip} = k_{MeCO_3\ precip} \cdot \left(Me^{2+}_{(aq)} \cdot CO^{2-}_{3(aq)} - K_{sp\ MeCO_3}\right) \quad (34)$$

while the rate of dissolution of metal carbonate correspondingly is given by the equation (35):

$$r_{MeCO_3\ dissol} = k_{MeCO_3\ dissol} \cdot \left(K_{sp\ MeCO_3} - Me^{2+}_{(aq)} \cdot CO^{2-}_{3(aq)}\right) \quad (35)$$

where $r_{MeCO_3\ precip}$ and $r_{MeCO_3\ dissol}$ are the volumetric rates of metal (Me^{2+}) precipitated or dissolved as $MeCO_3$, and $k_{MeCO_3\ precip}$ and $k_{MeCO_3\ dissol}$ are the corresponding apparent kinetic coefficients, respectively. Similar equations apply for the case of precipitated or dissolved $Me(OH)_2$.

Table 2 and Table 3 present the Petersen matrices of the biotic and abiotic processes included in the model. Water produced from reactions (4) and (8) is not included in the tables as does not affect the speciation of the metals in the wastewater. A list of variables included in the model is presented in Table S1.

3.5. Model calibration

Model calibration is an important step in the model development process, as it allows the model to be fine-tuned to better represent the real-world system or the processes being modeled. The goal of calibration is to find the set or the range of parameter values that produce the best agreement between the model's predictions and the observed data. Optimization-based calibration uses mathematical optimization algorithms to find the optimal parameter values that minimize the difference between the model's predictions and the observed data. However, there are several difficulties that can arise during optimization-based model calibration, including (Dochain and Vanrolleghem, 2001; Marsili-Libelli, 2018):

(a) Local minima: Optimization algorithms can get trapped in local minima, which are solutions that are not the global optimum. This can result in suboptimal parameter estimates.
(b) Sensitivity to initial values: The performance of optimization algorithms can depend heavily on the initial values of the

Table 2
Petersen matrix of the biotic processes included in the model.

		Component								
		Organic substrate $C_xH_yO_zN_w$	NO_3^-	NO_2^-	H^+	NH_4^+	Biomass $C_5H_7O_2N$	HCO_3^-	N_2	Reaction rate
Biotic Process	Nitrate reduction to nitrite	$-\frac{1}{4x+y-2z-3w}$	$-\frac{1-f_s}{2}$	$\frac{1-f_s}{2}$	$-\left((1-f_s)+\frac{24f_s}{20}-\frac{5x+y-2z-4w}{4x+y-2z-3w}\right)$	$-\left(\frac{f_s}{20}-\frac{w}{4x+y-2z-3w}\right)$	$\frac{f_s}{20}$	$\frac{x}{4x+y-2z-3w}-\frac{5f_s}{20}$		$\mu_{max,NO_3}\cdot\frac{C_{org}}{K_{sorg}+C_{org}}\cdot\frac{C_{NO_3}}{K_{NO_3}+C_{NO_3}}\cdot X$
	Nitrite reduction to nitrogen	$-\frac{1}{4x+y-2z-3w}$		$-\frac{1-f_s}{3}$	$\frac{4(1-f_s)}{3}+\frac{24f_s}{20}-\frac{5x+y-2z-4w}{4x+y-2z-3w}$	$\frac{w}{4x+y-2z-3w}-\frac{f_s}{20}$	$\frac{f_s}{20}$	$\frac{x}{4x+y-2z-3w}-\frac{5f_s}{20}$	$\frac{1-f_s}{6}$	$\mu_{max,NO_2}\cdot\frac{C_{org}}{K_{sorg}+C_{org}}\cdot\frac{C_{NO_2}}{K_{NO_2}+C_{NO_2}}\cdot X$

Table 3
Petersen matrix of the abiotic processes included in the model.

	Component (Me^{2+} metal ions such as Ca^{2+}, Cu^{2+}, Fe^{2+}, Ni^{2+} and Zn^{2+})											
Abiotic processes		H_2CO_3	HCO_3^-	CO_3^{2-}	H^+	NH_4^+	NH_3	OH^-	H_2O	Me^{2+}	$Me(OH)_2$	$MeCO_3$	Reaction rate
	Carbonic acid dissociation to bicarbonate	−1	+1		+1								$k_{H_2CO_3}\cdot(K_{a1(H_2CO_3)}\cdot H_2CO_3^*(aq)-H^+_{(aq)}\cdot HCO_{3(aq)}^-)$
	Bicarbonate dissociation to carbonate		−1	+1	+1								$k_{HCO_3}\cdot(K_{a2(H_2CO_3)}\cdot HCO_3^-(aq)-H^+_{(aq)}\cdot CO_3^{2-}(aq))$
	Ammonium dissociation				+1	−1	+1						$k_{NH_4}\cdot(K_{a1(NH_4^+)}\cdot NH_4^+(aq)-H^+_{(aq)}\cdot NH_{3(aq)})$
	Water dissociation				+1			+1	−1				$k_{H_2O}\cdot(K_w-H^+\cdot OH^-)$
	$Me(OH)_2$ precipitation							−2		−1	+1		$k_{Me(OH)_2\ precip}\cdot(Me^{2+}_{(aq)}\cdot(OH^-)^2_{(aq)}-K_{sp\ Me(OH)_2})$
	$Me(OH)_2$ dissolution							+2		+1	−1		$k_{Me(OH)_2\ dissol}\cdot(K_{sp\ Me(OH)_2}-Me^{2+}_{(aq)}\cdot(OH^-)^2_{(aq)})$
	$MeCO_3$ precipitation			−1						−1		+1	$k_{MeCO_3\ precip}\cdot(Me^{2+}_{(aq)}\cdot CO^{2-}_{3(aq)}-K_{sp\ MeCO_3})$
	$MeCO_3$ dissolution			+1						+1		−1	$k_{MeCO_3\ dissol}\cdot(K_{sp\ MeCO_3}-Me^{2+}_{(aq)}\cdot CO^{2-}_{3(aq)})$

parameters. If the initial values are not chosen carefully, the optimization may converge to a suboptimal solution.

(c) Computational time: Optimization algorithms can be computationally intensive, and the time required to find the optimal solution can be long, especially for complex models with many parameters.

(d) Numerical instability: Optimization algorithms can be sensitive to the numerical stability of the model. If the model is not well-behaved, the optimization may fail to converge or produce unreliable results.

(e) Overfitting: If the model is too complex and has too many parameters, it can lead to overfitting, where the model fits the noise in the data and not the underlying relationship.

(f) Lack of uncertainty quantification: Many optimization-based calibration methods do not provide uncertainty quantification of the model parameters.

(g) Lack of robustness: Optimization-based calibration methods can be sensitive to outliers or errors in the data.

AQUASIM provides the appropriate environment for parameters fitting and sensitivity analysis. However, in multiparametric models there is always the issue of the parameter's identification as multiple sets of parameters may fit equally well the experimental data (Reichert, 1994, 1998).

4. Results and discussion

4.1. Estimation of biokinetic parameters

The literature reports a broad range of biokinetic parameters for denitrification. Based on various carbon/electron donors, Table 4 presents example ranges for the values of the maximum specific growth rate (μ_{max}) for microbial denitrification. The values vary with the type of organic source/electron donor, the temperature, and the microbial culture (pure strain or mixed culture). Less biokinetic data is available for the intermediate stages of microbial denitrification. For example, the values of maximum specific growth rates are reported as 0.434 d^{-1} for

Table 4
Maximum specific growth rates for nitrate reduction for different carbon/electron donors.

Carbon source/Electron donor	(μ_{max}) for nitrate reduction (d^{-1})	Reference
Methanol	0.52 (10 °C) - 1.86 (20 °C)	(Stensel et al., 1973)
	0.4–0.5 (13 °C) - 1.0 (19 °C)	(Mokhayeri et al., 2006)
	0.56 (13 °C) - 6.29 (20 °C)	(Dold et al., 2005)
	0.77 (15 °C) - 2.06 (20 °C)	(Christensson et al., 1994)
	0.67–1 (15 °C)	(Lee and Welander, 1996)
	0.52 (10 °C) −1.86 (20 °C)	(Tchobanoglous et al., 2003)
	0.34 (10 °C) - 1.25 (20 °C)	(Onnis-Hayden and Gu, 2008)
	1.86	Rittmann and McCarty (2020)
	7.92	(Grady et al., 2011)
	0.3–1.3	(Cherchi et al., 2009)
	0.50	(Foglar et al., 2005)
Ethanol	1.89 (15 °C) - 4.8 (25 °C)	(Christensson et al., 1994)
Acetate	1.2 (13 °C) - 3.5 (19 °C)	(Mokhayeri et al., 2006)
	2.18 (15 °C)	(Lee and Welander, 1996)
Sucrose	7.4	(Petrović et al., 2015)
Municipal wastewater	3.12	Rittmann and McCarty (2020)
	3.60	(Stensel and Horne, 2000)
	3.20	(Phillips et al., 2009)
Sludge	0.61	(Æsøy and Ødegaard, 1994)
Corn Syrup	1.3 (13 °C) - 3.7 (19 °C)	(Mokhayeri et al., 2006)
Dairy waste	1.91	(Onnis-Hayden and Gu, 2008)
Winery waste	1.43	(Onnis-Hayden and Gu, 2008)
Brewery waste	1.08	(Onnis-Hayden and Gu, 2008)
Beet-sugar waste	1.89	(Onnis-Hayden and Gu, 2008)
Hydrogen	1.36	(Rittmann and McCarty, 2020)
Sulfur	0.81	(Rittmann and McCarty, 2020)

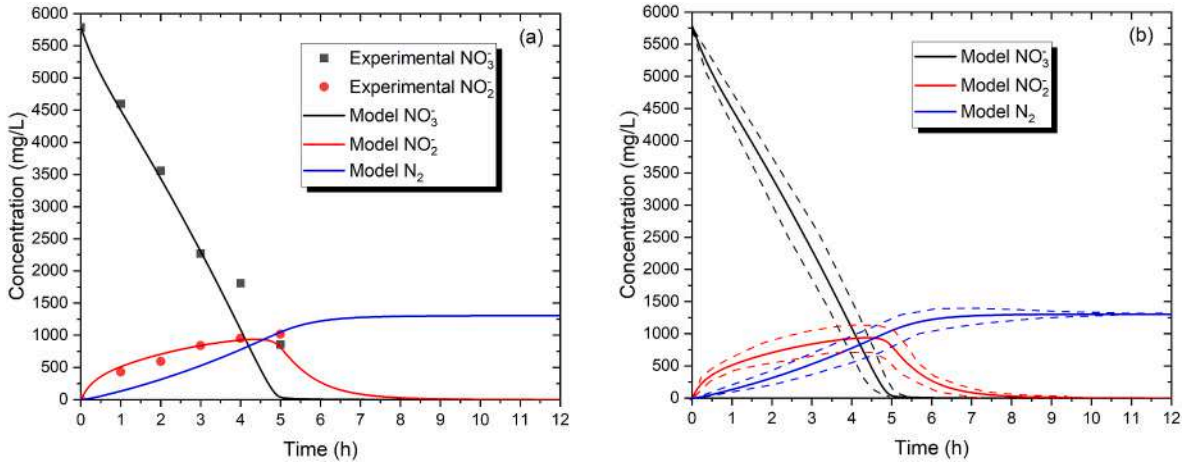

Fig. 2. (a) Example concentration profiles for nitrate, nitrite and nitrogen. Experimental results and model simulation; (b) Sensitivity analysis of the kinetic profiles during nitrate reduction.

the reduction of nitrate to nitrite and 0.121 d^{-1} for the reduction of nitrite to nitrogen, respectively (Lin and Gu, 2020).

The best fit parameters of our model for reproducing the kinetic profiles for nitrate reduction at 6000 mg/L NO_3^- (Fig. 2(a)) are $\mu_{max,NO3}$ = 0.35 h^{-1} (8.4 d^{-1}) and $\mu_{max,NO2}$ = 0.55 h^{-1} (13.2 d^{-1}) for the two stages of denitrification, respectively. These values are in the upper range of the values shown in Table 4, despite the fact that μ_{max} values for bacto peptone and yeast extract have not been published in the literature. However our estimates are comparable to the values of high energy molecules such as sucrose (μ_{max} = 7.4 d^{-1}) (Petrovič et al., 2015). In addition, the higher values can be justified if we consider that the nutrient medium used for denitrification as supplement in the wastewater is the one advised from DSMZ for optimal microbial growth of *H. denitrificans*. Furthermore, the acclimatization of the microbial culture in the wastewater environment for more than three years ensures that the microbial culture grows under optimal conditions. Nevertheless, it should be realized, that the uncertainty in the estimation of the biomass concentration, which is grown in the reactor environment, particularly inside the pores of the porous carrier, directly impacts the uncertainty in the estimation of the values of μ_{max}. The Monod kinetic equations (9) and (10) indicate that the product $\mu_{max} \cdot X$ can be kept constant by inversely changing the values of the two variables. As a result, the precision of the estimates of μ_{max} is dependent on the precision of the estimates of X.

In terms of the half saturation constant, literature provides a wide range of values in different units. For example, K_{sorg} is reported as: (a) for municipal wastewater 8.6 mg COD/L (Stensel and Horne, 2000), 1 mg/L (Rittmann and McCarty, 2020) and 5 mg/L (Phillips et al., 2009); (b) for methanol 9.1 mg donor/L (Rittmann and McCarty, 2020), 4.4 mg/L (Grady et al., 2011), 5 mg COD/L (Onnis-Hayden and Gu, 2008) and 15.6 mg COD/L (Cherchi et al., 2009); and (c) for acetate 38.1 mg COD/L (Cherchi et al., 2009). In our model the best fit parameter for K_{sorg}, which fits most of the experimental data series, is $2 \cdot 10^{-3}$ mol/L for the mixture of the peptones and yeast extract.

The Monod half saturation constant for nitrate reduction to nitrite (K_{NO_3}) is reported as 226.35 mg NO_3–N/L ($16.2 \cdot 10^{-3}$ mol NO_3^-/L) (Lin and Gu, 2020), 0.1 mg NO_3–N/L ($7.1 \cdot 10^{-6}$ mol NO_3^-/L) (Phillips et al., 2009) and as ranging between 0.1 and 0.2 mg NO_3–N/L (Grady et al., 2011). The corresponding value for nitrite to nitrogen (K_{NO_2}) is reported as 4.23 mg NO_2–N/L ($0.302 \cdot 10^{-3}$ mol NO_2^-/L) (Lin and Gu, 2020). The best fit values in our model are 0.02 mol NO_3^-/L for both K_{NO_3} and K_{NO_2}, respectively, which fits most of the experimental data series. Table 5 summarizes the best fit biokinetic parameters for the case of nitrate reduction at initial concentration 6000 mg/L NO_3^-.

4.2. Nitrate/nitrite kinetic profiles

Fig. 2(a) presents kinetic data for the reduction of nitrate at initial concentration 6000 mg/L NO_3^- in the bioreactor. In the same figure, the concentration of nitrite as intermediate product of nitrate reduction is shown. Both concentration profiles follow the pattern of reactions in series where the product of the first reaction (NO_2^-) is used as reactant in the second. Complete reduction of nitrate takes place within 5 h while the intermediate nitrite is completely reduced in 8 h. The solid lines depicted in the same figure represent the simulation of the experimental data by the model. The model predicts also the concentration profile of nitrogen gas produced by the reduction of nitrite, although N_2 concentration was not monitored experimentally. In the first 5 h the concentration of nitrite is the result of nitrite production from reaction (4) and concomitant nitrite consumption from reaction (8). Once nitrate has been completely reduced, nitrite is no longer produced, thus the concentration profile is determined solely by the kinetics of nitrite reduction. During nitrate reduction, nitrite concentration does not increase above 1000 mg/L indicating that the reduction of nitrite proceeds in parallel with the reduction of nitrate. This suggests that the strain *Halomonas denitrificans* is capable of completely reducing both NO_3^- and NO_2^- simultaneously. It is also beneficial for the proposed treatment process that the final product of nitrogen reduction is a harmless, inert gas that can be safely released into the environment.

In uncertainty analysis, the uncertainty of model parameters is propagated to the uncertainty of model results. Fig. 2(b) presents the sensitivity of the model on the values of $\mu_{max,NO3}$ and $\mu_{max,NO2}$. The solid lines represent the simulated concentration profiles of nitrate, nitrite and nitrogen on the best fit values. The dash lines represent the response of the model by ± one standard deviation when both parameters $\mu_{max\ NO3}$ and $\mu_{max\ NO2}$ vary by ±10% (Reichert, 1998).

4.3. pH variation

Fig. 3 presents an example of simulated pH profile. The pH of the medium increases from 3.5 to 6 within less than an hour. This outcome is expected, as the reduction of nitrate to nitrite according to reaction (4)

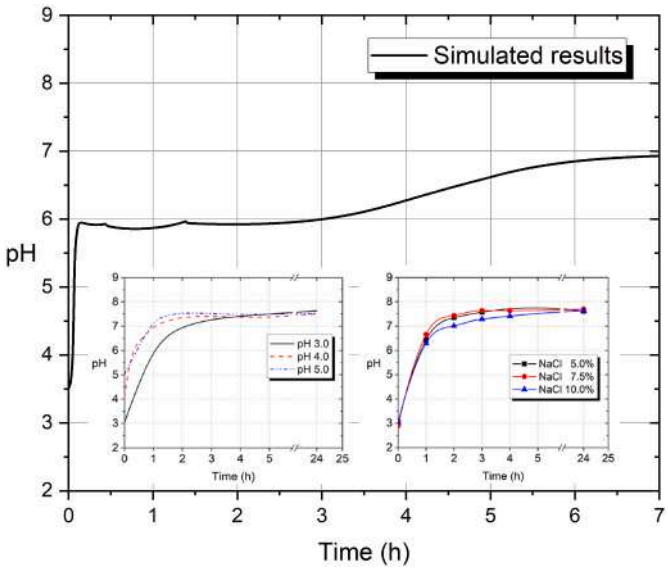

Fig. 3. Simulated pH profile during nitrate reduction. Insert figures at the bottom show experimental pH profiles at different initial pH values (left) and different salinity levels as expressed by the concentration of NaCl (right) (Mendrinou et al., 2021).

Table 5
Best fit biokinetic parameters for nitrate reduction at initial concentration 6000 mg/L NO3-.

Parameter	Symbol	Value	Units
Maximum specific growth rate for reduction of nitrate to nitrite	μ_{max,NO_3}	0.35	h^{-1}
Maximum specific growth rate for reduction of nitrite to nitrogen	μ_{max,NO_2}	0.55	h^{-1}
Monod half-saturation constant for organic substrate	K_{sorg}	0.002	mol/L
Monod half-saturation constant for nitrate	K_{NO_3}	0.02	mol/L
Monod half-saturation constant for nitrite	K_{NO_2}	0.02	mol/L
Fraction of electrons captured for biomass synthesis	f_s	0.50	–
Concentration of biomass	X	3500	mg/L

results in the consumption of protons and the production of bicarbonate ions. As a result, the pH of the wastewater rapidly shifts from the initial pH to more alkaline values. The reduction of nitrite to nitrogen, which is described by reaction (8), results in the formation of additional bicarbonate ions which neutralize the protons that are released. The overall balance of cations and anions, as described by equation (26) and the hydrolysis reactions discussed in section 3.3, is used to calculate the pH during the denitrification process. As illustrated in Fig. 3, the model predicts a final equilibrium pH of around 7, which deviates by 0.5 unit from the experimentally observed pH of around 7.5 (as shown in the inserts of Fig. 3). The slight deviation in pH can be attributed to other acid/base reactions that have not been taken into account in the model, such as the reactions between protons and the amino groups of the peptone used as a carbon source. The equilibrium constants for these reactions are not known.

4.4. Fate and mobility of metal ions – metal detoxification mechanism

The proposed treatment process aims to accomplish two objectives: (a) to completely reduce nitrates in the presence of metal ions, which may hinder microbial activity due to metal toxicity, and (b) to simultaneously sequester trace metals present in the wastewater through biological means. It has been experimentally and theoretically demonstrated that the pH and alkalinity of the wastewater increase significantly during biological denitrification (Mendrinou et al., 2021). The formation of insoluble compounds such as $Me(OH)_2$ and $MeCO_3$, facilitated by inorganic scavengers like OH^- and HCO_3^-, is the primary mechanism of trace metal removal known as biomineralization (Rajasekar et al., 2021; Reddy, 2013; Ren et al., 2023) or bioprecipitation (Benzerara, 2011; Remoudaki et al., 2007). Bioprecipitation acts as a complementary mechanism to biosorption, which is the process in which microorganisms remove pollutants from a liquid stream by adsorbing chemical species onto their surface (Tsezos, 2014). Research has shown that both bioprecipitation and biosorption contribute to the removal of metal ions in a moving bed sand filter (Remoudaki et al., 2003b) and the treatment of acidic metal bearing wastewater by sulfate reducing bacteria through the production of HS^- as a result of sulfate reduction (Kousi et al., 2011; Remoundaki et al., 2008).

During denitrification, the levels of soluble metal ions in the reactor were monitored as the concentration of nitrate was reduced over time (Mendrinou et al., 2021). Zn^{2+}, Cu^{2+}, and Fe^{2+} were removed from the synthetic wastewater within 6–24 h, even at the highest concentration levels tested up to 100 mg/L. However, Ni remained soluble for extended time at the same conditions, suggesting that the excess of OH^- or HCO_3^- in an organic rich environment does not lead directly to the formation of insoluble inorganic Ni precipitates. This has been largely attributed to complexing organic ligands which compete with OH^- or HCO_3^- and originate from the functional groups of the peptone hydrolysates or from simpler metabolic products formed during peptone catabolism (Mendrinou et al., 2021). Similar behavior regarding the precipitation of chromium has been observed in the presence of organic molecules (Remoudaki et al., 2003a; Remoundaki et al., 2007).

Fig. 4 illustrates the simulated concentration profiles for the soluble Fe^{2+}, Cu^{2+}, Zn^{2+}, Ni^{2+}, and Ca^{2+}, and the corresponding metal precipitates that are formed. The simulation results suggest that in the presence of carbonates and at pH around 7, the precipitated metal carbonates ($MeCO_3$) are dominant than the corresponding metal hydroxides $Me(OH)_2$. According to the solubility product constants for $MeCO_3$ presented in Table 1, for equimolar initial concentration of Fe^{2+}, Cu^{2+}, Zn^{2+}, Ni^{2+}, and Ca^{2+}, the order of formation of the insoluble $MeCO_3$ should be $FeCO_3 > ZnCO_3 \approx CuCO_3 > CaCO_3 \gg NiCO_3$. However, it is important to note that this order may vary significantly depending on factors such as the rates of nucleation and crystal growth, as well as the influence of physical factors such as the temperature and the pressure (in geological condition), and chemical factors such as the presence of other dissolved ions or organic moieties in the solution. Additionally, there is a significant degree of uncertainty when it comes to the solubility values of different crystallographic carbonate solids, as the solubility product constant of calcite ($3.36 \cdot 10^{-9}$) differs from that of aragonite ($6 \cdot 10^{-9}$) (Speight, 2017). It should be noted also that while calcium is not typically considered as toxic metal, its presence in wastewater can have negative effects on the long-term operation of the reactor. The formation

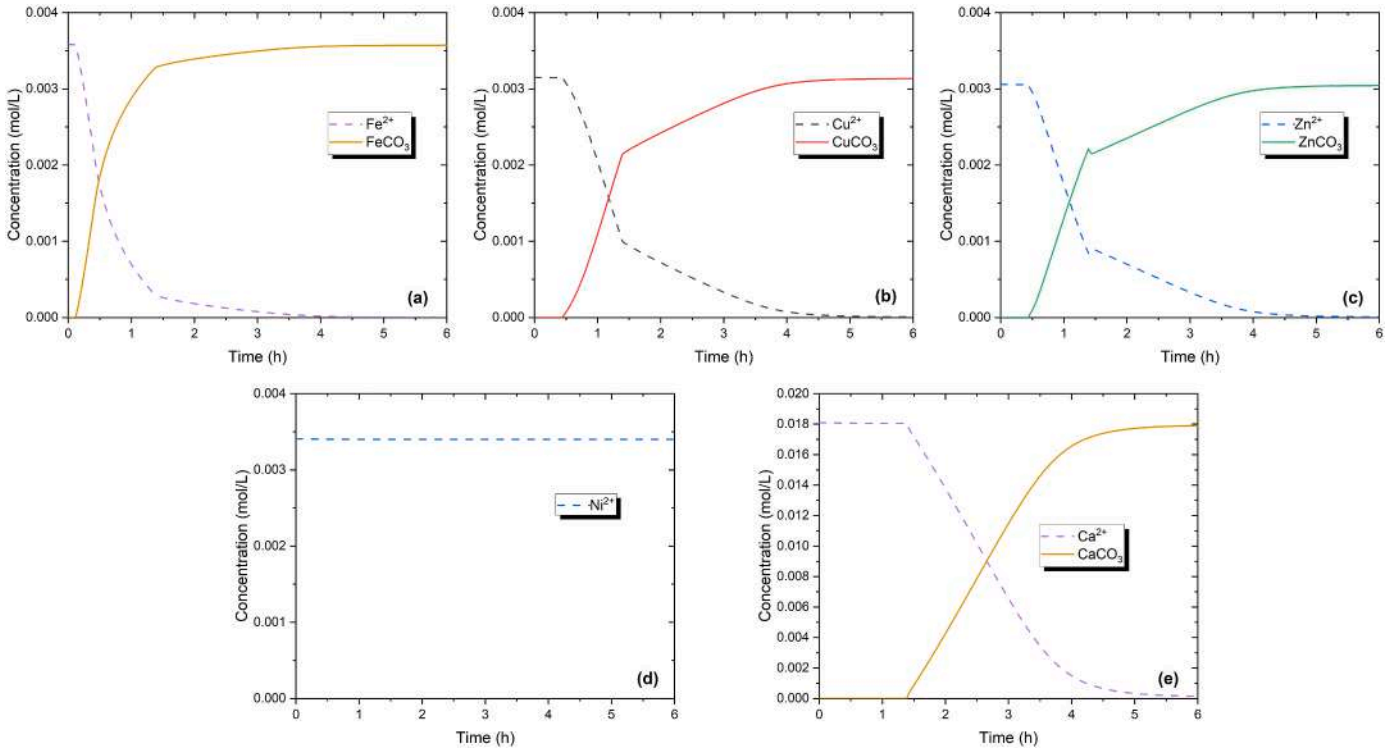

Fig. 4. Simulated concentration profiles for Fe, Cu, Zn, Ni and Ca and the corresponding precipitates.

of large amounts of calcium carbonate precipitates can clog the pores of the reactor, create a calcite crust over the cells, and decrease the reactor's efficiency. This may be a concern particularly when wastewater is rich in calcium or whenever calcium is added as an amendment for microbial growth.

Biomineralization is also reported in the work of (Ren et al., 2023) who have studied the fate of Ca^{2+} and Cd^{2+} in a hydrogel microbial reactor under nitrate reducing conditions. The authors confirm by X-ray diffraction (XRD) that the sediments contained $CaCO_3$, $CdCO_3$ and $Ca_5(PO_4)_3OH$ by a mechanism referred as microbially induced calcite precipitation (MICP). In a similar research, Ca^{2+}, trace concentrations of Ni^{2+} and nitrate are simultaneously removed by forming calcium-precipitated bio-crystals and $NiCO_3$ precipitates with parallel removal of nitrate (Liu et al., 2021). The biomineralization activity of *Neurospora crassa* for the precipitation of Ca^{2+} is also studied in the work of (Li et al., 2014) who reported that over 90% of Ca^{2+} could be removed from the media by the fungal biomass. In a similar study, the same fungus has been used for the precipitation of cerium as Ce carbonate $Ce_2(CO_3)_3{\cdot}8H_2O$ (Kang et al., 2022). Finally, in the review paper of (Rajasekar et al., 2021) the factors affecting MICP are summarized and the importance of biomineralization as a remediation technique for the removal of heavy metals is presented. However, to the best of our knowledge, the present paper is one of the few works which attempt to model the microbially induced metal precipitation under denitrifying conditions in high salinity environment.

The solubility of Fe^{2+}, Cu^{2+}, Zn^{2+}, Ni^{2+}, and Ca^{2+}, was also studied with Visual MINTEQ version 4 (https://vminteq.com/) at concentrations of 1 mM of each metal in the presence of 10 mM total inorganic carbon - expressed as carbonate - at different pH. The composition of the medium simulates the operating conditions. The saturation indices of different candidate minerals are illustrated in Fig. 5. For the case of Fe^{2+}, Siderite ($FeCO_3$) can be precipitated in the pH range 6.5–10. Above pH 11 the dominant precipitate is crystalline $Fe(OH)_2$. Copper can precipitate in the form of Malachite ($Cu_2CO_3(OH)_2$) at the pH range 5.5–8, while at pH 9 and above the precipitate of CuO dominates. Mixed mineral forms such as Malachite have not been included in the model. All other mineral phases of copper are undersaturated in the pH range 4.5–12. Zinc can form many alternative minerals among which Smithsonite ($ZnCO_3$) at pH range 6–8 substituted by Hydrozincite ($Zn_5(CO_3)_2(OH)_6$) at pH 9.5–10 and finally replaced by Zincite (ZnO) at pH above 11. $Zn(OH)_2$ precipitates are not favored under these conditions. Nickel could be also potentially precipitated as $NiCO_3$ in the pH range 6–9 which then is substituted by $Ni(OH)_2$ at pH above 10. Finally, calcium precipitates are dominated by the formation of Calcite ($CaCO_3$) at pH above 7.5 as shown in the SEM images and EDS spectra in Fig. S2.

To clarify further the likelihood of precipitate formation during denitrification due to alkalinity production and wastewater neutralization, we evaluated the influence of simple organic molecules on saturation indices. Table S2 shows the effect of increasing citric acid concentration on saturation indices of various potential minerals at the bioreactor's operating pH of 7.5. The results indicate that the progressive increase of citric acid concentration reduces the concentration of the wastewater with unbound metal ions, which could potentially lead to mineral precipitation. This trend can also be observed with other organic complexing agents like lactic acid, amino acids, and proteins (Remoudaki et al., 2003a; Remoundaki et al., 2007). However, this metal-ligand interaction is frequently neglected due to the high number of organic molecules present in a wastewater, their unknown nature and the uncertainty of the stability constants of these complexes.

Understanding and predicting the kinetics of metal precipitation is also essential for incorporating them into the model. In our model, a simple, fast linear relationship has been used which predicts faster precipitation for the minerals that are further from the equilibrium saturation state (equation (34)). Similar linear equation is used for the dissolution reactions (equation (35)). However, this approach cannot always depict the reality as there are cases where the precipitation kinetic is slow, non-linear or the metal appear dissolved even at a saturation index above one.

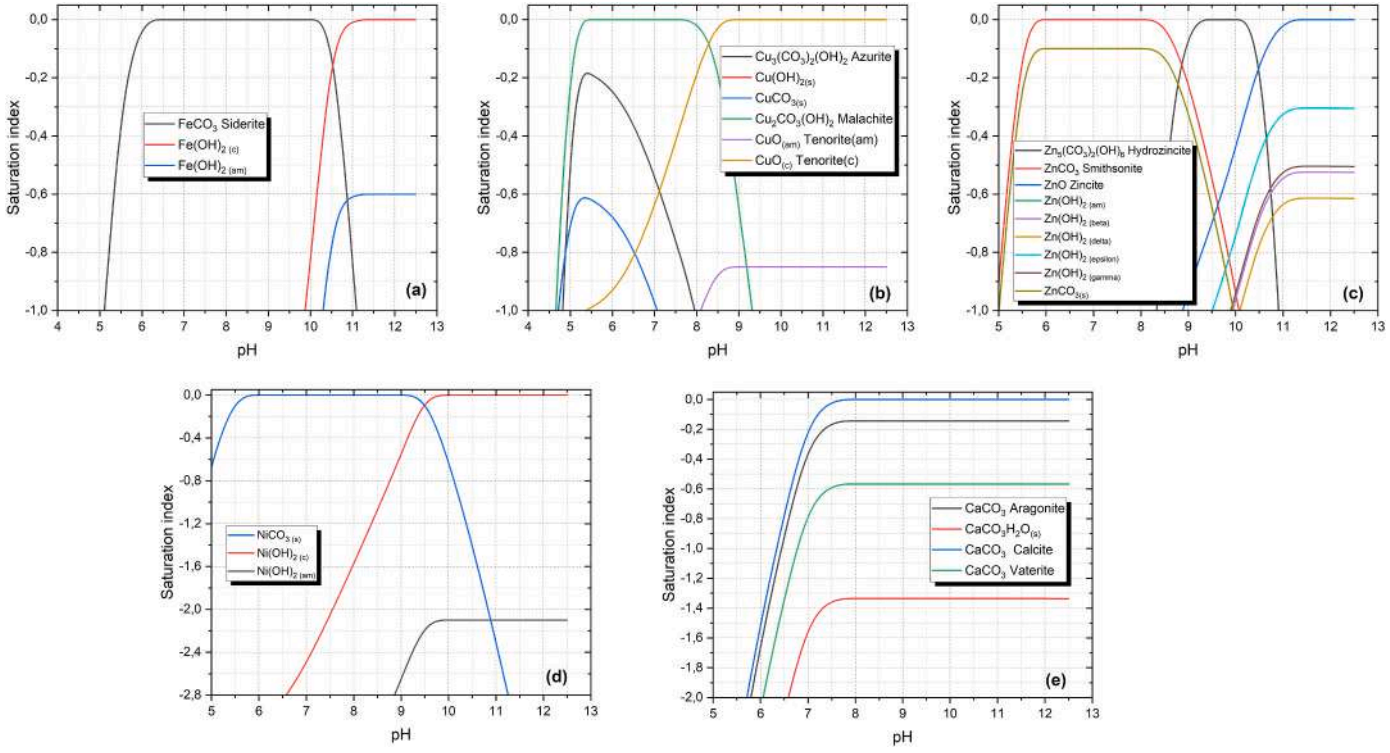

Fig. 5. Saturation indices of various minerals for Fe, Cu, Zn, Ni and Ca at concentration 1 mM in the presence of 10 mM total inorganic carbon (simulation results by visual MINTEQ).

5. Conclusions

This work presents a fundamental mathematical model for the biological treatment of synthetic wastewater containing nitrates, chlorides and metal ions simulating the wastewater originating from hydrometallurgical treatment of printed circuit boards for the recovery of base and precious metals. Abiotic chemical reactions supplement the main biological actions that simulate the reduction of nitrate to nitrite and eventually to elemental nitrogen. Microbial denitrification alters the chemical environment of the treated wastewater, which has a direct impact on metal ions mobility. Except nickel which remains soluble to a great extent, metal ions such as iron, copper and zinc as well as non-toxic metals such as calcium are removed from the wastewater by the mechanism of bioprecipitation. The accuracy of the model is limited by the available information provided and included in the model concerning the kinetics and the equilibrium of the abiotic reactions. Additional uncertainties could be identified in the biological actions as the denitrification process is described by overall stoichiometric reactions. Nevertheless, AQUASIM, as a model developing platform, facilitates the expansion of the model by enabling the simulation of specific experimental flowsheets, the incorporation of additional biological or physical processes according to the availability of the data, the fit of the model parameters to experimental data and also the determination of the process uncertainties.

Credit author statement

Assistant Professor Artin Hatzikioseyian: Conceptualization, model development, data curation, validation, visualization, writing - original draft, reviewing & editing; Panagiota Mendrinou: Design of experiments, data acquisition, model development, data curation, writing - original draft, reviewing & editing; Dr. Pavlina Kousi: Data curation, formal analysis, validation, visualization, writing - reviewing & editing; Professor Emmanouela Remoundaki: Project administration, funding acquisition, conceptualization reviewing & editing.

Declaration of competing interest

The authors declare the following financial interests/personal relationships which may be considered as potential competing interests: Panagiota Mendrinou reports financial support was provided by European Regional Development Fund of the European Union and Greek national funds through the Operational Program Competitiveness, Entrepreneurship and Innovation. State Scholarships Foundation of Greece (IKY).

Data availability

Data will be made available on request.

Acknowledgements

The experimental part of this study has been co-financed by the European Regional Development Fund of the European Union and Greek national funds through the Operational Program Competitiveness, Entrepreneurship and Innovation, under the call RESEARCH – CREATE – INNOVATE (project code: T1EDK-00219). Ms. P. Mendrinou also acknowledges the financial support she received from the State Scholarships Foundation of Greece (IKY) for the implementation of her doctoral thesis which was co-financed by Greece and the European Union (European Social Fund-ESF) through the Operational Programme "Human Resources Development, Education and Lifelong Learning" in the context of the Act "Enhancing Human Resources Research Potential by undertaking a Doctoral Research" Sub-action 2: IKY Scholarship Programme for PhD candidates in the Greek Universities".

Appendix A. Supplementary data

Supplementary data to this article can be found online at https://doi.org/10.1016/j.jenvman.2023.118285.

References

Æsøy, A., Ødegaard, H., 1994. Denitrification in biofilms with biologically hydrolysed sludge as carbon source. Water Sci. Technol. 29 (10–11), 93. https://doi.org/10.2166/wst.1994.0750.

Benzerara, K., 2011. Bioprecipitation. In: Gargaud, M., Amils, R., Quintanilla, J.C., et al. (Eds.), Encyclopedia of Astrobiology. Springer Berlin Heidelberg, Berlin, Heidelberg. https://doi.org/10.1007/978-3-642-11274-4_189, 200-200.

Bhatnagar, A., Kumar, E., Sillanpää, M., 2010. Nitrate removal from water by nano-alumina: characterization and sorption studies. Chem. Eng. J. 163 (3), 317–323. https://doi.org/10.1016/j.cej.2010.08.008.

Bhatnagar, A., Sillanpää, M., 2011. A review of emerging adsorbents for nitrate removal from water. Chem. Eng. J. 168 (2), 493–504. https://doi.org/10.1016/j.cej.2011.01.103.

Burghate, S., Ingole, N., 2014. Biological denitrification—a review. J. Environ. Sci. Comput. Sci. Eng. Technol. 14, 9–28.

Cherchi, C., Onnis-Hayden, A., El-Shawabkeh, I., Gu, A.Z., 2009. Implication of using different carbon sources for denitrification in wastewater treatments. Water Environ. Res. 81 (8), 788–799. https://doi.org/10.2175/106143009x12465435982610.

Christensson, M., Lie, E., Welander, T., 1994. A comparison between ethanol and methanol as carbon sources for denitrification. Water Sci. Technol. 30 (6), 83. https://doi.org/10.2166/wst.1994.0255.

Dochain, D., Vanrolleghem, P., 2001. Dynamical Modelling and Estimation in Wastewater Treatment Processes. IWA Publishing, London.

Dold, P., Murthy, S., Takacs, I., Bye, C., 2005. Batch test method for measuring methanol utilizer maximum specific growth rate. In: Proceedings of the 78th Annual Water Environment Federation Technical Exposition and Conference. Oct, Washington, DC. https://doi.org/10.2175/193864705783814871, 2005.

EPA, 2009. National Primary Drinking Water Regulations under the Safe Drinking Water Act. https://www.epa.gov/ground-water-and-drinking-water/national-primary-drinking-water-regulations.

Felgate, H., Giannopoulos, G., Sullivan, M.J., Gates, A.J., Clarke, T.A., Baggs, E., Rowley, G., Richardson, D.J., 2012. The impact of copper, nitrate and carbon status on the emission of nitrous oxide by two species of bacteria with biochemically distinct denitrification pathways. Environ. Microbiol. 14 (7), 1788–1800. https://doi.org/10.1111/j.1462-2920.2012.02789.x.

Foglar, L., Briški, F., Sipos, L., Vuković, M., 2005. High nitrate removal from synthetic wastewater with the mixed bacterial culture. Bioresour. Technol. 96 (8), 879–888. https://doi.org/10.1016/j.biortech.2004.09.001.

Gerardi, M.H., 2003. Nitrification and Denitrification in the Activated Sludge Process. John Wiley & Sons.

Golterman, H., 2013. Denitrification in the Nitrogen Cycle, vol. 9. Springer Science & Business Media.

González-Domenech, C.M., Martínez-Checa, F., Béjar, V., Quesada, E., 2010. Denitrification as an important taxonomic marker within the genus Halomonas. Syst. Appl. Microbiol. 33 (2), 85–93. https://doi.org/10.1016/j.syapm.2009.12.001.

Grady Jr., C.L., Daigger, G.T., Love, N.G., Filipe, C.D., 2011. Biological Wastewater Treatment. CRC press.

Hirata, A., Nakamura, Y., Tsuneda, S., 2001. Biological nitrogen removal from industrial wastewater discharged from metal recovery processes. Water Sci. Technol. 44 (2–3), 171–180. https://doi.org/10.2166/wst.2001.0767.

Holuszko, M.E., Kumar, A., Espinosa, D.C., 2022. Electronic Waste: Recycling and Reprocessing for a Sustainable Future. John Wiley & Sons.

Kang, X., Csetenyi, L., Gadd, G.M., 2022. Fungal biorecovery of cerium as oxalate and carbonate biominerals. Fungal Biology. https://doi.org/10.1016/j.funbio.2022.07.006.

Kaya, M., 2019. Electronic Waste and Printed Circuit Board Recycling Technologies. Springer.

Khan, A., Asiri, A.M., 2019. E-Waste Recycling and Management: Present Scenarios and Environmental Issues, vol. 33. Springer.

Kim, K.K., Jin, L., Yang, H.C., Lee, S.-T., 2007. Halomonas gomseomensis sp. nov., Halomonas janggokensis sp. nov., Halomonas salaria sp. nov. and Halomonas denitrificans sp. nov., moderately halophilic bacteria isolated from saline water. Int. J. Syst. Evol. Microbiol. 57 (4), 675–681. https://doi.org/10.1099/ijs.0.64767-0.

Kordosky, G.A., 1992. Copper solvent extraction: the state of the art. JOM 44 (5), 40–45. https://doi.org/10.1007/BF03223049.

Kordosky, G.A., 2002. Copper recovery using leach/solvent extraction/electrowinning technology : forty years of innovation, 2.2 million tonnes of copper annually. J. S. Afr. Inst. Min. Metall 102 (8), 445–450. https://doi.org/10.10520/AJA0038223X_2713.

Kousi, P., Remoundaki, E., Hatzikioseyian, A., Battaglia-Brunet, F., Joulian, C., Kousteni, V., Tsezos, M., 2011. Metal precipitation in an ethanol-fed, fixed-bed sulphate-reducing bioreactor. J. Hazard Mater. 189 (3), 677–684. https://doi.org/10.1016/j.jhazmat.2011.01.083.

Kumar, M., Chakraborty, S., 2006. Chemical denitrification of water by zero-valent magnesium powder. J. Hazard Mater. 135 (1), 112–121. https://doi.org/10.1016/j.jhazmat.2005.11.031.

Lee, N.M., Welander, T., 1996. The effect of different carbon sources on respiratory denitrification in biological wastewater treatment. J. Ferment. Bioeng. 82 (3), 277–285.
Li, Q., Csetenyi, L., Gadd, G.M., 2014. Biomineralization of metal carbonates by Neurospora crassa. Environ. Sci. Technol. 48 (24), 14409–14416. https://doi.org/10.1021/es5042546.
Lin, Y.-H., Gu, Y.-J., 2020. Denitrification kinetics of nitrate by a heterotrophic culture in batch and fixed-biofilm reactors. Processes 8 (5), 547. https://doi.org/10.3390/pr8050547.
Liu, J., Ali, A., Su, J., Wu, Z., Zhang, R., Xiong, R., 2021. Simultaneous removal of calcium, fluoride, nickel, and nitrate using microbial induced calcium precipitation in a biological immobilization reactor. J. Hazard Mater. 416, 125776 https://doi.org/10.1016/j.jhazmat.2021.125776.
Marsili-Libelli, S., 2018. Environmental Systems Analysis with MATLAB®. CRC Press.
Mendrinou, P., Hatzikioseyian, A., Kousi, P., Oustadakis, P., Tsakiridis, P., Remoundaki, E., 2021. Simultaneous removal of soluble metal species and nitrate from acidic and saline industrial wastewater in a pilot-scale biofilm reactor. Environmental Processes 8 (4), 1481–1499. https://doi.org/10.1007/s40710-021-00536-w.
Miao, Y., Liao, R., Zhang, X.-X., Liu, B., Li, Y., Wu, B., Li, A., 2015. Metagenomic insights into salinity effect on diversity and abundance of denitrifying bacteria and genes in an expanded granular sludge bed reactor treating high-nitrate wastewater. Chem. Eng. J. 277, 116–123. https://doi.org/10.1016/j.cej.2015.04.125.
Mokhayeri, Y., Nichols, A., Murthy, S., Riffat, R., Dold, P., Takacs, I., 2006. Examining the influence of substrates and temperature on maximum specific growth rate of denitrifiers. Water Sci. Technol. 54 (8), 155–162. https://doi.org/10.2166/wst.2006.854.
Murali, A., Zhang, Z., Shine, A.E., Free, M.L., Sarswat, P.K., 2022. E-wastes derived sustainable Cu recovery using solvent extraction and electrowinning followed by thiosulfate-based gold and silver extraction. Journal of Hazardous Materials Advances 8, 100196. https://doi.org/10.1016/j.hazadv.2022.100196.
Onnis-Hayden, A., Gu, A.Z., 2008. Comparisons of organic sources for denitrification: biodegradability, denitrification rates, kinetic constants and practical implication for their application in WWTPs. Proceedings of the Water Environment Federation 17, 253–273. https://doi.org/10.2175/193864708788735510.
Öztürk, N., Bektaş, TEl, 2004. Nitrate removal from aqueous solution by adsorption onto various materials. J. Hazard Mater. 112 (1–2), 155–162. https://doi.org/10.1016/j.jhazmat.2004.05.001.
Petrovič, A., Goršek, A., Simonič, M., 2015. A kinetic study on drinking water denitrification using a membrane bioreactor. Open Chemistry 13 (1), 901–909. https://doi.org/10.1515/chem-2015-0112.
Phillips, H.M., Barnard, J.L., deBarbadillo, C., Shaw, A.R., Steichen, M.T., Wallis-Lage, C., 2009. Denitrification rates: sampling, modeling and design considerations. Nutrient Removal and Recovery Symposium 2009 2009, 252–276. https://doi.org/10.2175/193864709793901301. Water Environment Federation.
Pintar, A., Batista, J., Levec, J., 2001. Catalytic denitrification: direct and indirect removal of nitrates from potable water. Catal. Today 66 (2–4), 503–510. https://doi.org/10.1016/S0920-5861(00)00622-2.
Rajasekar, A., Wilkinson, S., Moy, C.K.S., 2021. MICP as a potential sustainable technique to treat or entrap contaminants in the natural environment: a review. Environmental Science and Ecotechnology 6, 100096. https://doi.org/10.1016/j.ese.2021.100096.
Reddy, M.S., 2013. Biomineralization of calcium carbonates and their engineered applications: a review. Front. Microbiol. 4, 314. https://doi.org/10.3389/fmicb.2013.00314.
Reichert, P., 1994. Aquasim – a tool for simulation and data analysis of aquatic systems. Water Sci. Technol. 30 (2), 21–30. https://doi.org/10.2166/wst.1994.0025.
Reichert, P., 1998. Aquasim 2.0-user Manual. Swiss Federal Institute for Environmental Science and Technology Dubendorf, Switzerland.
Remoudaki, E., Hatzikioseyian, A., Kaltsa, F., Tsezos, M., 2003a. The role of metal-organic complexes in the treatment of chromium containing effluents in biological reactors. In: 15th International Biohydrometallurgy Symposium (IBS 2003), pp. 711–718, 2003a.
Remoudaki, E., Hatzikioseyian, A., Kousi, P., Tsezos, M., 2003b. The mechanism of metals precipitation by biologically generated alkalinity in biofilm reactors. Water Res. 37 (16), 3843–3854. https://doi.org/10.1016/S0043-1354(03)00306-3.
Remoudaki, E., Hatzikioseyian, A., Tsezos, M., 2007. Metabolically mediated metal immobilization processes for bioremediation. In: Proceedings of Balkan Mineral Processing Conference. Delfi, Greece, pp. 481–486, 2007.
Remoundaki, E., Hatzikioseyian, A., Tsezos, M., 2007. A systematic study of chromium solubility in the presence of organic matter: consequences for the treatment of chromium-containing wastewater. J. Chem. Technol. Biotechnol. 82 (9), 802–808. https://doi.org/10.1002/jctb.1742.
Remoundaki, E., Kousi, P., Joulian, C., Battaglia-Brunet, F., Hatzikioseyian, A., Tsezos, M., 2008. Characterization, morphology and composition of biofilm and precipitates from a sulphate-reducing fixed-bed reactor. J. Hazard Mater. 153 (1), 514–524. https://doi.org/10.1016/j.jhazmat.2007.08.094.
Ren, Y., Su, J., Wang, Z., Li, Y., 2023. Hydrogel microbial reactor based on microbially induced calcium precipitation for the removal of calcium, cadmium and nitrate from groundwater. J. Environ. Chem. Eng. 11 (3), 109867 https://doi.org/10.1016/j.jece.2023.109867.
Revsbech, N.P., Sørensen, J., 2013. Denitrification in Soil and Sediment, vol. 56. Springer Science & Business Media.
Richard, Y.R., 1989. Operating experiences of full-scale biological and ion-exchange denitrification plants in France. Water Environ. J. 3 (2), 154–167. https://doi.org/10.1111/j.1747-6593.1989.tb01503.x.
Rittmann, B.E., McCarty, P.L., 2020. Environmental Biotechnology:principles and Applications, second ed. McGraw-Hill, New York.
Schoeman, J., Steyn, A., 2003. Nitrate removal with reverse osmosis in a rural area in South Africa. Desalination 155 (1), 15–26. https://doi.org/10.1016/S0011-9164(03)00235-2.
Speight, J.G., 2017. Lange's Handbook of Chemistry. McGraw-Hill Education.
Stensel, H.D., Horne, G., 2000. Evaluation of denitrification kinetics at wastewater treatment facilities. In: WEFTEC 2000, 2000. Water Environment Federation, pp. 633–654.
Stensel, H.D., Loehr, R., Lawrence, A., 1973. Biological kinetics of suspended-growth denitrification. J. (Water Pollut. Control Feder.) 249–261.
Stumm, W., Morgan, J.J., 2012. Aquatic Chemistry: Chemical Equilibria and Rates in Natural Waters. John Wiley & Sons.
Tanaka, T., Koizumi, M., Yokoyama, T., Ishihara, Y., 1979. Kinetics and products of the reaction between sodium nitrite and bisulfite. Am Chem Soc, Div Pet Chem, Prepr; (United States) 24. CONF-790415-).
Tchobanoglous, G., Burton, F.L., Stensel, H.D., 2003. Wastewater Engineering: Treatment and Reuse, vol. 10. Metcalf & Eddy Inc. McGraw-Hill, Inc, New York, 0070418780.
Thakur, P., Kumar, S., 2020. Metallurgical processes unveil the unexplored "sleeping mines" e- waste: a review. Environ. Sci. Pollut. Control Ser. 27 (26), 32359–32370. https://doi.org/10.1007/s11356-020-09405-9.
Tsezos, M., 2014. Biosorption: a mechanistic approach. In: Schippers, A., Glombitza, F., Sand, W. (Eds.), Geobiotechnology I: Metal-Related Issues. Springer Berlin Heidelberg, Berlin, Heidelberg, pp. 173–209. https://doi.org/10.1007/10_2013_250.
Wan, D., Liu, H., Qu, J., Lei, P., 2010. Bio-electrochemical denitrification by a novel proton-exchange membrane electrodialysis system—a batch mode study. J. Chem. Technol. Biotechnol. 85 (11), 1540–1546. https://doi.org/10.1002/jctb.2465.
Wang, L., Shao, Z., 2021. Aerobic denitrification and heterotrophic sulfur oxidation in the genus Halomonas revealed by six novel species characterizations and genome-based analysis. Front. Microbiol. 12, 652766 https://doi.org/10.3389/fmicb.2021.652766.
WHO World Health Organization, 2017. Guidelines for Drinking-Water Quality, fourth ed. incorporating the first addendum edn.
Wisniewski, C., Persin, F., Cherif, T., Sandeaux, R., Grasmick, A., Gavach, C., 2001. Denitrification of drinking water by the association of an electrodialysis process and a membrane bioreactor: feasibility and application. Desalination 139 (1–3), 199–205. https://doi.org/10.1016/S0011-9164(01)00311-3.
Zhang, J., Hao, Z., Zhang, Z., Yang, Y., Xu, X., 2010. Kinetics of nitrate reductive denitrification by nanoscale zero-valent iron. Process Saf. Environ. Protect. 88 (6), 439–445. https://doi.org/10.1016/j.psep.2010.06.002.
Zou, G., Papirio, S., van Hullebusch, E.D., Puhakka, J.A., 2015. Fluidized-bed denitrification of mining water tolerates high nickel concentrations. Bioresour. Technol. 179, 284–290. https://doi.org/10.1016/j.biortech.2014.12.044.